

POLITECNICO DI TORINO

Collegio di Ingegneria Chimica e dei Materiali

**Master of Science Course
In Material Engineering**

Master of Science Thesis

Experimental study on the behaviour of composite materials subjected to water blast explosion. Naval application.



Supervisors

prof. Luca Marmo
prof. David Cendón

Co-supervisor

Victor Rey de Pedraza Ruiz

Candidate
Maria Luisa Scala

December 2019

*To my family,
for their love and support.*

POLITECNICO DI TORINO

Abstract

COLLEGIO DI INGEGNERIA CHIMICA E DEI
MATERIALI
DISAT
Master of Science Course in Materials Engineering

Experimental study on the behaviour of composite materials subjected to water blast explosion. Naval application.

Scala Maria Luisa

The present work is focused on the study of the behaviour of composite materials subjected to water blast explosion. The studied materials are those typically used in the naval and military structures. Studies are conducted simulating the blast wave caused by a possible explosion in the sea, caused by a mine, for example. The study is carried out using an equipment designed, manufactured and located at the university 'Politecnica de Madrid'. It is based on a modification of the original scheme of the Hopkinson bar and thus consisting essentially of a cylindrical projectile which hits a long incident bar in which a short compressive pulse is created. This incident bar is connected to a piston which closes a metallic box full of water. The tested composite panel is mounted at the back of the metallic box acting as a side of the testing chamber. The experimental set-up is instrumented with several sensors which provide record the values of the shooting time, of the pressure inside the chamber and of the deflection of the sample. Tested samples are rectangular panels in vinylester matrix reinforced with different types of fibers: carbon, glass, carbon and glass, basalt and glass. Therefore, the analysed samples are not-hybrids and hybrids panels, in order to observe the different behaviour depending on their configuration. Moreover, half of all the samples are subjected to saturation level with seawater and the results in both cases (saturated and not saturated) are compared. Finally, a developed analytical model of the deflection of the panel has been implemented in MATLAB. Experimental and analytical results obtained are compared by means of the panel deflection.

Contents

Abstract	v
Riassunto	x
1 Introduction and objectives	1
1.1 Introduction	1
1.2 Objectives.....	3
2 State of art	5
2.1 Composite Materials	5
2.2 Matrix	6
2.3 Dispersed phase.....	8
2.4 Laminate.....	9
2.5 Manufacturing process of composite materials.....	10
2.6 Composite materials used in the naval field.....	15
2.6.1 Matrix	16
2.6.2 Reinforcement fibers	18
2.6.3 Hybrids	25
2.7 Development of composite materials in naval field.....	25
2.8 Previous studies.....	28
3 Experimental study.....	31
3.1 Objectives.....	31
3.2 Materials.....	32
3.3 Manufacturing process	34
3.4 Materials characterization	39
3.5 Experimental device	46

3.6 Calibration of the experimental device	51
3.7 Experimental tests	52
4 Results	55
4.1 Data analysis	55
4.2 Experimental results	57
4.2.1 Carbon fiber composites.....	59
4.2.2 Glass fiber composites	62
4.2.3 Hybrid Basalt-Glass fiber composites.....	64
4.2.4 Hibrid Carbon-Glass fiber composites	67
4.3 Results comparison.....	71
5 Analytical model	74
5.1 Analytical model of blast effect on composite panels.....	74
5.1.1 Circular panel	74
5.1.2 Computation example	76
5.1.3 Rectangular panel.....	77
5.2 Model Implementation	79
5.3 Results	80
5.3.1 Carbon fiber specimen	80
5.3.2 Glass fiber specimen	82
5.3.3 Basalt-glass specimen	83
5.3.4 Carbon-glass specimen.....	84
5.4 Results discussion	87
Conclusion and future work	88
Appendix	92
Matlab software.....	92
References	95

Riassunto

Sin dai tempi più antichi l'uomo ha sempre utilizzato imbarcazioni piccole e grandi come mezzo di trasporto in acqua. Le navi sono utilizzate anche nel settore militare e queste, ancor più delle navi tradizionali, devono essere progettate in maniera molto efficiente, perché è previsto che non solo esse debbano avere una durabilità di oltre venti anni, ma soprattutto, debbano resistere a condizioni sfavorevoli, potendo essere oggetto di attacchi che possano comprometterne la vita. Nella progettazione di queste navi, ha grande importanza la scelta dei materiali utilizzati, in quanto da essi dipende la resistenza a vari fattori, ambientali e non, come corrosione, onde, impatti, possibili attacchi dovuti a proiettili, missili o mine sottomarine. I materiali da utilizzare in questa applicazione devono soddisfare vari requisiti, devono infatti essere leggeri, resistenti e avere bassi costi. Per tali requisiti, vengono perciò utilizzati, nel settore navale, metalli, polimeri e materiali compositi. Questi ultimi, in particolare, sono di grande interesse ed infatti sono utilizzati in moltissimi settori, in quanto posseggono eccezionali caratteristiche, quali, rigidità, flessibilità, durezza, durabilità, resistenza, alto rapporto resistenza-densità a buone proprietà meccaniche. In effetti, i materiali compositi, sono tra i materiali più innovativi, perché essi sono costituiti dalla combinazione di due fasi, una matrice ed una fase dispersa, permettendo così l'ottenimento di caratteristiche altrimenti non raggiungibili utilizzando singolarmente una delle due fasi.

La matrice nei materiali compositi rappresenta la fase maggioritaria, mentre la seconda fase o fase dispersa, viene introdotta per avere dei miglioramenti, essa può avere infatti diverse funzioni, (rinforzante, indurente, di abbassare il peso o il costo) e può essere sotto forma di fibre, particelle, whiskers. La matrice classifica il composito stesso, nel senso che è possibile avere un composito a matrice polimerica, ceramica o metallica a seconda appunto che la matrice sia un metallo, un ceramico o un polimero. I compositi più comunemente utilizzati sono quelli a matrice polimerica rinforzati con fibre ed in particolare i laminati in cui le fibre sono continue. Per questi compositi le metodologie di produzione sono piuttosto consolidate e i risultati ottenuti notevoli.

I materiali compositi hanno quindi suscitato grande interesse anche nel settore navale, essi sono infatti utilizzati per la fabbricazione della struttura principale, del ponte, dell'albero, delle eliche. I primi materiali compositi utilizzati in questo settore, comparvero già durante la Seconda guerra mondiale ed erano i GFRP (compositi a matrice polimerica rinforzata con fibre di vetro).

Molti progressi sono stati fatti in questo settore, ad esempio all'inizio non si potevano produrre imbarcazioni di grosse dimensioni in materiale composito, a causa della bassa rigidità dei primi compositi fabbricati e dei metodi di produzione poco efficienti. Con il corso degli anni, vennero ottenuti miglioramenti e furono osservati i vantaggi nell'uso dei materiali compositi sulle imbarcazioni, quali minor consumo di carburante, maggiore resistenza meccanica e alle condizioni ambientali che causano degradazione per idrolisi e corrosione. Tuttavia, sono necessarie ulteriori ricerche, nuovi metodi e nuovi studi su questi materiali che possano resistere alle varie condizioni estreme come quella oggetto di questo lavoro, ovvero lo studio del comportamento di materiali a possibili attacchi militari e terroristici. Il comportamento dei materiali compositi all'impatto statico e dinamico a bassa e alta velocità, è stato già ampiamente studiato, mentre pochi studi esistono su impatti dinamici balistici, come quelli appunto causati da missili e mine.

Questo lavoro di tesi ha perciò l'obiettivo di studiare il comportamento dei materiali compositi a esplosione sottomarina, simulando l'onda esplosiva che viene provocata dall'esplosione di una mina sottomarina. Tale lavoro è finanziato dall'ONR (Office of Naval Research) e prevede l'utilizzo di uno strumento sperimentale costruito alla *Politecnica de Madrid* e utilizzato per la prima volta in questo lavoro sperimentale. Poiché lo strumento è sperimentale, ovvero non standardizzato, un altro importante obiettivo è valutare il modo migliore per condurre i test e quindi ottenere risultati che siano quanto più possibile riproducibili e confrontabili tra loro, così da potere effettuare un'analisi qualitativa e quantitativa dei risultati e potere ottenere delle conclusioni valide. Dal punto di vista qualitativo, i materiali testati sono osservati dopo l'impatto dinamico subito, per valutare possibili danni visibili ad occhio nudo, questo soprattutto dopo i primi test effettuati, per potere calibrare lo strumento. Dal punto di vista quantitativo, i risultati ottenuti sperimentalmente analizzati e confrontati. Un ultimo obiettivo è lo sviluppo di un modello analitico implementato in Matlab che possa prevedere il comportamento dei materiali ad esplosione, in modo da potere confrontare i risultati sperimentali ed analitici.

La scelta dei materiali utilizzati in questo lavoro, è conseguenza di studi precedenti e materiali già in uso, che risultano essere quelli che hanno migliore comportamento rispetto

all'applicazione in oggetto, e sono materiali compositi a matrice polimerica. La matrice è in una resina termoindurente (per le migliori caratteristiche quali rigidità, resistenza, buona adesione con le fibre, buona resistenza alle condizioni ambientali, resistenza alla crescita della cricca, bassa emissione di gas nocivi, viscosità appropriata). In particolare, è scelto il vinilestere, perché esso, contenendo doppi legami carbonio-carbonio alla fine delle catene (siti reattivi) e basso numero di gruppi esteri (soggetti a idrolisi), ha buona resistenza ad acqua e attacchi chimici, resistenza a impatto e fatica, tenacità, facile fabbricazione e basso costo. Le fibre usate devono essere leggere, resistenti e stabili. Sono quindi scelte fibre minerali inorganiche quali vetro, carbonio e basalto. Le fibre di vetro sono tra le più utilizzate, vista la grande disponibilità, bassa densità, basso prezzo e facile produzione, in particolare è scelto il vetro di tipo S2 poiché presenta maggiore resistenza, soprattutto a impatto. Le fibre di carbonio hanno bassa densità, alta rigidità e resistenza, oltre che capacità di mantenere queste caratteristiche anche ad alte temperature. Le fibre di basalto sono ottenute da rocce vulcaniche, dunque la loro composizione dipende dal sito di estrazione, il loro costituente principale è silicato di alluminio, ossido di titanio e calcio. Sono scelte per la loro alta resistenza, alta tenacità, alto punto di fusione, bassa conducibilità elettrica, termica e acustica, alta resistenza a idrolisi e ad attacchi chimici e resistenza a impatti drastici.

I materiali studiati in questo lavoro sono laminati di tipo cross-ply (fibre orientate a 0/90), in vinilestere rinforzato con vetro, carbonio, vetro-carbonio, vetro-basalto. I materiali sono stati prodotti sotto forma di pannelli attraverso il metodo di fabbricazione VBI (Vacuum bag infusion), un metodo piuttosto semplice, economico e consolidato, che prevede la disposizione dei tessuti di fibra uno sull'altro all'interno di una sacca sottovuoto e l'iniezione della resina con il catalizzatore, in modo che impregni le fibre. L'indurimento avviene in un'ora all'interno di un semplice forno a 120°C, questo perché a temperatura ambiente impiegherebbe circa 24h. Nonostante la sua semplicità, questa tecnica di produzione permette di ottenere efficienti risultati. Alla fine del processo, infatti, viene effettuato un controllo C-Scan ad ultrasuoni, poiché i rischi sono di non uniformità di spessore e di porosità. La percentuale di difetti è molto bassa e quando comunque risulta superiore ad una certa percentuale limite, il pannello viene scartato.

È importante che i quattro tipi di pannelli abbiano tutti lo stesso spessore scelto di 3 mm, di conseguenza il numero di strati di fibre all'interno dei pannelli sarà diverso, infatti i GFRP (Glass fiber reinforced polymer) conterranno 20 strati, i CFRP (carbon fiber reinforced polymer) avranno 10 strati, HGC (Hybrid carbon.glass) conterranno 10 strati di vetro e 5 di carbonio e gli HGB (Hybrid basalt-glass) presenteranno 10 strati di vetro e 9 di basalto. I

pannelli fabbricati hanno dimensione 500x400mm², e sono ottenuti 2 pannelli di GFRP, di CFRP e di HGB, e 4 pannelli di HGC. La dimensione del campione deve essere un pannello di 225x170 mm², perciò ogni pannello fabbricato viene tagliato in laboratorio ottenendo così 8 campioni di GFRP, CFRP, HGB e 16 di HGC.

In questo lavoro sperimentale è stato, scelto di confrontare materiali compositi ibridi e non ibridi. Gli ibridi contengono appunto due tipi di fibre all'interno dello stesso composito, in modo da ottenere le migliori caratteristiche dei due. La disposizione delle fibre nei pannelli ibridi è non mista, ovvero da un lato del pannello ci saranno le fibre di un tipo e dall'altro lato l'altro tipo di fibra. Questo ha portato alla considerazione di testare i pannelli ibridi sia da un lato che dall'altro, in modo da osservare possibili differenze di comportamento quando il composito viene colpito dal lato del vetro, del carbonio o del basalto.

I materiali compositi utilizzati in questa applicazione, sono soggetti a varie condizioni critiche, tra cui l'immersione in mare. È dunque valutata la possibile influenza dell'immersione in acqua, portando metà dei campioni a livello di saturazione. È preparato un bagno di acqua salata (3.5% di sale) dove sono immersi i campioni. Essi sono pesati prima dell'immersione e dopo circa un mese e poi dopo qualche settimana, il livello di saturazione è raggiunto quando la differenza in peso tra due misure è minore dell'1%. Durante le pesature, è stato notato che i campioni dello stesso tipo avessero peso leggermente diverso (dell'ordine del grammo), questo perché l'operazione di taglio in laboratorio non è stata effettuata in maniera molto precisa. Quando i campioni immersi nel bagno raggiungono il livello di saturazione, essi sono pronti per essere testati, vengono estratti dal bagno solo prima del test e sono avvolti usando una pellicola di plastica in modo da non perdere acqua dal campione.

Per quanto riguarda lo strumento sperimentale, esso è stato progettato sulla base della barra di Hopkinson, un metodo verificato e consolidato per testare il comportamento dei materiali in condizioni dinamiche. La barra di Hopkinson è infatti costituita da due barre, una incidente e una trasmessa, tra le due viene posizionato il campione, la barra incidente viene colpita da un percussore (alimentato ad aria compressa ad esempio) e trasmette l'onda d'urto al campione che a sua volta la trasmette alla barra trasmessa, la quale produce un'onda riflessa che ritorna al campione, provocandone la deformazione. Lo strumento sperimentale è una modifica di quest'ultimo, infatti consiste nella combinazione della barra incidente con una cassa di alluminio e nell'eliminazione della barra trasmessa. Praticamente vi è un lungo tubo che contiene un proiettile (un cilindro metallico di circa 1.20 m) alimentato ad aria compressa grazie ad una bombola di pressione, esso colpisce la barra incidente avvitata ad un pistone che costituisce una delle facce della cassa di alluminio. La camera di alluminio è riempita di

acqua e il campione è posizionato proprio dietro questa cassa. L'obiettivo è infatti quello di simulare l'onda esplosiva di una mina sottomarina ed in effetti, il proiettile che colpisce la barra incidente e quindi il pistone, permette di convertire l'impatto in un'onda piana all'interno della camera che colpisce il campione, proprio come se fosse colpito dall'onda provocata da una mina in mare. Il proiettile contenuto nel lungo tubo del dispositivo prevede il posizionamento di due cilindri cavi di nylon alle due estremità, che hanno la funzione di tenere allineato il proiettile nella barra. La cassa di alluminio possiede tre pareti fisse (laterali e inferiore) mentre le altre tre sono smontabili, ovvero la parete superiore che viene avvitata alle laterali, quella anteriore che è costituita dal sistema pistone-barra incidente e la parete posteriore che è costituita da una cornice dove il campione è posizionato. Per evitare il contatto diretto tra campione e cassa, si utilizza una cornice di gomma. La cassa viene riempita di acqua per ogni test grazie a un foro presente sulla parte superiore, che poi viene chiaramente richiuso con un'apposita vite. La capacità della camera è di oltre sette litri. La cassa deve essere sigillata per evitare perdite di acqua, anche se in realtà si crea un gap tra pistone e cassa, che viene riempito con della semplice plastilina per evitare eventuali perdite di acqua.

Lo strumento sperimentale è inoltre provvisto di una parte strumentale, che costituisce appunto il sistema di misura e permette di ottenere le misure sperimentali. Tale sistema comprende: un laser posizionato dietro al campione per potere misurare la deformazione del pannello, un sensore di pressione collocato su una delle pareti laterali della cassa che misuri la pressione dell'onda di impatto ogni volta che questa lo attraversa, un cronografo costituito da due pezzi, ognuno dei quali possiede un sensore a infrarosso, che permettono di misurare il tempo che il proiettile impiega a passare attraverso questo strumento e dunque ricavare la sua velocità (nota la distanza tra i due sensori). Il cronografo ha anche la funzione di "trigger", ovvero quando il proiettile passa, innesca il sistema strumentale, che inizia dunque a registrare la misura da quel momento in poi. I sensori sono collegati ad un condizionatore di segnale che amplifichi appunto i segnali, un contatore digitale che permetta di visualizzare il tempo misurato dai sensori a infrarosso ed un oscilloscopio digitale che permetta di visualizzare e registrare i segnali delle misure effettuate.

Uno degli obiettivi del progetto è quello di calibrare lo strumento di misura posseduto, in modo da potere confrontare i vari test. Sono stati, perciò, condotti dei test preliminari su dei pannelli di alluminio. Innanzitutto, è stato posizionato un ulteriore sensore di pressione sul campione di alluminio, questo per verificare che il segnale di pressione misurato sul campione fosse simile a quello misurato sulla parete. In effetti si osserva che il segnale non solo ha lo

stesso andamento, ma presenta anche gli stessi valori, soprattutto lo stesso picco di pressione, di conseguenza, la pressione misurata sulla parete può essere considerata la stessa che sente il campione. Successivamente è stato verificato che l'andamento della deformazione misurata dal laser fosse simile a quella misurata per il campione composito. Infine, è stata decisa la sequenza di step da seguire durante il test e la pressione minima per alimentare lo sparo di 3 bar, visto che con tale pressione si è raggiunta una evidente deformazione plastica sui pannelli di alluminio. Tuttavia, la pressione di sparo scelta è stata poi successivamente modificata in seguito a dei test su un campione di CFRP e uno di GFRP, ed è stata scelta pari a 5bar circa, in quanto con questa pressione si è ottenuta una rottura sul campione di carbonio che non veniva modificata molto con una pressione superiore, mentre i campioni di vetro rimanevano intatti anche con 6bar.

I risultati ottenuti dai test vengono analizzati come segue. Le misure registrate vengono salvate in formato "csv", e vengono manipolate su un foglio di lavoro chiamato "QtiPlot", questo perché permette di lavorare su un numero così alto di valori (125000 in 42ms). Ogni misura è in Volts, quindi bisogna innanzitutto convertire nell'opportuna unità di misura ogni risultato (in mm per la deformazione e in MPa la pressione) attraverso specifici fattori di conversione.

Tutti i campioni presentano gli stessi pattern di pressione e deformazione. La pressione raggiunge un picco massimo e poi presenta altre oscillazioni, il primo picco rappresenta l'onda incidente, gli altri le onde riflesse, dunque l'unica parte del pattern importante è il picco iniziale, poiché esso può causare il maggior danno al campione testato.

La deformazione ha un andamento crescente fino a raggiungere un picco, questo perché appunto il campione viene deformato dal lato opposto rispetto a cui è colpito dall'onda, e quindi flesso dall'impatto subito, poi la deformazione torna a zero per poi raggiungere valori negativi e ripetere lo stesso comportamento con valori di deformazione più bassi, questo perché appunto il campione tenta di tornare nella sua posizione iniziale e applica una forza sull'acqua, infatti si nota sempre la presenza di un gradino che rappresenta il maggiore sforzo esercitato dal provino sull'acqua per potersi flettere dal lato opposto. Ad ogni modo, l'unico valore importante è quello di picco, che rappresenta appunto la massima deformazione subita dal campione e causata dall'impatto, anche perché nella realtà l'acqua non si trova in un contenitore chiuso e dunque l'andamento non sarebbe quello osservato sperimentalmente.

È possibile inoltre calcolare la velocità con cui il proiettile colpisce la cassa conoscendo il tempo impiegato per attraversare il cronografo e la distanza attraversata in questo tempo (15cm). I risultati mostrati sono la pressione con cui è alimentato lo sparo (sempre intorno ai

5bar), la velocità del proiettile, il picco di deformazione e di pressione, il possibile danno subito dal campione ed infine viene introdotto un nuovo parametro che è l'impulso per unità di area. Quest'ultimo non è altro che l'integrale numerico della curva di pressione rispetto al tempo, ma viene considerato solo appunto il picco iniziale, visto che, appunto, il resto dell'andamento della pressione è dovuto alla serie di onde riflesse che si generano all'interno della camera. L'impulso iniziale per unità di area viene calcolato integrando il picco iniziale di pressione rispetto al tempo, applicando la regola del parallelogramma. Per ogni tipo di campione vengono inoltre ricavati dei grafici che riportano i picchi di deformazione rispetto ai picchi di pressione e i picchi di deformazione rispetto agli impulsi per area, evidenziando con diversi colori i campioni saturi e secchi. Infine, vengono ricavati gli stessi grafici (deformazione-tempo; deformazione-impulso) mostrando con diversi colori i vari tipi di campione sia nel caso della condizione satura che secca, in modo da capire quale materiale si comporta meglio rispetto all'applicazione in oggetto.

Per quanto riguarda i CFRP si osserva una deformazione massima che varia da 9 a 21mm, anche se la maggior parte dei campioni ha un valore intorno ai 15 mm, questo perché, per questi campioni, la pressione di sparo utilizzata non è stata la stessa. Infatti, il campione che presenta una deformazione di 9 mm è il primo testato e sparato con una pressione molto bassa di 2 bar, mentre tutti gli altri campioni sono testati con una pressione mediamente di 5 bar. Il campione che invece presenta una deformazione di 21 mm è stato sparato con una pressione di 6 bar che ha causato la rottura ed la saturazione del segnale. Inoltre, nel caso dei CFRP il numero di campioni secchi testati è 4, mentre quello dei campioni saturi è 2, questo perché altri 2 campioni sono stati soggetti ad un ciclo termico che non è oggetto di questo lavoro. Dunque, come risultato non si osserva una grande differenza tra campioni saturi e secchi, anche perché il numero di campioni è troppo basso per potere ottenere una conclusione obiettiva. Ad ogni modo, i CFRP si sono tutti fratturati in seguito al test, escluso il primo test effettuato a bassa pressione. Il pattern di rottura è sempre lo stesso per tutti i campioni, ovvero, ha la forma di una T capovolta posizionata sulla parte inferiore del campione.

Per quanto riguarda i GFRP, anche in questo caso il numero di campioni secchi e saturi sono rispettivamente 4 e 2, nessuno dei campioni in seguito al test ha mostrato alcun segno di danneggiamento ed anche in questo caso le pressioni di sparo sono state piuttosto varie. Le deformazioni massime raggiunte variano intorno ai 13-16 mm con picchi di pressione tra i 4 e 6 MPa, senza mostrare praticamente alcuna evidente differenza tra condizione satura e secca.

Gli HGB sono come detto 8, metà in condizione di saturazione e metà secchi, inoltre metà dei campioni è testata dal lato del basalto e metà dal lato del vetro, con pressioni di sparo sempre

intorno ai 5 bar. Tutti i campioni hanno un comportamento molto simile, raggiungendo deformazioni massime intorno ai 16 mm, con pressioni massime raggiunte intorno ai 6MPa, eccetto un campione che raggiunge a una deformazione di quasi 20 mm con un picco di pressione di quasi 8MPa. Dunque, non si notano apprezzabili differenze di comportamento né in caso di saturazione né in caso di differente lato testato. Per quanto riguarda i danni subiti, i campioni presentano praticamente tutti delaminazione visibile ad occhio nudo, soprattutto dal lato del vetro, poiché il vetro è molto chiaro ed il basalto molto scuro.

Infine, vi sono i campioni ibridi HGC, di essi si posseggono 16 campioni ed anche in questo caso metà dei campioni è stata immersa nel bagno di acqua salata fino a saturazione ed anche in questo caso i campioni sono testati metà dal lato del carbonio e metà dal lato del vetro. Tali campioni ibridi raggiungono deformazioni massime che variano tra 13 e 17mm, con picchi di pressione tra 4 e 7MPa. Per quanto riguarda il lato in cui è posizionato il campione durante il test, non ci sono apprezzabili differenze, nonostante il maggior numero di campioni a disposizione. Per quanto riguarda la differenza di condizione (satura e secca), anche in questo caso non ci sono differenze molto evidenti, sembrerebbe che i campioni saturi si deformino mediamente leggermente di più, ma anche le pressioni e gli impulsi sono in media maggiori rispetto a quelle raggiunte nel caso dei campioni secchi. Per quanto riguarda i danni subiti, poco più della metà dei campioni mostra una visibile delaminazione, anche più evidente del caso precedente visibile a occhio nudo ed ancora una volta dal lato del vetro è più evidente, ma semplicemente perché il vetro è chiaro e il carbonio scuro.

Come ultimo risultato sperimentale mostrato, sono confrontati tutti i materiali sia nel caso di condizione satura che secca. Il risultato è difficile da analizzare, ma concentrandosi nell'intervallo tra 4 e 6 MPa, dove vi è la maggiore densità di risultati. In effetti, si osserva che i campioni ibridi HGC hanno i valori più bassi di deformazione massima e i CFRP la maggiore deformazione massima. Stesso risultato è osservato se si considerano i grafici rispetto all'impulso per area. In effetti tale risultato concorda con il fatto che i campioni compositi rinforzati con fibre di carbonio siano gli unici ad essersi fratturati in modo evidente. Si può dunque sicuramente concludere che i CFRP sono quelli che si comportano peggio in questa specifica applicazione. Per quanto riguarda i campioni ibridi, essi sono quelli che presentano deformazioni massime minori, ma mostrano anche evidenti segni di delaminazione che può chiaramente compromettere la resistenza residua del materiale. Tuttavia, probabilmente con una disposizione più omogenea delle fibre si potrebbe evitare la delaminazione e dunque sarebbero necessari futuri test per potere osservare un possibile comportamento migliore rispetto all'applicazione in oggetto. Infine, si può affermare che i

GFRP mostrano il comportamento migliore, visto che nessuno dei campioni ha mostrato alcun segno di frattura. Ovviamente, tali conclusioni sono applicabili solo al caso preso in esame, un contenuto diverso di fibre o uno spessore differente o un altro metodo di fabbricazione del pannello potrebbe portare risultati differenti. Per quanto riguarda i campioni saturi, le conclusioni sono le stesse, potendo quindi concludere che l'immersione in acqua non ha influenza apprezzabile su questi compositi.

Ultimo obiettivo di questo lavoro di tesi è quello di confrontare i risultati sperimentali ottenuti con i risultati di un modello analitico sviluppato e implementato in Matlab. Il programma di calcolo utilizzato è stato sviluppato sulla base di equazioni scritte dal professor Vicente Sánchez sull'effetto di pannelli compositi soggetti ad esplosione. Lo scopo è quello di ottenere una risposta simile se non uguale a quella ottenuta dal test utilizzando le stesse condizioni del test e ponendole come dati nel programma. I risultati di deformazione sperimentale e analitica sono confrontati così da valutare la possibilità di studi futuri con l'utilizzo di questo programma e confermare la validità dei risultati ottenuti.

Il codice del programma prevede la presenza di variabili sulla geometria e sulle proprietà dei pannelli. Le variabili geometriche sono altezza, larghezza e spessore e saranno le stesse per ogni campione, visto che tutti i campioni hanno le stesse dimensioni. Le proprietà che devono essere modificate per ogni tipo di campione sono modulo di Young, distanza tra le fibre, numero di strati, densità, sforzo critico di rottura, sezione delle fibre. Per quanto riguarda queste ultime, sono note le proprietà singolarmente delle fibre di vetro, carbonio e basalto, perciò nel caso dei materiali ibridi, le proprietà sono ricavate utilizzando la regola della leva.

Dal punto di vista pratico, il programma viene alimentato in ingresso con la pressione sperimentale misurata ed in uscita calcolerà la deformazione. Come detto, la pressione è un archivio di 125000 valori, sarebbero troppi e il programma impiegherebbe molto tempo per calcolare la soluzione. Dunque, i dati pari a zero vengono tagliati all'inizio e alla fine, ricavando così un archivio di circa 5000/9000 dati che permetteranno di ottenere l'archivio di deformazione calcolato dal programma in qualche minuto. Questo è stato fatto per ogni campione permettendo così di sovrapporre tutte le curve di deformazione-tempo sperimentale e analitiche. Si osserva che le curve del modello si accostano notevolmente alle curve sperimentali, soprattutto come picco massimo di deformazione. La pendenza talvolta non è così simile, questa leggera differenza è dovuta al comportamento imperfetto della provetta nel dispositivo sperimentale, infatti, il campione non è perfettamente fissato sulla parte inferiore della camera e questo può modificare il suo comportamento. Un altro fattore che influisce tale risultato è il fatto che alla massa d'acqua è aggiunta anche la massa del pistone e della barra

incidente, ciò ha permesso di ottenere il picco di deformazione uguale e anche una pendenza di discesa molto simile, anche se questa non è di grande interesse. È stato infatti provato che considerando solo la massa dell'acqua la pendenza iniziale è la stessa del modello sperimentale. Questo accade perché inizialmente è solo l'acqua a causare la deformazione del materiale, ma poi quando viene raggiunto il picco di deformazione e la provetta tenta di tornare nella sua posizione originale, essa deve spingere contro la massa di acqua e contro il pistone che in tutti gli esperimenti viene anche spinto nella cassa a causa del colpo subito, ed è anche questo suo spostamento che determina una maggiore deformazione raggiunta dal campione.

In conclusione, il modello analitico sviluppato predice molto bene il comportamento dei materiali compositi ad esplosione osservando che le curve di deformazione sperimentali e analitiche sono sempre molto simili, in ogni caso analizzato (materiali ibridi, non ibridi, secchi e saturi).

Il potenziale del modello analitico è dato dalla possibilità di potere essere utilizzato in futuro per predire il comportamento dei materiali compositi ad esplosione, anche di materiali differenti da quelli in oggetto in questo lavoro, semplicemente cambiando le variabili di ingresso.

Riguardo, invece, al modello sperimentale, esso ha permesso di testare i materiali a esplosione in acqua, simulando l'onda d'urto di una mina sottomarina. Nonostante varie difficoltà e imprevisti, conseguenza ovviamente della sperimentabilità del progetto, si è riuscito a portare a termine il lavoro, ottenendo validi risultati che possano essere considerati come punto di partenza e stimolo per ricerche future che possano confermare tali risultati ed ottenerne altri. Un interessante studio futuro potrebbe riguardare il comportamento di tali materiali in seguito a un ciclo termico subito oltre che un numero di test maggiore sulla possibile influenza dell'assorbimento di acqua. Inoltre, in futuro, potrebbe essere progettato uno strumento migliore per condurre tali test, poiché la potenza degli impatti ha portato a dovere eseguire molte riparazioni, che hanno rallentato il lavoro oltre che talvolta compromesso la riuscita dello stesso. Ad esempio, durante i test preliminari effettuati sui pannelli di alluminio, veniva utilizzato una parete superiore in metacrilato che è stata distrutta dal test, in seguito fu usata una parete in alluminio, ma troppo sottile che infatti si è deformata, infine è stata utilizzata una parete più spessa. Nonostante questi vari miglioramenti, durante i test successivi gli impatti subiti hanno comunque provocato dei danneggiamenti, come il fatto che le viti utilizzate sono state piegate o spezzate e la cassa stessa durante gli ultimi test risultava praticamente deformata. Nonostante ciò, l'obiettivo di studiare il comportamento dei materiali

compositi ad esplosione è stato conseguito e sono stati ottenuti risultati ripetibili e paragonabili che confermano la validità del dispositivo sperimentale usato e permettono di confrontare i vari tipi di materiali.

Un ulteriore lavoro futuro riguarda la caratterizzazione dei materiali testati, ad esempio ai raggi X, in modo da potere quantificare i danni subiti e potere dunque verificare possibili cambiamenti microstrutturali che possano compromettere i materiali stessi oltre che confrontare i vari tipi di materiali e confermare quale si sia comportato meglio.

Chapter 1

Introduction and objectives

1.1 Introduction

The oldest mode of transport used in water comprises the ships. Ships, in general, but military ships are designed very efficiently, because they must have a durability greater than twenty years. This is the reason why it is very important the appropriate choice of the materials and the study of their behaviour facing with adverse and unfavourable situations, like corrosion, impact, wave and, in particular in the case of military vessels, also to air attack, such as the ones caused by missiles and projectiles, and water attacks, such as those caused by a submarine mine.

Therefore, the materials used in the shipbuilding sector have to satisfy various requirements, such as weight, fabrication costs, durability and so on. Generally, the materials used for these purposes are metals, non-metals (wood, rubber...) and in particular composite materials that are of great interest, especially in recent years.

Composite materials present excellent performance and properties required in this sector and in particular for this application. The composites, studied in this work, have a vinylester matrix and a dispersed phase in fibers of carbon, glass and hybrids with fibers in carbon-glass, basalt-glass.

The considered materials are the most common materials used for small and medium sized ships, because of the properties of these materials, such as stiffness, strength, high strength-density ratio, hardness, flexibility, durability and good mechanical properties. In fact, composite materials have always been of great interest and have experienced a deep and constant improvement along the last years, becoming a very competitive material used for many applications today.

The progress reached for these materials made them very suitable for the naval industry, especially during the Second World War, when FRP (Fiber Reinforced Polymer) were developed. The increasing interest led to new studies and research, new manufacturing methods, new fibers and matrices used, in order to improve the quality and the behaviour of these materials, and because of the results reached, composite materials started to be used in many sectors: automotive, sport, construction and in all application where better qualities were required.

In the case of the naval application the first vessels made up of composite material and in particular in GFRP (glass fiber reinforced polymer) appeared in 1947 in the USA. Small ships were manufactured which presented better characteristics respect to the traditional materials used, like less weight, transparency to the radiofrequency, high mechanical strength, but also higher cost that limited the use in large scale.

Moreover, the marine structures must support not only stresses but also harder conditions due to the environment and to the seawater that make the situations worse. In fact, the durability decreases, and corrosion conditions worsen, and then it's faster the degradation of the physical properties (hardness, resistance) and of the chemical properties, because of the hydrolysis mechanism. As said, the military vessels are also obviously subjected to various threats and dangers, then the conditions to what the materials are subjected are not only statics and quasi-static, but also dynamic, such as missile, projectiles, mines and other possible impacts. This is the reason why it is important to study the behaviour of these materials subjected to dynamics and ballistic impacts.

Composite materials used in this naval field have been studied under quasi-static and dynamic regimes, it means that traditional tests like traction tests have been conducted, the results evidenced the better behaviour respect to the traditional materials. More innovative tests have been conducted, like impact tests with low and high speed, in order to study the behaviour and in order to compare different composite materials reinforced with different types of fibers, or to compare the behaviour in different conditions, such as temperatures, saturation. The high velocity impacts are ballistics and explosions, and in order to study the behaviour of the materials it is important not only to conduct a test, but also to compare the results with some analytical or numerical models.

This led to the present master thesis work which has been financed to Vicente Sánchez by the ONR (office of naval research) an organization that promotes scientific programs through

schools, universities, profit and no profit organizations. It has been developed an experimental set-up and an analytical model implemented in matlab that can simulate the submerged impact to which some panels in composite materials are subjected. The results obtained with the model and with the experiments are compared in order to prove its validity and to implement it for future studies on the behaviour of composite materials subjected to dynamic loads.

1.2 Objectives

This master thesis work aims to study the behaviour of composite materials subjected to underwater blast explosion which a military ship can suffer due to explosions caused by submarine mines or projectiles.

Regarding the dynamic characterization of these materials for this particular behaviour there are not many studies or tests done. Even though that experiments using explosive loads have been conducted, due to military and confidentiality reasons, it was not possible retrieving any information or experimental result.

In order to obtain the simulation of the wave blast, and then to study and to characterize the behaviour of the materials tested, in this experimental work, an innovative set-up has been used (not standardized) able to recreate the wave blast caused by a submarine mine in the seawater, obtained by shooting a metallic cylindrical projectile with compressive air which hits and introduces a compressive pulse inside the incident bar. The compressive pulse travel through the incident bar which is linked to a steel piston closing an aluminium chamber full of water and equipped with the sample in the back part. Thus, the sample is in contact with water and subjected to the wave blast introduced by the piston, just like the walls of a ship in the seawater.

The objectives were not only the tests themselves, but also the design and the development of the method used, because the equipment is not standardized, so it was important to find the best way to conduct the tests, in order to obtain a certain reproducibility.

Another important objective involves the materials used, the choice, the manufacturing method and also the different test types to carry out. Therefore, the tests are performed over different types of composite materials, considering different cases, for example in the case of the hybrids materials (that contain two types of fibers) and not-hybrids, in the case of sample

at the saturation level, considering the influence of the face in contact with water (only in the hybrid case).

At the end of the tests a qualitative analysis is done. The materials are observed to evaluate the damage suffered, especially in the first tests, in order to calibrate the appropriate pressure to employ in the test campaign. The idea of this calibration is to find the optimal (minimal) shooting pressure which produces the failure of the tested panel. Then, the experimental results are analysed and compared.

Finally, the results are compared with the results obtained with a developed analytical model, very useful for possible future analysis.

Chapter 2

State of art

2.1 Composite Materials

Composite materials are multiphase materials, consisting of a continuous phase, defined matrix, and a dispersed phase, that can be in the form of fibers, particles or mixed. Both phases are distinct from the presence of a net interface which, also, allows to transfer the stresses from the matrix to the dispersed phase. The interface can be considered a real part of the material, in such a way that, sometimes, it is said that a composite comprises three different parts: the matrix, the reinforcement and the interface (*figure 2.1*). The matrix is the principal phase, the reinforce is the dispersed phase in the matrix and the interface is the contact zone between the two phases.

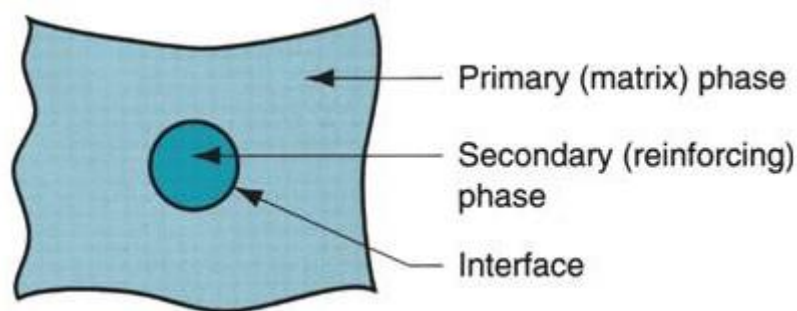


Figure 2.1: Schematic representation of a composite material [1].

Composite materials are used in many fields and applications, but especially where better properties and characteristics are required and common materials cannot satisfy these needs, while these materials are able to join the properties of the two phases showing performance levels otherwise unreachable.

Indeed, even though these materials are heterogeneous, the properties are homogeneous between all the volume and they vary from a composite to another depending on the present phases, on the fabrication process, on the way of disposition of the phases and so on.

In nature, they exist some heterogeneous materials, like wood, but the majority of the materials appertained to this class are artificial, meaning that they are fabricated and designed in order to obtain the desired properties and characteristics.

It is for the best characteristics reachable that these materials are of so great interest in many fields, such as civil, structural, automotive and naval.

2.2 Matrix

The matrix is the majority phase and the continuous phase of the composite material.

It has to satisfy various characteristics, in particular, it is necessary that it transfers the load to the reinforce, to the fiber, and that it holds the fiber spaced, that it protects them from chemicals, atmospheric agents and from mechanical damage, that it provides to fracture-retarding and that it makes that the compression and shear loads propagate in orthogonal direction respect to the fiber.

Both, matrix and dispersed phase influence and determine the final characteristics and properties of the material.

The matrix, in particular, has a role in determine the density, the load transferring, the interlaminar shear strength, the compression stability (micro buckling) and the machinability.

Composite materials can be classified and distinguished depending on the nature of the matrix in:

- **PMC:** composites with polymeric matrix
- **MMC:** composites with metallic matrix
- **CMC:** composites with ceramic matrix

The composites with polymeric matrix (PMC) are the most common ones, they have been developed to enhance many properties of the polymers, but keeping their features, like the low density.

The polymeric matrices can be of two types: thermoplastic and thermosetting. The different properties showed from these two types depend obviously on the chemical nature of the monomers, then from the crystallinity degree, in the case of the thermoplastics, and on the degree of crosslinking, in the case of the thermosetting.

In the structure of a thermosetting polymer, the carbon atoms form with themselves and with other atoms a three-dimensional and rigid network, in fact, they have all bonds with covalent nature.

This particular structure is obtained via curing, a technique in which the liquid resin forms the above-mentioned bonds at room temperature or at a certain pressure and temperature, thanks to specific catalysts.

The resulting matrix is easy to obtain, but it is also brittle respect to a thermoplastic matrix. Indeed, thermoplastic matrices do not have permanent bonding, instead they have weak bonds, however, they are more difficult to process, because of the high molecular weight that they have to reach in order to show good mechanical properties.

As a result of the different type of bond, the two type of matrix have different properties, as it is shown in the next table (*table 2.1*).

<i>Property</i>	<i>Thermosetting</i>	<i>Thermoplastics</i>
<i>Young Modulus [GPa]</i>	1.3-6.0	1.0-4.8
<i>Tensile Strength [MPa]</i>	20-190	40-190
<i>K_{Ic}</i>	0.5-1.0	1.5-6.0
<i>G_{Ic}</i>	0.02-0.2	0.7-6.5
<i>Max service T [°C]</i>	40-450	25-230

Table 2.1: properties comparison of thermoplastic and thermosetting resins [1].

2.3 Dispersed phase

The dispersed phase is a non-continuous phase that, like the matrix, have to satisfy some requirements, first of all, it has to support the loads applied to the material and that are transferred to it. This phase will then determine the final properties of the material.

The contribution of this phase depends on its own properties. The final characteristics of the composite material depend on the volumetric fraction of the two phases, on the interface, and on the distribution, dispersion and orientation (in the case of fiber) of the second phase.

In particular, the fiber influence the Young Modulus, the tensile and compression strength, the density, the fatigue resistance, the electric and thermic conductivity, the thermal expansion coefficient and the cost.

The second phase can be used for various purposes: toughening, strengthening, hardening...

Moreover, the second phase can be in different geometry: long fiber, short fiber, particles, whiskers (*Fig. 2.2*).

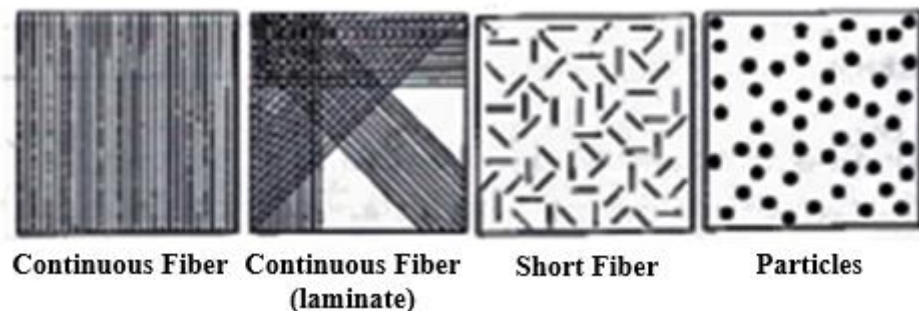


Figure 2.2: Morfology of the dispersed phase in the matrix of composite materials [1].

The most common second phase in composite material with polymeric matrix is fiber.

Fiber can be natural or artificial. The natural fiber are not commonly used, if not in the case in which the objective is an economic polymer without any enhanced property or characteristic. They are very similar from one to other, characterized with a structure very similar to wood, meaning that they consist in cellulose filament in a matrix of hemicellulose or lignin. This type of fiber have very poor mechanical properties, it is the reason why they are not so common in PMC and the reason why organic and inorganic synthetic fiber were designed, in order that they allow to obtain a composite material with excellent features.

The synthetic fiber more used for this scope are essentially:

- Glass fibres
- Aramid fibres
- Carbon fibres
- Basalt fibres (more recent fibres)

Contribute and efficiency, of these above mentioned fibres to the composite material, depend on various factors: their chemical composition, obviously, their intrinsic properties and features, such as length, diameter, dimensional uniformity, surface quality, interaction and compatibility with matrix, fabrication process.

2.4 Laminate

Composite materials are blended in order to obtain a sandwich or a laminate.

The so-called sandwich are panels, generally isotropic, used in bending. Laminate are, instead, precisely foils contained the unidirectional fibres overlapped in such a way that the fibres have different orientation and are bonded in a chemical or physical bonding.

Laminate are the commonly used structure, because they have better mechanical and physical properties.

According to the orientation angles of the foils that form the composite, laminates are classified in unidirectional, cross-ply and angle ply.

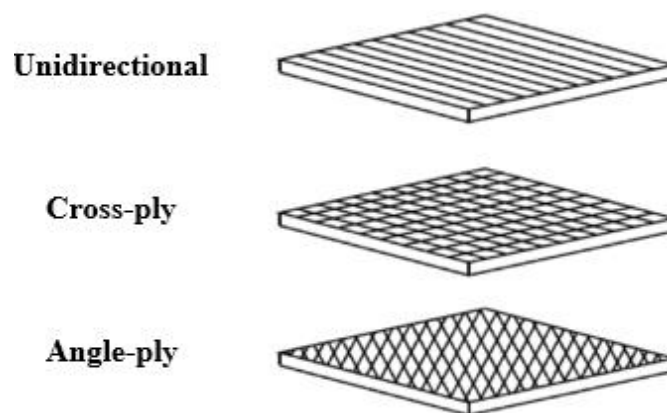


Figure 2.3: laminate types [7].

Nevertheless, laminate show some problems that common materials do not have, such as:

- **Delamination:** it is the separation between the foils, due to the interlaminar stresses (this is also called interlaminar failure)
- **Residual stresses and tensions at the edges:** they can be the consequence of the fabrication process, they are typically difficult to detect and to evaluate and, then, they can lead to the delamination failure.
- **Fracture analysis:** failure in a laminate is typically a progressive process, difficult to analyse and, therefore, very difficult to predict.

2.5 Manufacturing process of composite materials

A fundamental phase in the design of a composite material is the manufacturing process, in fact the final properties and features of the material depend on the phases and on how they are situated. Therefore, it has a great influence the fabrication method.

The manufacturing processes of the composite materials with metallic matrix (MMCs) and with ceramic matrix (CMCs) are still to be improved, meaning that they do not led to excellent results. Instead, the fabrication techniques of the composite material with polymeric matrix (PMCs) is pretty conformed and efficient. In fact, the fabrication process of a PMC essentially consists in forming the material and in its contemporary or following consolidation through cooling, in the case of thermoplastic resins, and reticulation, in the case of thermosetting resins.

Following they are described the different methods used for the manufacturing of an FRP (fiber reinforced polymer) composite:

- **Hand lay-up technique:** it is the simpler method used when it is needed to produce large size product with a specific geometry (vessel, pool...) and the fibres fraction is small (25-30%). Fibres in the form of felt or tissue are overlapped on the floor of an open mould, then the melted resin, containing the possible curing agent (thermosetting resins), is casted and smooth with rollers. In the case of thermosetting resins, an energy source (warm, UV lamp) makes the resins reticulated. The drawback of this technique is the probability of some trapped air.

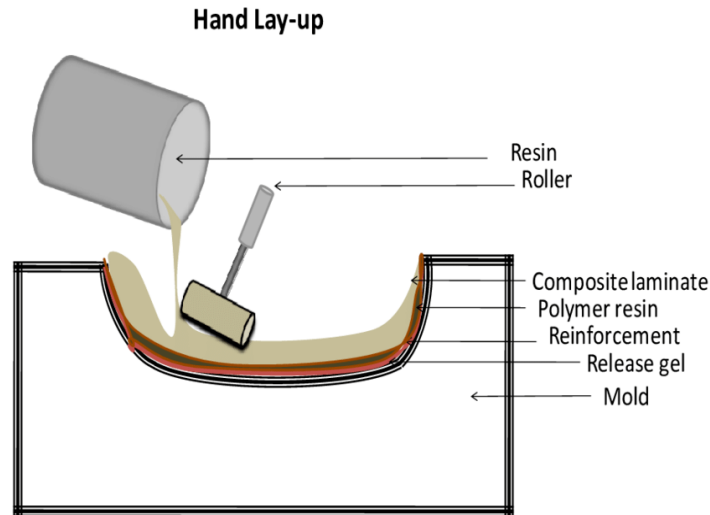


Figure 2.4: Hand lay-up of a composite material [20].

- High pressure moulding:** this technique is used for production of small size parts and for mass production. The resin containing the eventual curing agent and the reinforce, is pre-heated to shorten the curing time, it is hot moulded. The pressures used are around 10-50 MPa and they act on the foils of the composite (prepreg) or a slurry (in the case of short fibres). In the following figure it is shown the scheme of the process that also illustrates the pre-impregnation of the layers with the resin (*figure 2.4*).

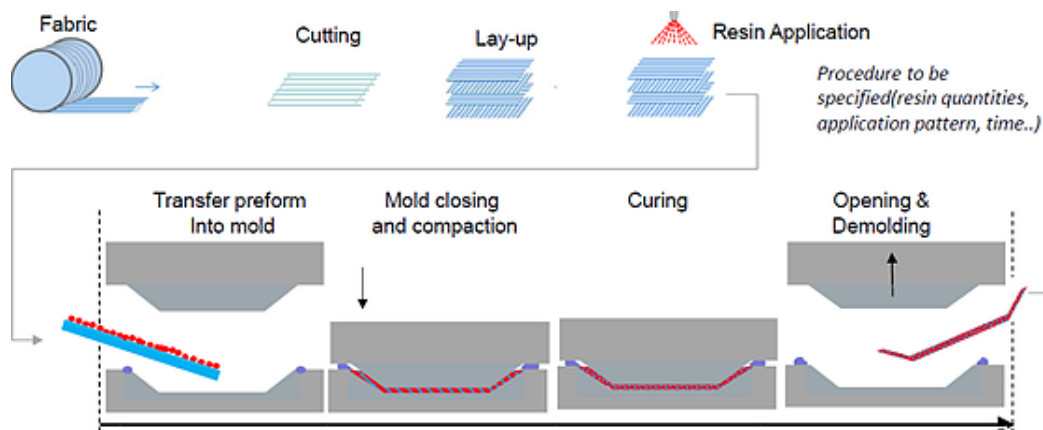


Figure 2.5: Hot moulding of PMCs [21].

- **Low pressure moulding in open mould:** in this technique the pre-impregnated fibers (prepreg) and the resin layers are deposited on the mould. Then the mould is sealed outward with a plastic shell, or it is closed in a plastic shell put on the mould. Anyway, the objective is to form the vacuum in the preform in order to prevent inclusions. Therefore, a pressure is applied in order that the shell join the mould and finally it is heated. The vacuum can be done with various techniques, the most common is in autoclave.

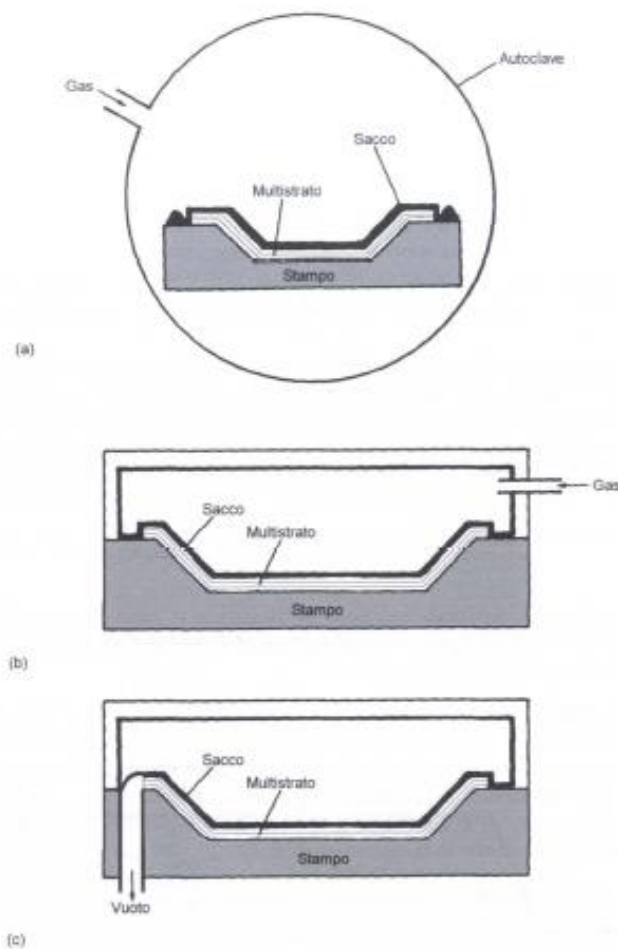


Figure 2.6: moulding in open mould of composite materials with polymeric matrix: a) in autoclave; b) hot and high pressure; c) hot and vacuum. [1]

- **Low pressure moulding in closed mould:** in this case the reinforce is put in the mould and then the resin is injected and so permeates the fibres, while air is driven off through aeration channels. The advantage of this technique is that it is possible to obtain product with complex geometry and that contain a high volumetric fraction of

fibres until 50%. The disadvantage, instead, is that also the mould is a composite material, therefore too high temperatures cannot be reached and, consequently, curing times are rather long. To shorten the curing time, it is possible to add to the resin a curing agent in a pre-heated chamber.

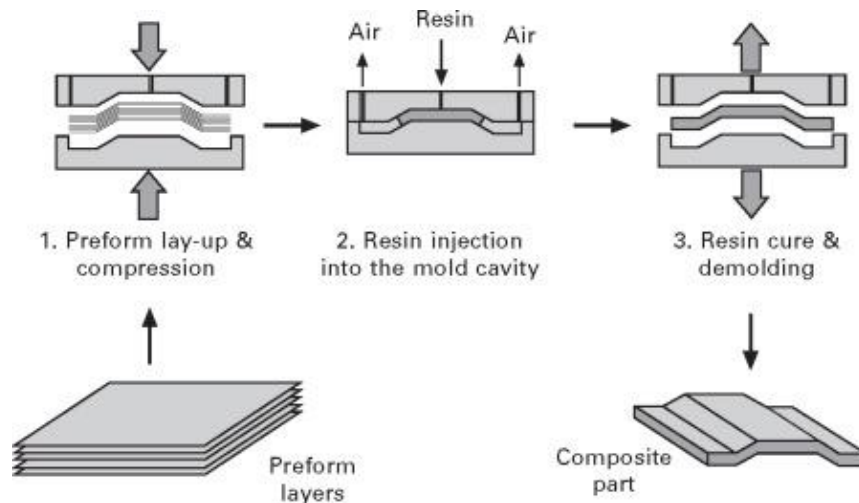


Figure 2.7: low pressure hot moulding of a PMCs [22].

- Pultrusion:** in this technique fibers in form of fabric or felt, are impregnated in a bath containing the resin. Then, the pre-impregnated fibers are transported in a pre-heated mould where it starts the curing which then is typically finished in a furnace. This method is very similar to the extrusion, except for the dragging, in fact, in this case, there are some rollers downstream of the system (pulling system), that allow to the dragging (it is the reason why this technique is called pultrusion). Just as the extrusion, there are a limit in term of the possible geometries, but there is a high productivity, indeed, pultrusion is used to obtain continuous products with constant section (e.g. bars) in short time.

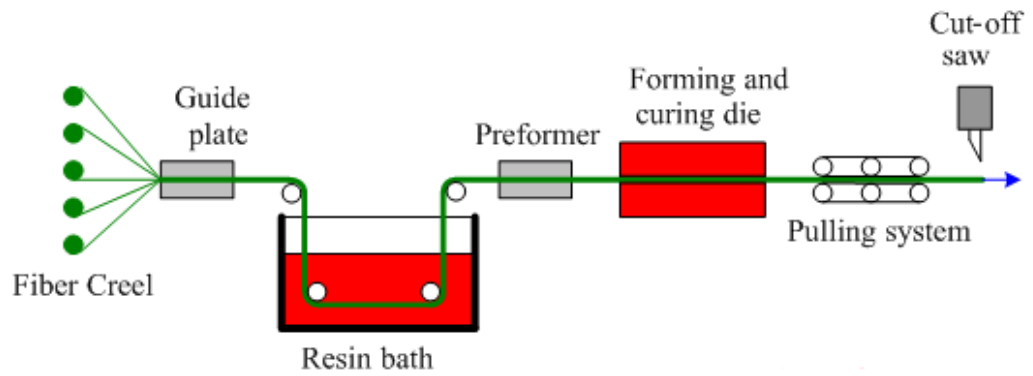


Figure 2.8: Poltrusion technique [23].

- Filament winding:** in this technique the prepreg fibres are wrapped and crossed on a rotating mandrel that allow to obtain a predetermined geometry. Subsequently, heat is applied in order to obtain the curing and finally the product is extracted. With this technique it is possible to obtain particular items, such as helicopter rotor blades, tanks, etc.

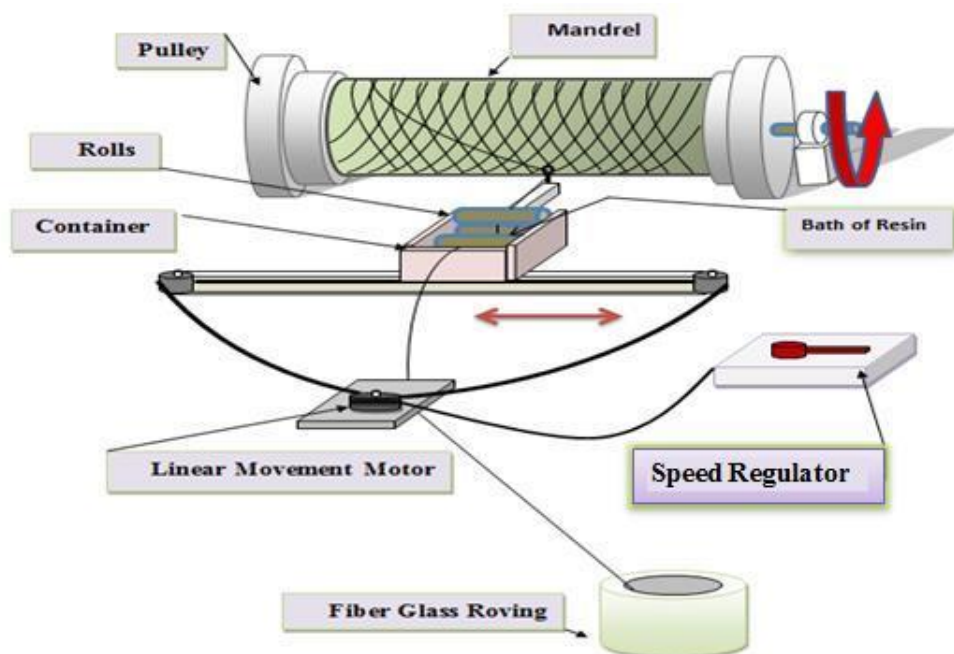


Figure 2.9: filament winding technique [24].

In the following table, the different techniques are compared in term of costs, times and efficiency.

<i>Method</i>	<i>Production cycle [time]</i>	<i>Equipment cost [€*1000]</i>	<i>Mould cost [€]</i>	<i>Value per cycle [€]</i>	<i>Value per hour [€]</i>	<i>Efficiency [*]</i>
<i>Moulding</i>	3 min	75	7500-30000	1.5-7.5	30-150	547-2142
<i>Autoclave</i>	8 h	225	1500	15-150	1.8-18	12-118
<i>Filament welding</i>	4 h	30-150	1500	15-150	3.7-37	178-375
<i>Forming</i>	10-60 min	7.5-15	450-1500	1.5-15	9-15	1500-1800
<i>Spray lay-up</i>	3 h	7.5	150-750	7.5-37	3-12	600-2400
<i>Manual</i>	5 h	0	150-750	7.5-37	2	15000
<i>Pultrusion</i>	0.5-3m/min	75-150	3000-15000	4.5/m	120-810	4326-8100

**(value*hour*10⁶)/(invested capital)*

Table 2.2: comparison of the different techniques in terms of costs and efficiency [1].

2.6 Composite materials used in the naval field

The most common material used in the naval industry are composite materials, especially the polymeric matrix composites (PMCs) and in particular FRP (fiber reinforced polymers).

2.6.1 Matrix

The most common matrix used in this field are the thermosetting resins. The most used matrices appertaining to this class are polyester, vinylester and epoxy resin. Indeed, they reflect the required properties for this application:

- Mechanical properties: stiffness and strength
- Resistance to the crack growth
- Good adhesion with fibers
- Good resistance to the weather conditions
- Proper viscosity
- Low emission of noxious agents
- Low shrinkage during the fabrication

The *polyester resins* result from the polycondensation of alcohol and polyvalent acids, depending on whether they are saturated or unsaturated it will be obtained a thermoplastic or a thermosetting product. The thermosetting resins resulting from the polycondensation in reactor, in which unsaturated chains are formed, followed by the in-situ polyaddition in which the chains reticulate bonding across between each other. These resins easy to process and cheap with good mechanical properties. In the nautical field, orthophthalic and isophthalic polyester resins are used, of which, the firsts are cheaper but with worst properties, then, typically, are used the orthophthalic because they also have a better resistance to water.

The *epoxy resins* are so called because they contain epoxy groups at the ends of the chains before of the reticulation. The most epoxy resin used is obtained by the polycondensation in basic environment between bisphenol A and epichlorohydrin-ethylene, followed by the solidification with an appropriate hardener (diamines, phenols, organic dioxides). The curing can be done at room temperature or in a furnace, in which better mechanical properties will be obtained. The epoxy resins are characterized by long chains with reactive groups at the ends and benzene rings in the middle. The benzene rings absorb the thermal and mechanical stresses making the resin resistant to impacts and to heat. Moreover, the resin resists to water and to chemicals, it is flexible, it has good adhesive characteristics thanks to polar groups that also make it adapt to many reinforce types, allowing to obtain tough and lightweight layers.

Therefore, they are incomparable in this field, but they are expensive and difficult to product and these reasons restrict their use.

The *vinylester resins* have a similar structure to the polyester ones. They are the result of an unsaturated monofunctional acid and a di-epoxide bisphenol. The reagents are diluted with styrene, typically, because it results a product very viscous and finally it is used a catalyst that allows that actives the cross-linking reaction. This type of resin is easy to obtain, like the polyester ones, but differently from those, they have carbon-carbon double bonding (reactive sites), just at the ends of the chains, also, they have a less amount of ester groups (they are susceptible to hydrolysis degradation), so the result is a resin with better resistance to water and to chemicals. Because of the smaller cross-linking density and of the presence of reactive sites only at the ends of the chains, the vinylester resins have good mechanical properties: impact resistance, toughness, fatigue resistance. Hence, these resins are suitable either as layer resin or as gelcoat, because they have excellent characteristics comparable to epoxy resins, but they also are cheaper than the epoxy ones.

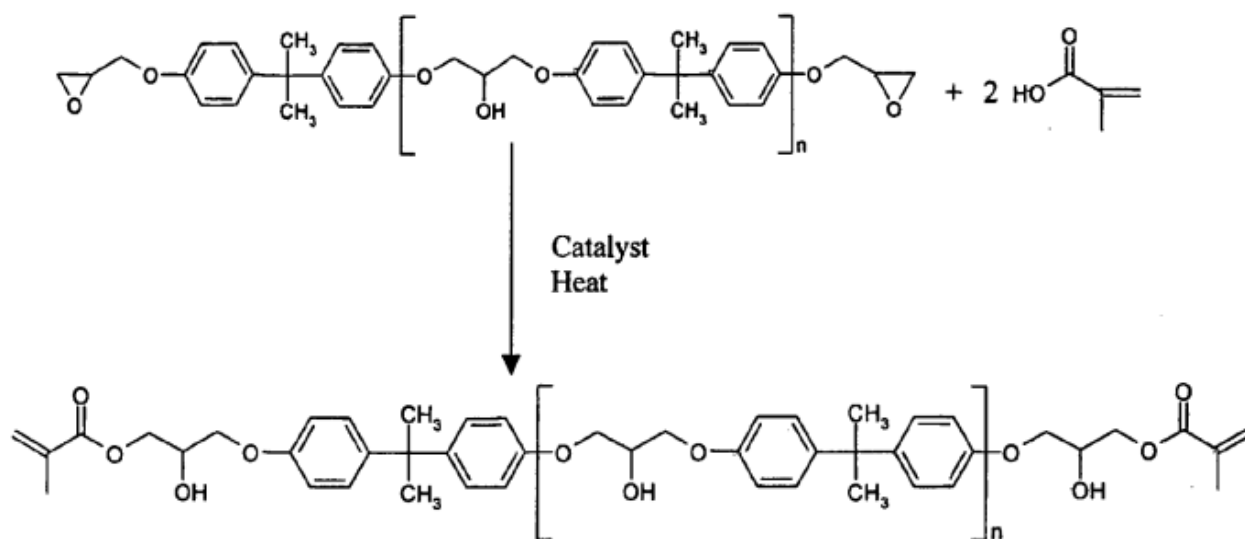


Figure 2.10: vinylester resin formula and structure [25].

Summarizing, the epoxy resins have the best mechanical and adhesive properties, but they are expensive and difficult to produce; while, vinylester resins have similar properties but they are cheaper and easy to obtain. These resins are often used as gelcoat in order to make the

surface impermeable and to protect it from ultraviolet rays, chemicals, atmospheric agents and for aesthetic reasons.

2.6.2 Reinforcement fibers

Naval structures required lightweight, resistant and stable fibres, that have strong covalent bonding between atoms. This is the reason why the fiber used are those inorganic synthetic fibres, like fiberglass, carbon fiber, organic fiber, aramid fiber, basalt fiber.

In the following table there are some properties of different fibers. The values in the table are indicative, meaning that they can be different depending on various factors, like the production technique, the processing.

<i>Fiber</i>	ρ [g/cm ³]	<i>E</i> [GPa]	σ_R [MPa]	ϵ_R [%]
<i>E- glass</i>	2.55	72	2400	3.0
<i>S2-glass</i>	2.50	88	3400	3.5
<i>SM carbon</i>	1.76	230	3530	1.5
<i>IM carbon</i>	1.80	294	6370	2.2
<i>HM carbon</i>	1.77	377	4410	1.2
<i>UHM carbon</i>	1.91	588	3920	0.7
<i>Kevlar</i>	1.45	125	2800	2.8
<i>Basalt</i>	2.75	89	4840	3

Table 2.3: properties of different type of fibers [1][26].

The *fiber glass* are the most used in the polymeric composites matrix in the naval industry, this is because of their characteristics, their cost and their availability. This fibers are made of

silica SiO_2 containing metallic oxides, so that the product has a certain machinability and appropriate properties to the use. There are various type of glass fiber:

- **Glass A:** similar to the glass used for glass bottle and glass plates, it has a low resistance to chemical attack in aqueous solution
- **Glass C:** is a variation of the glass A, but with better resistance to chemical attack
- **Glass D:** has good dielectric characteristics, low density and resistance to chemical attack
- **Glass E:** it is electric and it is the most used thanks to the balanced properties; **glass E-CR** is a variation that also present a good corrosion resistance
- **Glass S (strong):** it has a better resistance and for it is called strong
- **Glass M:** has a higher Young Modulus
- **Glass Z or AR (alkali resistant):** it is a glass made of zirconia, and so it is expensive because this oxide makes higher the softening temperature and then the fabrication is easier. It is a glass used in the concrete, because it is resistant to alkaline environment, resulting during the hydration of the Portland concrete.

The composition of the different glasses is showed in the next table.

<i>Glass</i>	<i>SiO₂</i> (%)	<i>Al₂O₃</i> (%)	<i>B₂O₃</i> (%)	<i>CaO</i> (%)	<i>Na₂O</i> (%)	<i>MgO</i> (%)	<i>Other (%)</i>
<i>A</i>	72	0.6-1.5	-	10	14.2	2.5	0.7 SO ₃
<i>C</i>	65	4	6	1.4	8	3	-
<i>D</i>	74	0.3	22	0.5	1	-	0.5 Li ₂ O
<i>E</i>	52-56	12-16	5-13	16-25	0-2	-	0-1.5 TiO ₂
<i>E-CR</i>	58-63	10-13	1-2.5	21-23	0-12	-	1-2.5 TiO ₂ 0-3.5 ZnO
<i>M</i>	53.7	-	-	12.9	-	9	2 ZrO ₂ ; 8BeO; 8 TiO ₂ ; 3 CeO ₂
<i>S</i>	65	25	-	-	-	10	-
<i>Z</i>	71	1	-	-	11	-	16 ZrO ₂ ; 2TiO ₂

Table 2.4: chemical composition of different types of glass [1].

Regarding the manufacturing process (*figure 2.10*) of the glass fibers, they are obtained with extrusion through a perforated plate containing thousands of holes from which the fibers emerge in stranded wire (hundreds of filaments) and then they are rolled up on a winding where they solidify. The stretching speed (about 50 m/s) determines the fiber's diameter, generally of around ten microns. During the solidification it is sprayed with an agent which gives the finishing to the fiber and acts as a former, as a lubricant, as a binding agent.

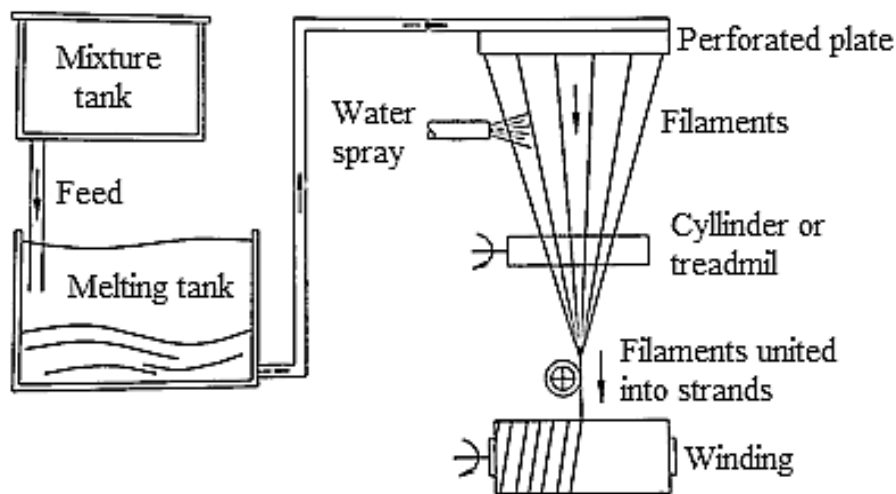


Figure 2.11: schematic manufacturing process of glass fibers [27].

The *carbon fibers* are the most used fibers in composite materials, because of their high stiffness and strength, because of their characteristics and properties: Young Modulus up to 900 GPa, longitudinal tensile strength up to 5000 MPa. They maintain their properties also at high temperature up to 1300 °C, nevertheless they are affected by oxidation from a temperature of about 400 °C and this causes the need for appropriate coatings when the application is at a temperature over that temperature.

Carbon fiber can be obtained from three different precursors: cellulose fibres (or rayon), polyacrylonitrile fibres (PAN) and pitch. In all cases, fibers obtained have graphite elements.

The final features of the product fiber depending on the origin and on the manufacturing process. IUPAC classify carbon fibers in the following ways, according to the mechanical properties:

- **UHM** (ultra-high modulus): Young modulus $E > 500$ GPa
- **HM** (high modulus): $E > 300$ GPa and tensile strength-modulus ratio $< 1\%$
- **HT** (high strength): tensile strength $\sigma > 3$ GPa and σ/E between 1.5 and 2%
- **IM** (intermediate modulus): $E < 300$ GPa and $\sigma/E > 1\%$
- **LM** (low modulus): $E < 100$ GPa and not-oriented structure.

PAN (polymer precursor with high melting point and containing polar nitrile groups) is the most used precursor for carbon fibers, because it led to a higher yield (percentage of product versus raw material), despite the higher cost. The manufacturing process includes the following steps:

- **Spinning (100-150°C):** melted PAN fibers are spinned in order to have a certain orientation.
- **Thermal stabilization-Oxidation (200-250°C):** this step is in air or in oxygen in order to obtain dehydrogenation and oxidation that lead to a double chain structure, thermally stable. This step and the following one are crucial for the production of high-quality carbon-fibers.
- **Carbonization (up to 1500°C):** this step is carried out in inert atmosphere, N_2 or Ar atmosphere, followed by removal of nitrogen and oxygen from the chains, in order to obtain many condensed cycles.
- **Graphitization (1500-2800°C):** this step is also conducted in an inert atmosphere with rising temperature. In this phase the fibers are submitted to a tensile stress that allows to align the rings to the fiber axis. This alignment or orientation rate is called graphitization rate and it depends on the temperature of this step, on the heating rate, on the tensile load applied, on the retention time. Depending on the graphitization rate it will be different the resulting young modulus: generally higher temperature means higher young modulus, but lower tensile strength (*figure 2.13*).

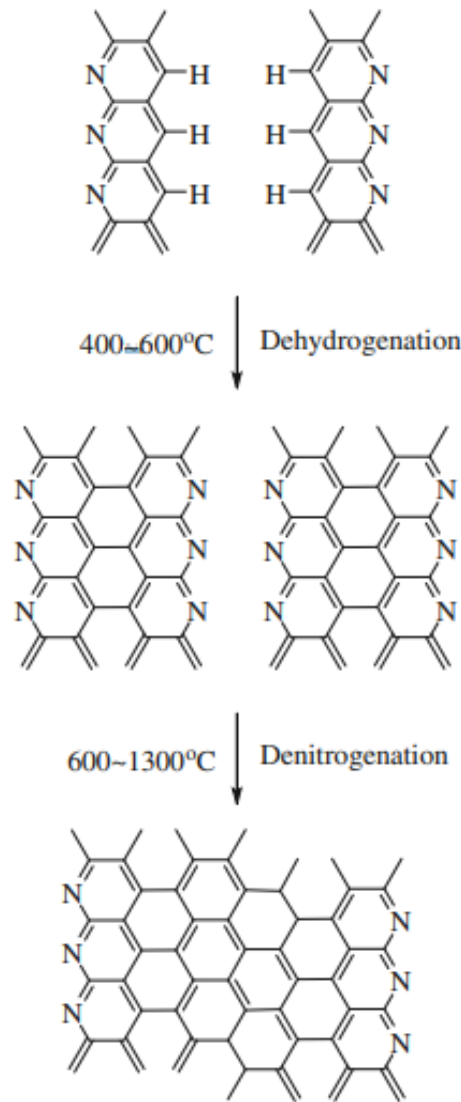
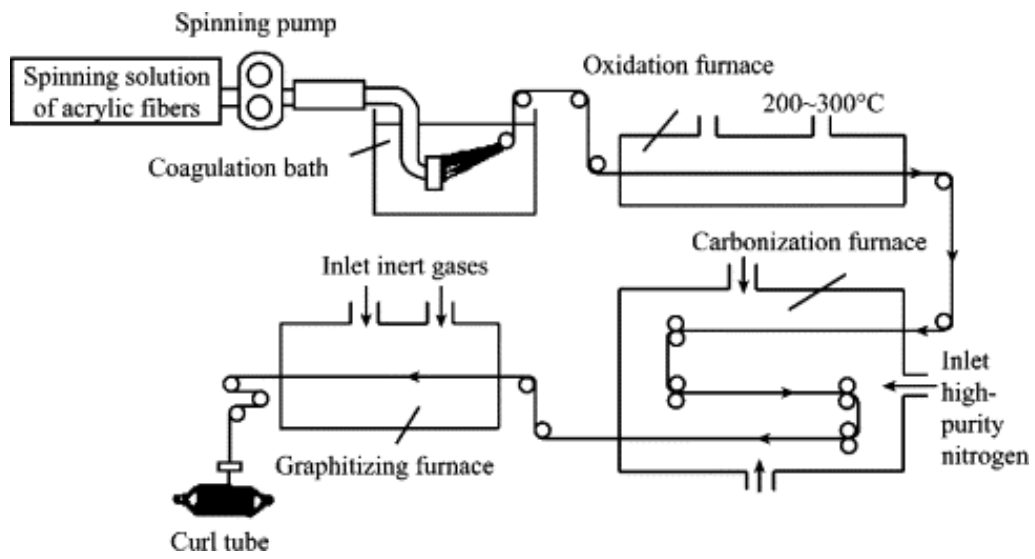


Figure 2.12: manufacture of carbon fibers from PAN [28][29].

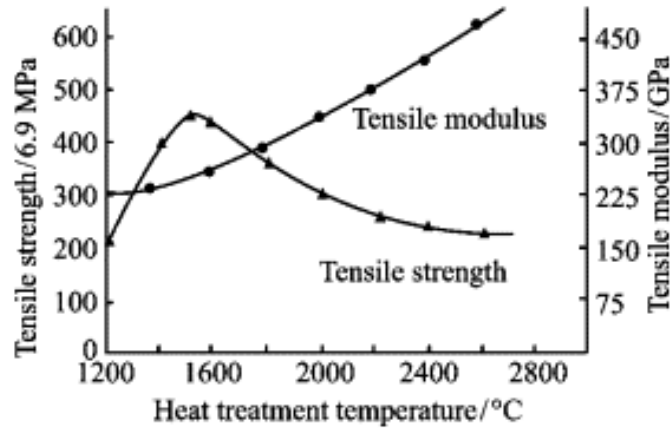


Figure 2.13: Young modulus and tensile strength respect to the heat treatment [28].

The *basalt fibers* are produced from volcanic rocks and therefore the chemical composition depends on the extraction site, but mostly they contain aluminium-silicate, titanium oxide and calcium. These fibers have excellent properties, such as high strength, high strain at break, high toughness, high melting point, low thermal, electrical and acoustical conductivity, resistance to chemicals and to hydrolysis. Because of their excellent features and their low cost, they are used in many fields and applications. In fact, they are a good alternative where better performances, like high stiffness, fire resistance, corrosion resistance, resistance to drastic impacts (blast, shot), are required.

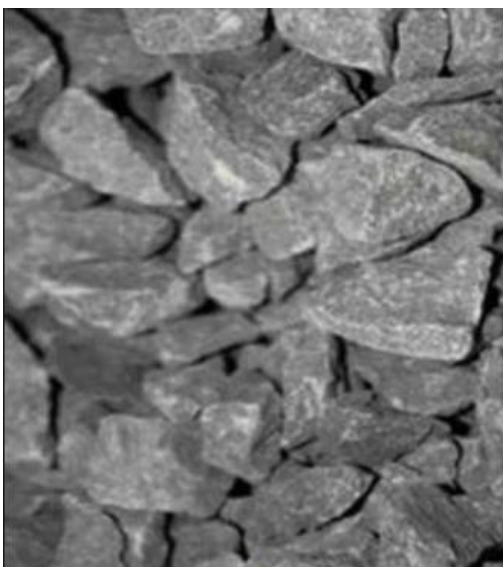


Figure 2.14: basalt: from rock to fiber [30].

Regarding the manufacturing process, it is very similar to that of the fiber glass, except for the precursor that in this case is made of just one component.

The steps of this process are:

- melting in a furnace of the basaltic rock at 1400 °C, in order to obtain the appropriate viscosity for the spinning step
- extrusion that lead to continuous filaments
- winding on a bobbin in order to obtain a diameter reduction of about ten micrometers.

It is noticeable that there is an high content of iron oxide in the chemical composition and this is the reason why basalt has a dark colour and it makes basalt able to absorb in the infrared range, making difficult that temperature is homogeneous into the melt, while glass is transparent, for this reason it is needed a furnace projected in appropriate way to have a homogeneous melt during the process. Therefore, it is typically used the vertical melting with electrodes submerged in bath (arc furnace).

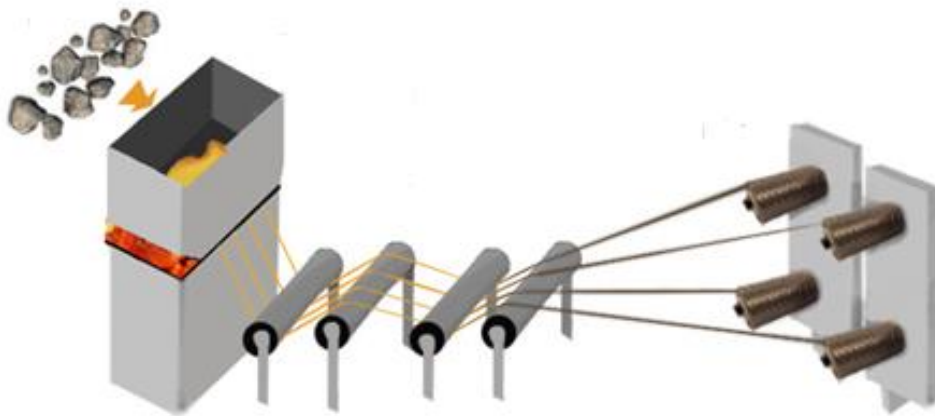


Figure 2.15: manufacturing process of basalt fibers [31].

2.6.3 Hybrids

Composite material can contain two or more reinforcement types and this type of composite is defined hybrid composite material. It is an innovative composite that allows to obtain better properties and features that comes from the fibers types and the matrix, or it is possible to obtain characteristics that would be achieved with just one fiber type, but with a lower price.

One of the most common hybrid composites is the result of the combination of glass fiber and carbon fiber into the same polymeric matrix. Indeed, carbon fibers have excellent properties, such as low density, stiffness, but they are expensive; while, glass fibers do not show so excellent properties, but they are cheaper and have better performances to impact. Therefore, to join these fibers seems to be a good solution, especially for the application of this work.

A hybrid composite with the combination of fiber glass and carbon fiber has higher strength, hardness and low-cost respect to materials containing just one type of the mentioned fibers.

There are various techniques to join the different fibers and depending on the method used the resulting features will be different. An important aspect is that properties will be still anisotropic.

Finally, hybrid composite materials are the best choice where the objective is to promote the best qualities of a fiber type and at the same time to avoid to its drawbacks.

2.7 Development of composite materials in naval field [36] [37]

Composite materials have been used in naval industry for several years. The reason of this choice, just like in other fields, is the objective of a structure as light as possible with advanced performances suitable to the application. Therefore, composite materials are the best choice considering the desired objectives, in fact, they are used for the main frame, the deck, the mast, propellers, etc.

Composite materials were used for the first time during the second world war, when vessels in GFRP (glass fiber reinforced polymers) were fabricated, instead of wood, aluminium and steel. In fact, in 1947, twelve boats in composite materials were built for the United States of

America Marina. Naturally, they had still not the appropriate knowledge on these materials, techniques and manufacturing technique are not well known and developed, and, therefore the resulting materials were not resistant and durable.

In the '60s, first commercial vessels, fishing boats and small ships were manufactured, mostly of those were in polyester reinforced with fiber glass. Meanwhile, just ten years later, composite materials were manufactured in epoxy and vinylester resins.

In fact, between '50s and 60's, first military ships in composite material were manufactured, the only limitation was the dimension, indeed the dimension of the fabricated ships were reduced. In fact, it was not possible to exceed the length of 20 meters, because the vessel was not enough stiff: materials have low young modulus and they would not resist to loads.

In 70's, it was fabricated an innovative composite material called "single skin design", with higher stiffness and it allows to obtain vessels of about 50 metres. This composite was made of a laminate with a thin layer in fiberglass containing longitudinal and transversal fibers with a sandwich structure.

The need to produce large sized structures has carried to further progress in manufacturing process, trying to make single-component structures of a specific thickness, a sandwich structure with a core between the two layers of the laminate. However, it was observed that it was not possible to obtain vessels in composite materials with dimensions over 100 metres long, to use steel was less expensive and safer in this case.

Between the '70s and 80's it was felt that there was a need of manufacturing techniques quicker, because of the growing market, therefore, advanced manufacturing techniques were developed.

In 1990 it was developed the technique of resin vacuum infusion, that led to the manufacturing of materials with better performances. In the same years carbon fibers and Kevlar fibers were used for the first time.

The advantages in the use of these materials were noted from the first moment. First of all, it was observed a lower fuel consumption respect to boat in steel, because of the lower weight, but maintaining the same boat speed. Moreover, these materials were not corroded over the time, thus reducing the needed maintenance work. Indeed, wood required a careful and

periodically maintenance, because it is submerged for long time into the water, thus it deteriorates, and rots and it is attacked from sea worms. Aluminium corrodes and decomposed by electrolysis. Steel lead to high weight construction such as to get worse the features' structure. Contrary, polyester and vinyl, submerged for long time, did not rot and were not attacked form sea worms, reducing costs and needed inspections.

In 1992, the first warship in composite material was built and it was called “*La Fayette*” (figure 2.16). It has the control deck, the battlefield and telecommunication sites, the ammunition storage and the weapon zone in steel, in order to have these parts safer and protect; while the superstructure of the stern was built in composite with a sandwich structure.



Figure 2.16: *La Fayette* photo [32].

In 2000 year, it was manufactured the first ship with the superstructure entirely in composite material, it was known as “*FNS Tornio*” (figure 2.16). Hull was in aluminium and the superstrustures were in composite material reinforced with carbon fibers.



Figure 2.17: *FNS Tornio* photo [33].

Actually, the main threat for a world ship is due to terrorist attacks, thus the ship structure must be able to maintain its integrity during these attacks. For this reason, it is interesting to study the behaviour of materials used for the superstructure of the ship facing with an attack like a blast due to a projectile or a mine. In the following figure it is shown a map in which it is possible to observe where there are the largest amount of enemy attack and then it is possible to understand the importance and the interest of this experimental study.



Figure 2.18: map of pirate attacks [34].

2.8 Previous studies

Several studies on the behaviour of composite materials used in naval field have been performed during the years. Some of these studies regard the behaviour to impact and to explosion. The most part of these studies are based on analytical and experimental models designed for this scope, only few of those are based on practical tests that allow to observe the effects of the blast on the tested materials and then the results were compared with the models in order to assess if they are similar.

Some of the studies consider the effect of the absorbed water by the material during its life before of the blast that it can suffer and thus the effects due to the various conditions of the water absorption.

In 2016 [16], it was conducted a test in which it was studied the behaviour of composite materials reinforced with carbon and glass facing with a water blast explosion in an aluminium box. Different types of materials were compared by quantify the damages with X-rays analysis. In this study it is shown the reason why the tested materials are chosen for this application. In fact, they have several advantages: high strength-weight ratio, good mechanical properties and so on. Ships must be designed in such a way that the materials have to resist to blasts and attacks and so it is fundamental to test the behaviour of these materials both in the air and in the water. In this case, the panels were welded in the box and then subjected to one kg of plastic explosive charge from one metre distance. Materials showed very similar behaviour, by resulting in debonding damages in the same tested time.

A study published in 2017 [14] regards the effect of the sea water on laminate in carbon fiber after explosion. Thanks to experimental and numerical techniques it is observed how mechanical and physical properties change after the blast of the tested panels. These samples were subjected to different water absorption level, until the saturation level. In this case, the equipment was provided of a tube from which a projectile was shot against a chamber containing the composite material panel and it was observed the results by using of a photographic system. The results analysed were the panel deflection, the damage resistance and the properties after the blast. Panels were in vinylester matrix reinforced with carbon fibers intertwined to form a laminate. The choice of the tested materials was the fact that fiber reinforced materials are the best appropriate materials for this application. They, in fact, show low weight, less fuel consumption, better corrosion resistance, low detonation probability dye to magnetic mines and so on. The drawback is that these materials could lost their stiffness, strength and their magnetic properties because of the water absorption. Consequently, it is possible that the properties' deterioration lead to a drop in the deformation and in the damage resistance and then there is a danger because ships as submarines are often subjected to underwater explosions due to mines or torpedoes and in air explosions due to missiles or projectiles. The work first involves the water immersion and durability study, then blast test is performed in a closed aluminium box covered with concrete and equipped with some transparent windows that allow to see inside. After tests, panels are studied using X-rays

(microtomography technique) and SEM (scanning electron microscope), in order to reveal the rising in the deterioration of the interfaces respect to the absorbed water rate. This type of revealed damage causes the worsening in compression, bending and interlaminar shear behaviour, while tensile modulus and fracture strength do not suffer of the damage.

Another study is carried out in London and published in 2017 [15], it regards the blast in air and in water of composite panels used in the naval structure. Even then, in this case the materials analysed were FRP and damages were observed with a visual technique using a 3D digital image correlation (DIC), with X-rays and tomography. It is tested the stability of these materials facing with blast explosion and impact caused by an explosive charge. Composite materials tested were reinforced with carbon-glass (hybrid materials) and the tests showed the benefits into join these fibers, in fact a reduction in the deflection and less damage was seen. Furthermore, these hybrid materials evidenced a higher resilience to blast explosion respect to composites containing just one fiber type. In this study, again, it is shown the reason why FRP are the best choice for this application, in fact, they have high strength-weight ratio and good mechanical properties. Always considering that military ships, contrary to common ships, must be designed in such a way to resist to attacks and high velocity impacts. The blast explosion is realized by using a gas gun which shot a steel projectile in a chamber where the sample is located. It is observed that all samples show the greatest deformation and dislocation in the centre of the plate, that CFRP (carbon fiber reinforced polymer) are more brittle and absorb less impact energy, GFRP (glass FRP) have a visible damage but greater deformation, while hybrids gave better response, in fact stress is reflected between the interfaces. It is also observed a shape effect due to the steel container and to the holders. The conclusion is that hybrids are the best solution for the application of military ships facing with blast explosion, due to less damages shown.

Chapter 3

Experimental study

3.1 Objectives

The objective of this study is to test experimentally the materials used in naval sector that must better resist to ballistic impact.

First of all, it has been chosen the best composite materials that can behave better in the case of this application, knowing the state of art (*chapter 2*), the choice is obviously a fiber reinforced polymer.

Another objective is to fabricate the composite materials, and then the choice of the fabrication process and the layers arrangement.

One of the greatest difficult and then objective has been the performance and the consolidation of the test with the owned experimental equipment, in order that all the tests were universal but especially comparable in terms of results.

Moreover, it has been decided the samples types (different materials comparisons and hybrids vs not-hybrids) and the status subjected by the samples (dry vs saturated).

The results have been collected in order to analyse and to compare the responses (*chapter 4*).

3.2 Materials

In this project thesis there are four types of materials studied. All of them are FRP because of the known best properties for this proposed application. Matrix is in vinylester and the four types of samples differentiate for the fiber type:

- | | | |
|-----------------|---|-------------|
| 1. Carbon | } | Not-Hybrids |
| 2. Glass | | |
| 3. Carbon-glass | } | Hybrids |
| 4. Basalt-glass | | |

As marked with graphs there are not-hybrid and hybrid materials.

The choice of a vinylester matrix comes from its exceptional water resistance and resilience. Additionally, it has low viscosity, appropriate to the manufacturing process used.

Regarding the second phase, it is in form of fabric, meaning that three types of fabric are needed:

- **Glass fabric** (*figure 3.1*): the fiber glass chosen for this work is the S2 type, because of its good mechanical properties, in fact, glass is generally brittle, but, in the form of fibers, its size is so reduced that drawbacks and weakness are minimized, achieving a material with high strength, lightweight and low cost. S2-glass is more expensive than other glass fiber types, but that with the best features, especially considering the application. It has, in fact, higher tensile strength and higher elastic modulus. The fabric used is the *Style 6580* with a density of 190 g/m^3 supplied by *Swiss-composite*.



- **Figure 3.1:** Glass-fiber fabric [17].

- **Carbon fabric** (*figure 3.2*): it is often chosen for its excellent properties of stiffness, high tensile strength, low density, resistance at high temperature. It shows higher surface density than S2-glass, it is the reason why a CFRP will have lower layers in order to obtain similar features between the two different composites. The carbon fiber used in the designed composites is *SIGRATEX PL1/ICW305* manufactured by *SGL Technologies*.



Figure 3.2: Carbon-fiber fabric [17].

- **Basalt fabric** (*figure 3.3*): basalt fiber is a very interesting fiber because of its intrinsic energetic-ecological features, in fact, it has an original nature, high chemical inertia, high durability, good thermal and acoustic insulation, good mechanical properties, high fire resistance, low cost and low impact of the cycle production.

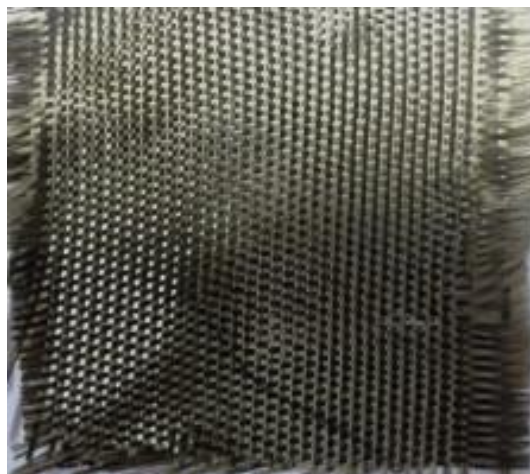


Figure 3.3: basalt fiber fabric [18].

The properties of the manufactured samples are shown in the next table, where the parameters will be useful not only for the experimental part, but especially for the analytical model.

<i>Property</i>	<i>Glass</i>	<i>Carbon</i>	<i>Basalt</i>
E [GPa]	87	230	74
ρ [Kg/m ³]	2100	1770	1950
$\epsilon_{critical}$	4.12	1.676	3.5
Cross-over distance [m]	$2.82 \cdot 10^{-4}$	$2.6 \cdot 10^{-3}$	$2.13 \cdot 10^{-4}$
Cross section area [m ²]	$1.2 \cdot 10^{-7}$	$2.3 \cdot 10^{-8}$	$1.3 \cdot 10^{-11}$

Table 3.1: properties of the fiber fabrics.

3.3 Manufacturing process

The technique used for the manufacturing of the materials in this project is the vacuum bag infusion (VBI). VBI is a technique well established, quick and very cheap.

The manufacturing process is carried out at IMDEA, a materials institute located in Getafe (Madrid).

The process requires the use of a preform, the resin mixed with an appropriate catalyst which initiates the curing, an under-vacuum cylinder, an infusion network with high permeability, a peelable tissue, a vacuum bag, sealing tape, feeding, distribution and collecting channels, vacuum system (to which the collecting channel is connected).

The infusion network allows the distribution of the resin, in fact, the network consists of a mesh placed on the peelable tissue itself located on the preform of the laminate. The vacuum bag is a bendable bag in which the several parts are enclosed. Vacuum is formed thanks to the sealing tape that is in nylon or, anyway, it is a transparent film that allows to check the flow

during the process and that will suit to the panel. The tape must be resistant to chemicals in the resin and it must be easy to remove when the process ends.

The feeding channel and the output channel are on the two sides of the prepared preform, they are two helicoidal tubes of the same size and the same length of the preform. The feeding channel connects the resin container with the distribution channel. The output channel connects the vacuum pump with collecting channel.

To avoid that the resin adheres to the bottom, all the system is on a Teflon support. It is, also, important and needed to clean everything before of the infusion process, in order to avoid that dirty forms defects like inclusions and vacancies in the panels and it is important that panels do not have visible defects. Feeding networks are situated above and below of the preform and between them and the tissues there is a peelable layers in order to avoid that the resin adhere with metallic networks and also in order to easily peel off the resin, including the excess of resin that accumulates in the surface layers.

The mesh located on the Teflon, allows not only the resin distribution but also allows to evacuate the air that is present in the laminate.

The vacuum-bag infusion is like a closed moulding technique, in which the Teflon on the bottom and bag on the top act like the two faces of the moulding.

The vacuum-bag system is shown in the next figure.

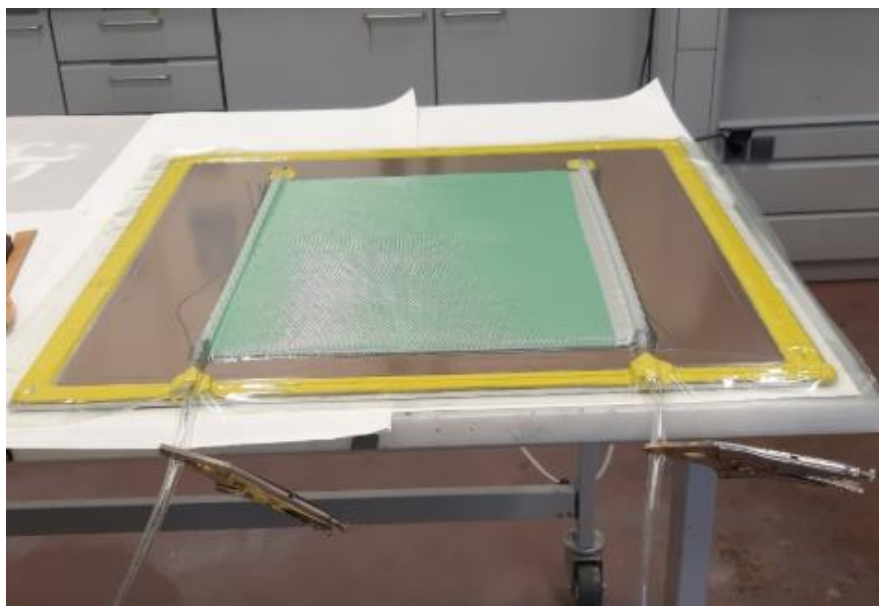


Figure 3.4: vacuum-bag system containing the preform.

Before of the infusion process, the resin is collected and it is added the catalyst that starts the curing process. The catalyst added is methyl ethyl ketone and the needed amount in the resin is about 1% and not more of 2%, for this reason it is important the weighting.



Figure 3.5: a)resin and b)catalyst.

Resin and catalyst are mixed and thus placed in a degasser for about ten minutes, in order to remove air bubbles. It is very important to remove bubbles, because they could negatively influence the behaviour of the manufactured panel, constiuing defects points in the laminate.



Figure 3.6: mixing and degassing step.

It is now possible the feeding: the resin passes through the channel and starts the distribution. It is observed that the resin is, initially, distributed quickly, until a certain level, then the distribution becomes very slow, this is because the resin is distributed transversally respect to the feeding direction, following the mesh of the network, but the distribution through the layers need more time, and as a consequence, when the distribution reach a certain level becomes low and low. In the next figures is shown this explained distribution behaviour. This is the reason why the mesh is not placed at the end of the preform, in such a way that the impregnation slows down and would be homogeneous in the longitudinal direction, giving the appropriate time to impregnate all the fibers. In fact, it is possible to see in the next figures that there is a gap, a space visible in white in which there is not the mesh.



Figure 3.7: feeding step of the vacuum-bag system.

It is very important that during all the process the feeding and collecting tubes (the spirals) are well stretched, in order to facilitate the resin flow. The resin is injected in surplus, because it is important to ensure that it impregnates all the layers and all the fibers; then the surplus resin is collected, in fact, there is a “resin trap” between the collecting channel and the vacuum pump, that collect the resin that comes out, avoiding that the resin goes in the vacuum pump. The resin impregnates the panel transversally respect to the feed direction and the distribution is facilitated thanks to the pressure difference between the two sides (feed and collecting).

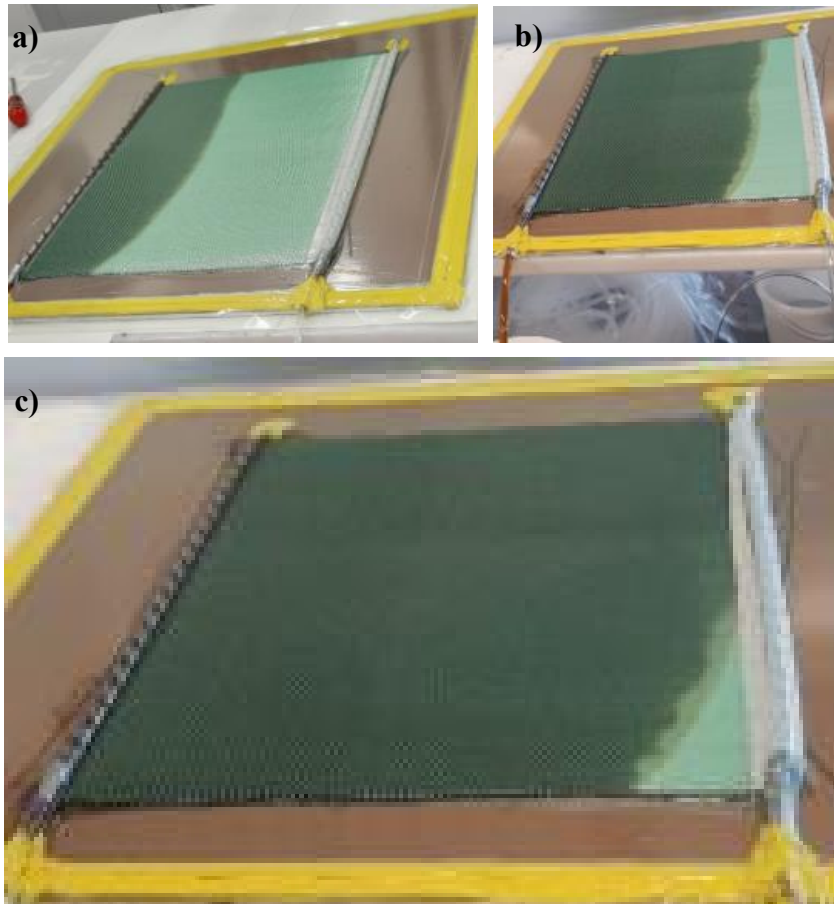


Figure 3.8: resin distribution a)quick phase and b)slow phase; c)mesh interruption.

When the infusion process is completed, the feeding channel is closed with a simple gripper.



Figure 3.9: collecting channel.

The curing of the resin occurs at room temperature, meaning that starts the chemical polymerization reaction and viscosity rises, it is needed one day until the completion of the process, but in order to speed up the curing, the vacuum-bag systems, containing the impregnated panels, are put in a oven at 120°C for three hours.

At the end of the curing it is possible the demolding: the nylon film, the mesh, the peelable fabric and the teflon plate are removed.



Figure 3.10: curing process in the oven.

In this manufacturing process it is important to pay attention to the uniformity of the thickness, in fact, because of the pressure difference between the two sides of the panel, the side with pressure equal to the vacuum one will be more compact respect to the side with atmospheric pressure. Furthermore, there is the risk of porosity. Because of these possible defects, it is important that at the end of the process, there will be an ultrasonic inspection called C-Scan (if the panel contains defects beyond a certain level, it is discarded).

Despite the low cost of this technique, despite the simplicity and the possible defects, the results of the manufactured panels are excellent, in fact, there is a very low percentage of porosity and defects in the samples and the panels are very homogeneous in thickness.

3.4 Materials characterization

IMDEA produced four different panels in vinylester reinforced with carbon (two panels), glass (two panels), carbon-glass (four panels) and basalt-glass (two panels).

The panel's dimension in of 500x400 mm² with thickness of 3 mm.

In order to obtain the same thickness for all panels the amount of the fiber's fabrics will be different, because the fabric's thickness is different (for example carbon's fabric has higher thickness). Knowing the thickness of the fabrics the panels' configuration and schematization will be as follows:

- Carbon: the panels contain 10 carbon fabrics with orientation $[0^\circ/90^\circ/0^\circ/90^\circ]$
- Glass: panels contain 20 glass fabrics with orientation $[0^\circ/90^\circ/0^\circ/90^\circ]$
- Carbon-glass: panels contain 5 carbon fabrics and 10 glass fabrics with orientation $[0^\circ/90^\circ/0^\circ/90^\circ]$
- Basalt-glass: panels contain 9 basalt fabrics and 10 glass fabrics with orientation $[0^\circ/90^\circ/0^\circ/90^\circ]$

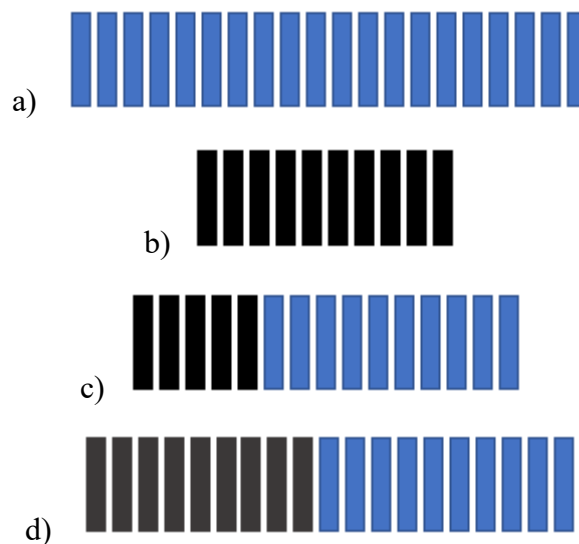


Figure 3.11: panels composites schematization a)glass; b)carbon; c) carbon-glass; d) basalt-glass.

As previously said there are hybrid and not-hybrid panels, in not hybrids there is just one type of fiber, while in hybrids types there are two different types of fiber but not mixed, meaning that in one side of the panel there is one fiber type and on the other side the other fiber type.

It suggests the possible materials characterization:

- Hybrids vs not-hibrids characterization
- Different sides (in the same hybrid type) characterization
- Dry vs saturated samples

Considering the testing apparatus has been designed to test sample of 170x225 mm², it means that for each panel is possible to obtain four specimens. In fact, the panels were been taken to the material's science department laboratory of the university, where they have been cut in order to obtain the specimen of the appropriate size, obtaining:

- 8 carbon fiber specimens
- 8 glass fiber specimens
- 16 carbon-glass specimens
- 8 basalt-glass specimens

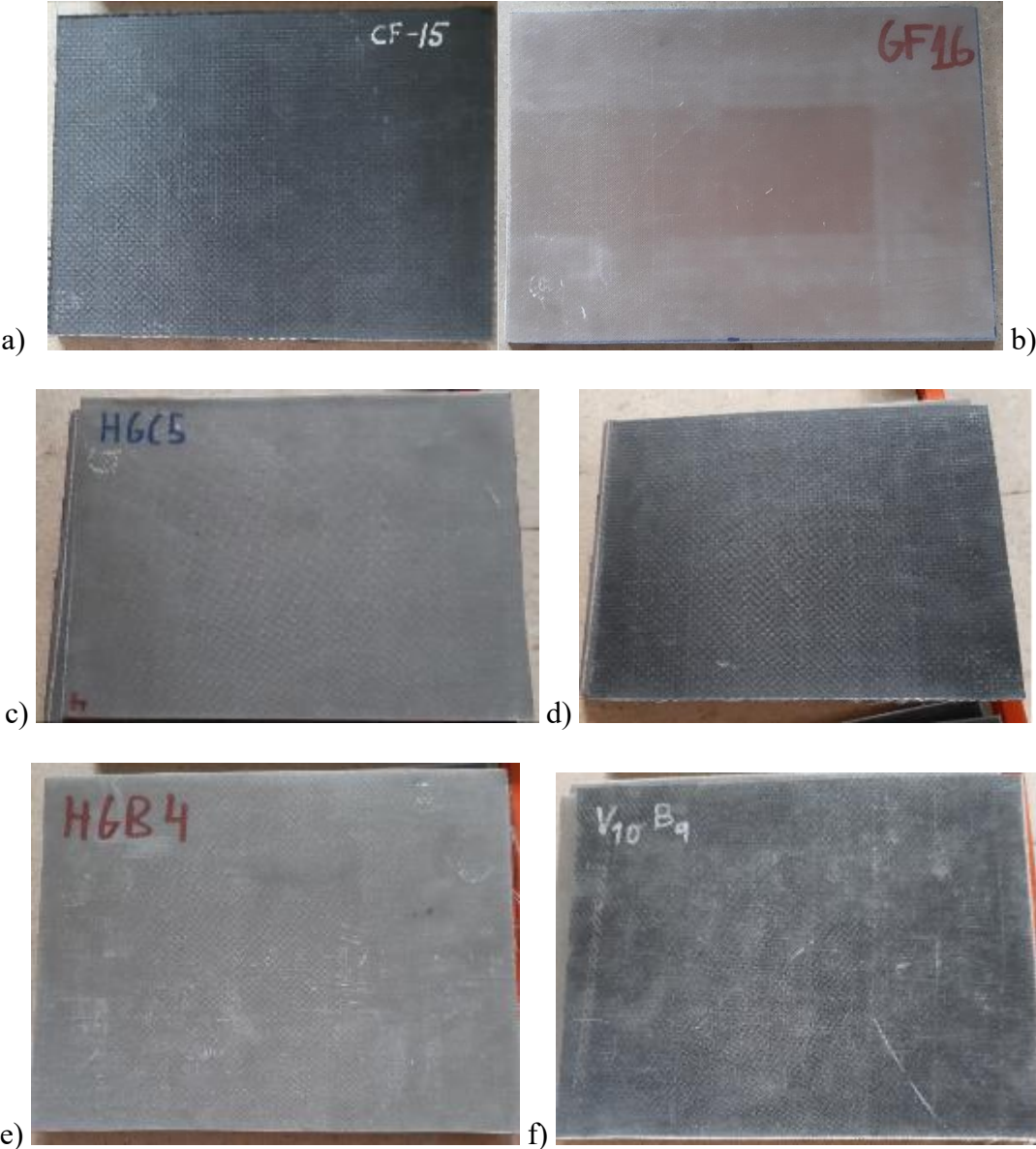


Figure 3.12: cut specimens photos: a)carbon,b) glass; c)d)carbon-glass; e)f)basalt-glass.

The objective of this study is to test the behaviour of the materials used in ships subjected to water blast explosion. It is considered that these materials will face various conditions that can cause the degradation. One of the most critical is the exposition to sea-water, thus it is immediate to think about the possibility to study the behaviour when materials are non-conditioned (dry specimens) and when they have been exposed to the saturation level caused by the sea-water. Then, in order to obtain the saturated samples, it is needed to prepare the salt-water, put the specimens and test it just when they reached the saturation level. The procedure adopted is schematized as follow.

First of all, it is important to establish when the samples reach the saturation, in order to understand it, the weight difference is considered and it was established that the saturation level is reached when the difference in weight, between two weighing of the same sample immersed in the salt water is less of 1%. Then, it is important to weigh the sample before to put it in the salt-water, weigh it after a considered time and then after a couple of days, in order to evaluate water uptake. When the saturation level is reached the samples are ready to be tested.

The bath of salt-water is prepared in laboratory in a very easy way: it is mixed 96.5% of water with 3.5% of salt. It is used a becher of 2.5L filled with water and it is added 80g of salt, then, in order to facilitate the dissolution of the salt in the water and to obtain an homogeneous solution, it is used a magnetic stirrer (*figure 3.13*).

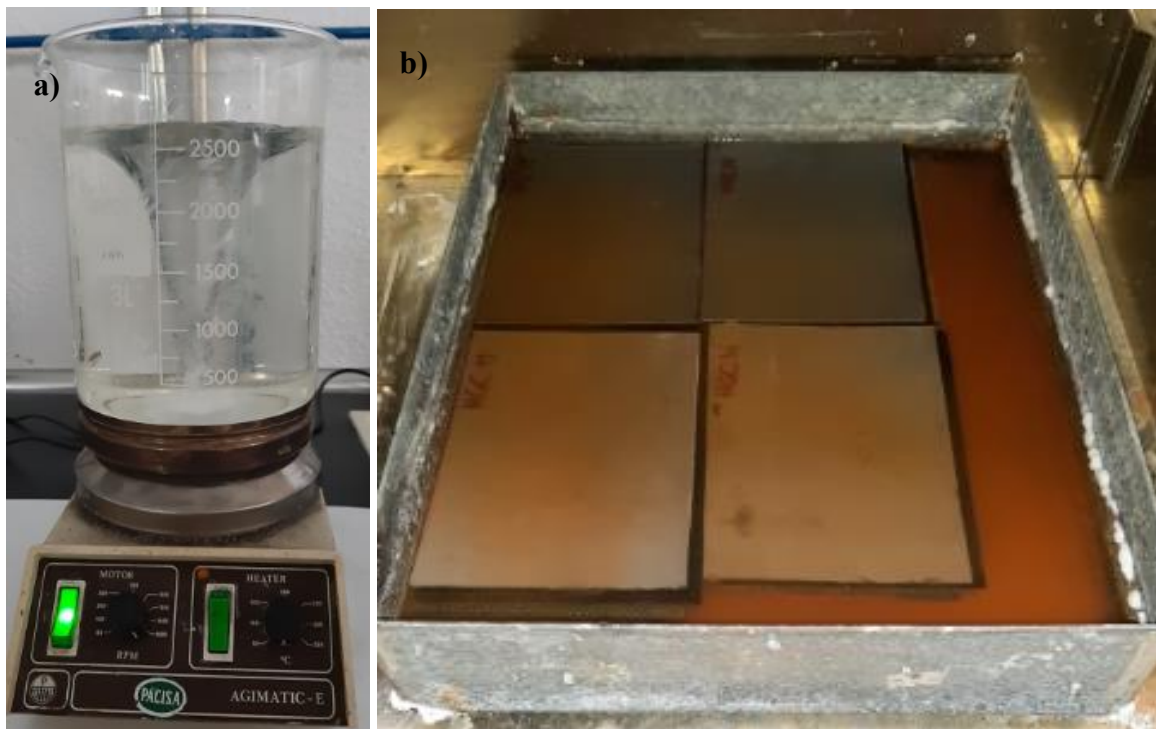


Figure 3.13: a) magnetic stirring of the salt-water solution; b) samples immersed in the bath.

The samples are weighed and the weight is annotated, then they are put in the bath that is then filled with the salt-water prepared until the complete immersion of the samples (*figure 3.13-b*). After about twenty days the weight is again measured and annotated. The procedure of weighing is repeated after seven days until the saturation level that is as said:

$$\Delta_w = \frac{w_2 - w_1}{w_1} \cdot 100$$

$\Delta_w =$ weight difference percentage

w_1 and $w_2 =$ weight at two different days

In the table 3.2-3.6 there are the weight and the day of the measure until the saturation level.

As we can see in the table, the specimens have not the same weight, meaning that the saturated mass will not be the same, as seen. The reason of these differences is that the cutting was not so accurate, it means that specimens are not all 175x225 mm², but there are some variations of the order of mm.

<i>Glass fiber specimen</i>	<i>W₀ [g]</i> <i>30/4/19</i>	<i>W_f [g]</i> <i>20/5/19</i>	<i>W_f [g]</i> <i>28/5/19</i>	<i>W_f [g]</i> <i>30/5/19</i>	<i>Δ_w [%]</i>
<i>GF11</i>	232	239	239	239	0
<i>GF12</i>	230	236	236	236	0
<i>GF13</i>	232	238	238	238	0
<i>GF14</i>	231	236	236	236	0

Table 3.2: weight and percentage difference measures of glass fiber samples.

<i>Carbon fiber specimen</i>	<i>W₀ [g]</i> <i>28/5/19</i>	<i>W_f [g]</i> <i>12/6/19</i>	<i>W_f [g]</i> <i>17/6/19</i>	<i>Δ_w [%]</i>
<i>CF10</i>	179	184	183	0.54
<i>CF11</i>	178	183	183	0
<i>CF12</i>	179	184	183	0.54

Table 3.3: weight and percentage difference measures of carbon fiber samples.

<i>Basalt-glass specimen</i>	<i>W₀ [g]</i> <i>31/5/19</i>	<i>W_f [g]</i> <i>12/6/19</i>	<i>W_f [g]</i> <i>17/6/19</i>	<i>Δ_w [%]</i>
<i>HGB1</i>	236	241	241	0
<i>HGB2</i>	251	257	257	0
<i>HGB5</i>	225	230	230	0
<i>HGB6</i>	238	243	243	0

Table 3.4: weight and percentage difference measures of basalt-glass fiber samples.

<i>Carbon-glass specimen</i>	<i>W₀ [g] 28/5/19</i>	<i>W_f [g] 12/6/19</i>	<i>W_f [g] 17/6/19</i>	<i>Δ_w [%]</i>
<i>HGC1</i>	214	219	219	0
<i>HGC2</i>	211	215	215	0
<i>HGC3</i>	211	216	216	0
<i>HGC4</i>	214	218	218	0

Table 3.5: weight and percentage difference measures of carbon-glass fiber samples.

<i>Carbon-Glass specimen</i>	<i>W₀ [g] 12/6/19</i>	<i>W_f [g] 27/6/19</i>	<i>W_f [g] 2/7/19</i>	<i>Δ_w [%]</i>
<i>HGC10</i>	211	215	215	0
<i>HGC11</i>	212	216	217	0.46
<i>HGC14</i>	211	214	215	0.47
<i>HGC15</i>	205	209	210	0.48

Table 3.6: weight and percentage difference measures of carbon-glass fiber samples.

Saturated specimen can be tested, like others, but first is necessary to envelope them in a plastic film, because it is important to not lose water, in fact, for this reason, the extraction and envelopment (*figure 3.14*) of each specimen must be immediately before of the test.



Figure 3.14: sample enveloped in the plastic film after the saturation in salt-water.

3.5 Experimental device

The device used to test the behaviour of the composite materials to water blast explosion was designed considering the Bertram-Hopkinson bar, which allows to test the strain-stress dynamic response of the tested materials. The Bertram-Hopkinson bar is composed of an incident bar, a transmitted bar, a projectile and the material to test. The material is located between the two straight bars. The incident bar produces the wave, called incident wave, which propagates towards the sample and then it is divided in two smaller waves called reflected wave and transmitted wave. The transmitted wave causes the plastic deformation of the sample, while, the reflected one only returns from the sample toward the incident bar.

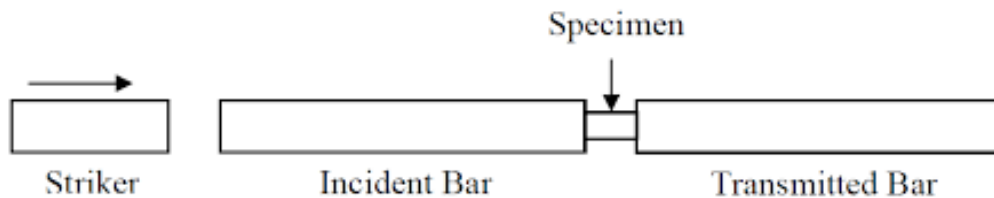


Figure 3.15: Bertram-Hopkinson bar schematization [12].

The device designed and located in the laboratory of the materials science department of the *Politecnica de Madrid*, is a little bit different (photos and schematizations of the experimental device in the figure 3.16-3.17). In particular, the experimental device is based on the combination of the incident bar of the Hopkinson bar with an aluminium box filled with water and equipped with the sample. The modification results in the abolition of the transmitted bar, while the incident bar is fixed to the aluminium box through a piston (the piston is also the frontal wall of the aluminium chamber). The water inside the box is incompressible and has the function of the propagation of the impact in order to convert this impact in the impact wave. In fact, the walls of the aluminium chamber are rigid with the sample mounted at the bottom of the box. In the cylindric Hopkinson bar there is the projectile that is shot launched by the gun at a certain pressure and it hits against the actuator. The actuator (2.193 kg) generates the wave in the chamber and this impact wave is finally generated through the water toward the specimen. In fact, the idea is that the full power of the projectile is transmitted to the centre of the front side of the chamber (through the incident bar and piston), then this

power is absorbed by the water in the chamber that converts it in impact wave, that finally hits the sample on the back side of the chamber, just like the mine that generates the impact wave in the sea that hits the ships.



Figure 3.16: experimental device.

A schematization of the complete device, composed of the experimental and instrumental system, is represented in the next figure.

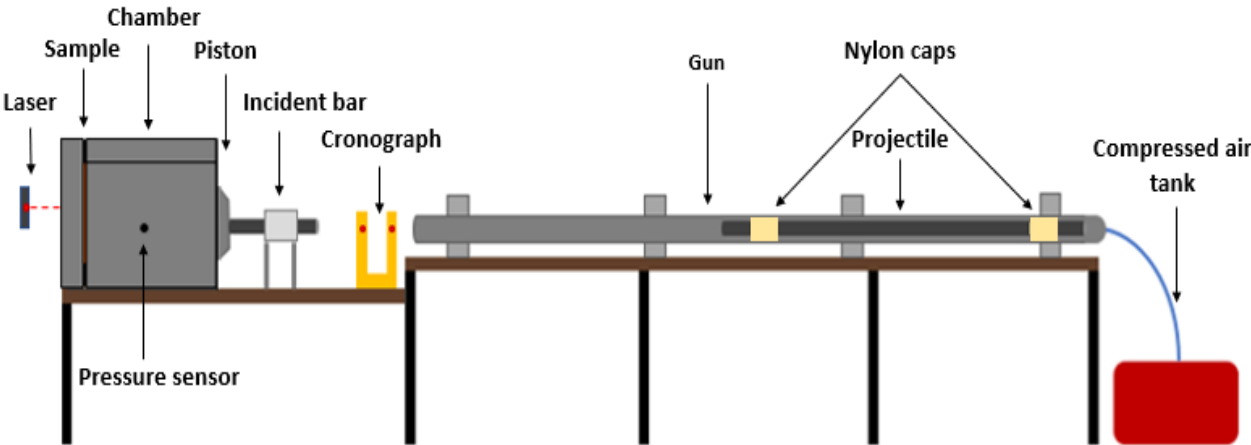


Figure 3.17: schematic drawing of the experimental device.

Regarding the characteristics of each part:

- The Hopkinson bar, actually, consists of two continuous bars and they represent the “gun” from which the projectile is shot. In fact, in this long tube of 360 cm of length and 3 cm of diameter there is the projectile. The bar is also provided of a valve that is opened to produce the shot obtained allowing the passage of the compressed air that fuel the projectile.
- The projectile is an aluminium cylinder with length of 120 cm and diameter of 2.54 cm. It is provided of two nylon caps that have the function of holding the projectile aligned in the bar and to ensure the transmission of the pressure.
- The compressed air tank is the power source that allows the shot of the projectile. It is provided of a pressure gauge, of a valve and of a knob that allow to fill the tank of air and to establish the pressure of the shot.
- Incident bar (actuator) and piston: the projectile hits the incident bar that is screwed to the piston, which represents one of the walls of the aluminium chamber.



Figure 3.18: some elements of the experimental device a)bar with valve;b)piston and incident bar; c)air pressure tank.

- The aluminium box is a fundamental part of the experimental device, in fact it is where the plane wave is generated caused by the impact. The chamber is provided of three fixed walls (lower and laterals), the front wall is the piston, the back wall is an aluminium framework where the specimen is located, and the top wall is an aluminium plate that is screwed to the chamber. The lower wall has a sealed hole, provided with a tube and a valve that allows the water evacuation after each test. The top of the box is provided with a nozzle, plugged during the test, which is used to add water to the chamber. The dimensions of the box without the framework are 25x26x26 with a capacity of 7350 cm³.
- The aluminium framework on the back of the chamber is like a rectangular window where the sample is located. Framework and sample will be the back wall of the chamber. It is very important that the sample is well sealed between the framework and the back part of the chamber, and that the chamber itself is well sealed. To assure sealing, the framework screwed to the chamber every time.
- A rubber gasket avoids the direct contact between specimen and the aluminium chamber.

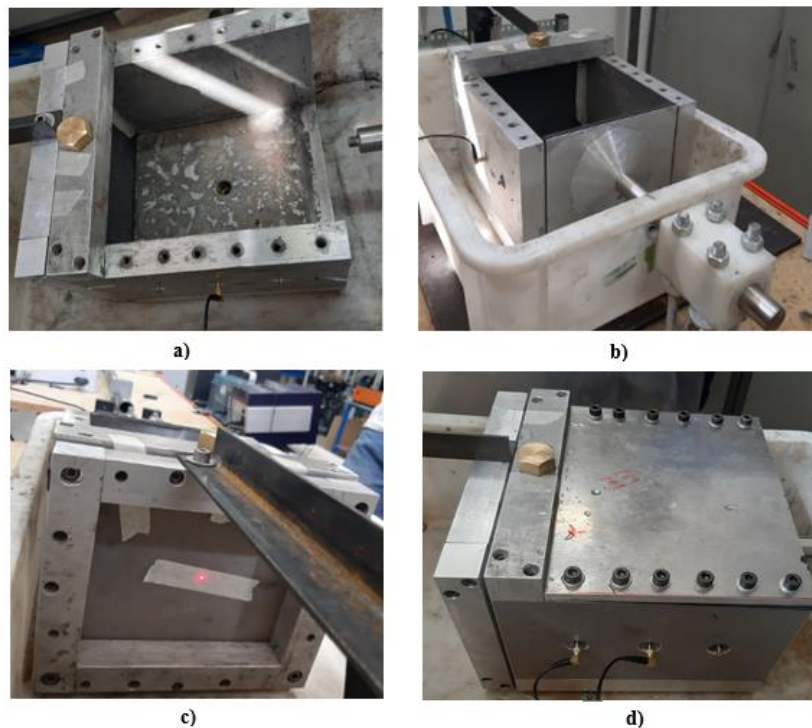


Figure 3.19: aluminium box a) fixed walls and hole of water evacuation; b) piston mounted; c) aluminium framework and specimen; d) top plate.



Figure 3.20: *instrumental system a) laser; b) pressure sensor; c) chronograph; d) digital counter; e) oscilloscope; f) sensor signal conditioner.*

The experimental equipment used for testing is then equipped of various devices like sensors and laser that allow to obtain the various measures and data useful to the study and to develop a model. The devices used in the project are:

- Pressure sensor: it is located at the middle of one of the lateral walls of the chamber. It allows the measure of the pressure during the shot. The sensor used is the PCB (Piezoelectric 102 B 0.001 Hz).
- Laser: it is located on the back side of the chamber. It allows the measure of the sample's deflection during the time. The laser used is the M70LL, it presents a frequency's measure of 100 kHz in the range distance of 0.5-200 mm.
- Chronograph: it consists of two infrared sensors. It is used to measure the speed of the projectile. In fact, when the projectile passes through the first

sensors it is registered as time 0, then when it crosses the second sensor it is registered the second time. In this way, knowing the time of passage of the projectile, and knowing the distance between the two sensors (15 mm), it is easily calculated the speed of the projectile. Moreover, the chronograph has the function of a trigger, it means then when the projectile crosses the sensor, it starts the measurement.

Moreover, the experimental setup is equipped with a signal conditioner (ICP 482C05 series), which provides the electric adjustment and amplify the signals of the laser and of the pressure sensor; a digital counter (PHWE) that measures and show the time of the projectile to cross through the chronograph; a digital oscilloscope (DPO2024), which registers the response of the measures and displays the results on the monitor. The oscilloscope is provided of 4 channels, meaning that four different sensors can be connected and thus four measure can be done. In this work just three channels are used, which are the chronograph, the pressure sensor and the laser. (Actually, in the beginning four channels were in use, the fourth being connected to an accelerometer located on the piston. Its measure allows the development of a numerical model, but it often got damaged by the impact. It has then been removed to avoid its damage and because the measures for the model development were enough.

3.6 Calibration of the experimental device

In order to rely on the results obtained calibration of the instruments is fundamental. This is the reason why several previous tests on aluminium samples were conducted. It was important to calibrate the instrumentation system, to find the way to conduct the testing without errors and with a good repeatability, then it is important that the bar transits impacts and converts this impact in plane wave and especially it is needed to verify that the measures, and the registered signals, are correct. In order to verify these challenges, located in the middle of the sample was used in some preliminary test. The comparison of the two measures provided indications about the reliability of the measure itself, In fact, it was proved that the pressure trend registered was the same and that the values, especially the peaks, of the pressure were

very similar. Finally, it was concluded that the location of the pressure sensor on the box is appropriate for the study.

The laser was calibrated too to ensure precise measurement of the displacement of the sample. To this purpose, the deformation trend obtained testing aluminium plate was compared with that obtained testing a composite material and it was verified that they have the same trend described in the next chapter.

Finally, many tests on the aluminium plate were conducted in order to define the most appropriate subsequence of the steps to conduct the experiments.

It was also decided the shooting pressure, which was in the range 3-5 bar because in this pressure range aluminium specimens were enough deflected. The shooting pressure was then calibrated on the composite samples.

3.7 Experimental tests

Summarizing, the tests were conducted with the experimental device consists of the combination of Hopkinson bar-chamber, as previously designed. The results of displacement, pressure and projectile speed, were registered thanks to the instrumental system and subsequently analysed and compared. Half of the sample were put in the artificial sea-water bath until the saturation level was reached, but the testing procedure was always the same for all sample types, the only difference is that it is needed to envelop the saturated sample with a plastic film, and to remove them from the bath just on the day of the test, and obviously just when they have reached the saturated level.

Each test is conducted following the next steps:

1. All the sensors to be used during the test are located in the right positions and connected to the oscilloscope, to the signal conditioner and to the digital counter (in the case of the infrared sensors). It is also verified that devices like oscilloscope, counter and conditioner are in the right measure settings.
2. Placement of the specimen and of all the moving wall of the chamber. Therefore, the rubber cover is located on the specimen (keeping attention, in the case of hybrids, to the right side on which it is wanted to conduct the test) is placed in a way that does not

obscure the holes, in order to allow the sealing with the framework through the screws. Then is placed the piston and the incident bar is screwed on it, it is important to ensure that this wall, because removable, is perfectly orthogonal. Finally, the top plate is screwed. Obviously, between the chamber and the piston there is a tiny space that is important to close, in order to ensure a perfect sealing of the box, and thus to avoid water leaks especially during the shot, and above all to try to reach a higher pressure in the chamber. To close these narrow gaps, it is manually applied a layer of polymeric insulating material, as it can be appreciated in the figure. Practically, this is the only point where this application is needed, but it was noted that after several tests, the chamber was practically deformed, and then it was needed this manually application also on the sides of the top.



Figure 3.21: Chamber with piston, incident bar, framework and plastiline placed.

3. Pushing of the projectile until the end of the bar using a long thin metallic bar. It is important to not forget this step because otherwise the projectile would not be affected by the pressure generated by the shot.
4. Close the water discharge valve.
5. Filling of the chamber: the box is filled with about 7L of water through the opening on the top of the box. During the filling is important to pay attention to avoid losses of

water from any part of the box, especially from the narrow gaps previously manually sealed; if necessary, the leaks must be eliminated by applying other more plasticine. When the box is filled, the hole is closed with the screw.

6. Sensors verification: it is verified that laser works correctly through a voltmeter. It is also controlled the correct working of the infrared sensors, it is simply done resetting the screen of the digital counter, crossing the chronograph with one hand, if the system registers the time, it works correctly, then the screen is again resetting and considered ready for the measure. It is also verified that the oscilloscope shows all the curves relative to the sensors connected and thus that the trigger is started the measurement.
7. Preparing of the air pressure tank: the valves of the tank are opened allowing to pressurize the tank to the desired pressure, that can be controlled thanks to the manometer. The pressure used for each test is of about 5 bar.
8. Blast: the valve on the top of the Hopkinson bar is opened to shot at the pressure set. The shot is immediate, as it takes a few milliseconds, therefore it is important to open this valve just when everything is ready for the test. Right after the shot this valve and the valves of the tank are closed.
9. Opening of the valve that allows the evacuation of the water from the chamber.
10. The specimen is removed from the framework in order to verify the damages. Some other parts are disassembled, so that the device is ready to run another test.

Data measured are saved to allow the later analysis.

Chapter 4

Results

In this chapter, the results of the tests are shown, it is also shown how the data are analysed, how the results are obtained and the comparison between the critical parameters for this application. The measures of the sensors are saved in a “.csv” format file. The data are recorded in a range of 45 ms, meaning that each measure consists of 125000 values. This number is so high that is not possible to work on it through excel, but it is needed another software, thus it is used QtiPlot. This program allows to analyse data and to get the scientific graphing, it is also very intuitive and easy to use.

4.1 Data analysis

Data saved are imported in QtiPlot, and a table like that showed in the next figure is obtained.

	TIME[X]	CH1[Y]	CH2[Y]	CH3[Y]	CH4[Y]	
1	-0.00152	4.56	0.6	0.008	0.08	
2	-0.00151968	4.56	0.6	0.008	0.12	
3	-0.00151936	4.56	0.64	0.008	0.08	
4	-0.00151904	4.56	0.64	0.008	0.08	
5	-0.00151872	4.56	0.6	0.008	0.08	
6	-0.0015184	4.56	0.6	0.008	0.08	
7	-0.00151808	4.48	0.6	0.008	0.08	
8	-0.00151776	4.56	0.6	0.008	0.12	

Figure 4.1: imported data on QtiPlot of glass fiber example.

As it is possible to see, there are five columns, one is referred to the time (that is the same abscissa for all other data), then CH1-2-3-4 are the measures of the four channels used, these are respectively the projectile speed, the displacements value obtained with the laser, the

pressure and the last is not used. It is important to remember that the signal response is always in Volt. Then first all the signals are converted in the respective unit of measure with a simple mathematical operation on each column which is multiply the measurement in Volts by a conversion factor which depends on the experimental set-up.

Regarding the displacement, in order to obtain the value in mm, the conversion factor is 5.11mm/V, then it is possible to add a column that will be equal to the column of the displacement in Volts multiplied by the factor.

Regarding the pressure, to obtain the values in MPa the conversion factor is 0.1452 mV/MPa , then a new column is added that will be equal to the pressure column in Volt divided by that factor.

Another operation is to arrange the displacement, in order that it starts from 0, then a new column is added and it will be equal to the displacement's column in mm minus the first value.

After the conversion, the curves of pressure and displacement are obtained. The curves of all samples shows the same behaviour, as shown in the next figure.

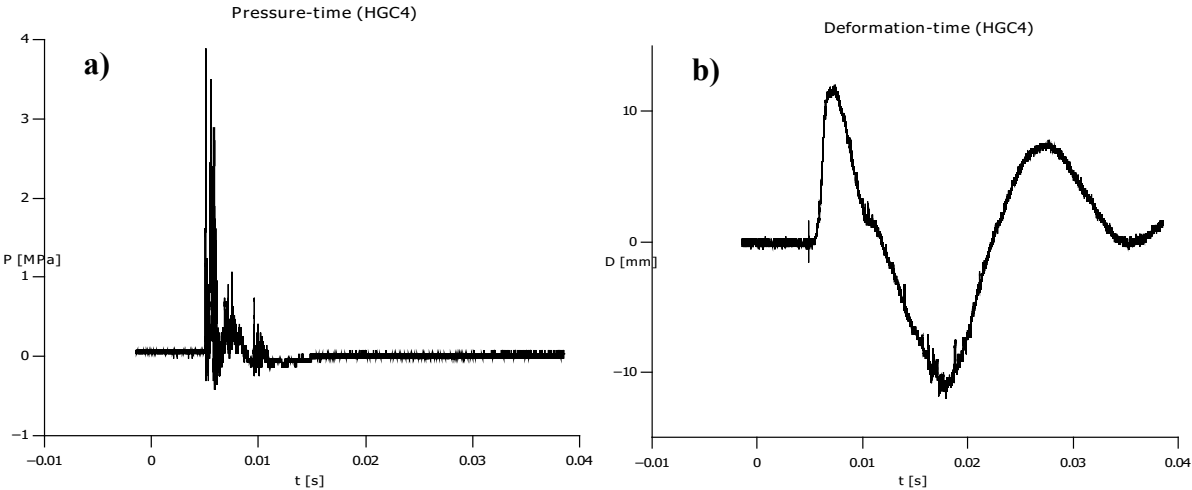


Figure 4.2: *esample of a)pressure trend and b)displacement trend.*

As can be seen, the pressure reach a peak followed by oscillations with smaller values. The trend is, effectively, coincident to forecasts, in fact, it is due to the collision of the projectile against the incident bar and the piston of the box, then the impact is converted in planar wave inside the box filled of water, and obviously it decreases its relevance. In fact, it is important only the first peak, because it has the bigger value that can cause the higher displacement and a possible damage on the sample.

Regarding the displacement, when the planar wave hits the sample, it bends because of the impact, after reaching the maximum displacement the panel rebounds and applies a force against the water, in fact one can observe that the displacement returns with lower slope until the zero point and there is always a step due to the higher effort that specimen has to do in order to apply its compressive force against water, in fact, then the deformation becomes negative, meaning the negative bending of the sample. There is also a similar behaviour due to the force applied to the water and the reaction done by the sample. For the analyses made in this work, it is considered only the positive bending of the first displacement peak, that is only the first part of the curve until the maximum value, and the maximum deformation value itself. In fact, the first part of the curve represents the maximum deformation caused by the impact, that can cause the biggest damage to the sample. Also because, in fact, water is not in a box, then it does not act another force on the sample.

Moreover, knowing the time registered by the chronograph (showed on the digital counter), when projectile crosses it, and knowing the distance crossed (15 cm) it is possible to obtain the speed with which the projectile hits the box.

4.2 Experimental results

In the next paragraphs are shown the experimental results obtained for each composite type and for each condition imposed (saturated, dry, hybrids, not-hybrids). The results discussed are the maximum pressure reached during the shot, the maximum deflection of the specimen, the speed of the projectile, the shot pressure and a new variable that is going to be introduced that is the impulse per unit area. This last mentioned is just the integral of the pressure along the time, because deflections of the samples depends more on this parameter than on peak pressure. However, it is important to consider the initial impulse per area, meaning that only the initial pressure peak is integrated. It is because the planar wave generated in the box hits the specimen, but as consequence it is generated a reflected wave and because of the enclosed chamber there will be several reflections. Only the initial impulse causes the deflection of the sample and not the reflections.

Regarding the parameters obtained and showed in the next paragraphs: the pressure of the shot is the pressure of the air in the reservoir; the speed with which the projectile impacts is calculated considering the time showed on the digital counter and the distance crossed of 15

cm ($v=s/t$); pressure peak and deformation peak can be seen on the curves, but because of the high number of points is better to consider a function of QtiPlot that is the “statistics on column” that shows all statistic related values of a select column, like the maximum; finally the impulse per area is obtained by the numerical integral of the peak pressure-time, obtained applying the parallelogram law in this range, the value obtained is a scalar which represent the impulse of the initial incident wave. It means that it is needed to calculate the speed of the wave propagation, that is:

$$v = \sqrt{\frac{E}{\rho}} \tag{1}$$

E and ρ are the elasticity modulus and density of the water, respectively. Because of the unidimensional deformation, it can be considered the water compressibility modulus K ($K=2.2GPa$), while water density is equal to $1000kg/m^3$. Then the propagation wave speed is $v=1483 m/s$. Considering that the internal length of the chamber is $L=210mm$, the time that wave needs to reach the pressure sensor position can be calculated as follows:

$$t = \frac{L}{v} \tag{2}$$

From (2), the time will be 0.141s and represents the time the wave will take to reach the pressure sensor. In order to better understand the mentioned statements, magnifications of the pressure plot of a sample are shown.

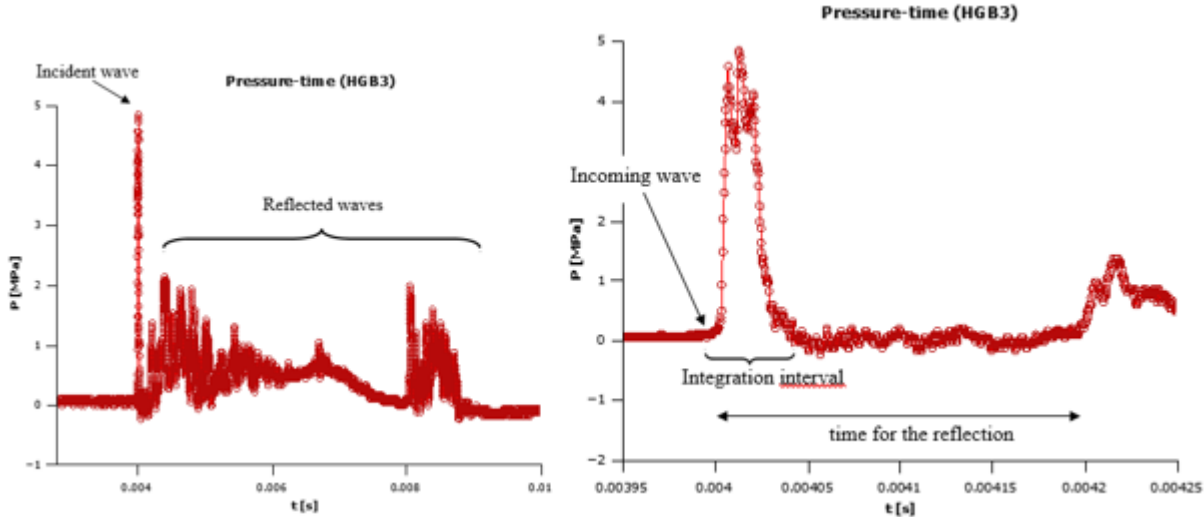


Figure 4.3: Pressure plot magnifications.

For each sample type are also shown the graphs of maximum deformation versus maximum pressure and versus impulse per area and finally some photos of the specimens after tests where one can see the damages provoked by the blast.

4.2.1 Carbon fiber composites

Table 4.1 shows the results from carbon fiber type samples in dry condition..

<i>Specimen</i>	<i>P_{shot} [bar]</i>	<i>v_{projectile} [m/s]</i>	<i>P_{max} [MPa]</i>	<i>D_{max} [mm]</i>	<i>I/A [Mpa·s·10⁻⁵]</i>	<i>Damaged</i>
CF14	2	4.6	2.09	9.10	6.55	No
CF14-2	3.6	13.5	4.35	14.71	12.85	Yes
CF14-3	4	13.7	3.09	15.74	8.03	Yes
CF15	4.6	13.9	3.53	15.94	8.51	Yes
CF16	6	12.3	4.79	21.67	9.51	Yes
CF17	6	12.9	6.67	17.78	8.09	Yes

Table 4.1: results obtained of the carbon fiber dry specimens.

Half the specimens were saturated with salt water. Two of these specimens were then wrapped with plastic film and tested. the two remaining panels were subjected to a heat-cycle that is not part of this study. The results obtained are shown in the next table.

<i>Specimen</i>	<i>P_{shot} [bar]</i>	<i>v_{projectile} [m/s]</i>	<i>P_{max} [MPa]</i>	<i>D_{max} [mm]</i>	<i>I/A [Mpa·s·10⁻⁵]</i>	<i>Damaged</i>
CF10	4.6	14.5	3.97	18.40	14.82	Yes
CF12	4.5	13	5.79	16.15	8.20	Yes

Table 4.2: results obtained of the carbon fiber saturated specimens.

In the next graphs are shown the maximum deformations reached versus the maximum pressure detected in the chamber and versus the impulse per unit area calculated.

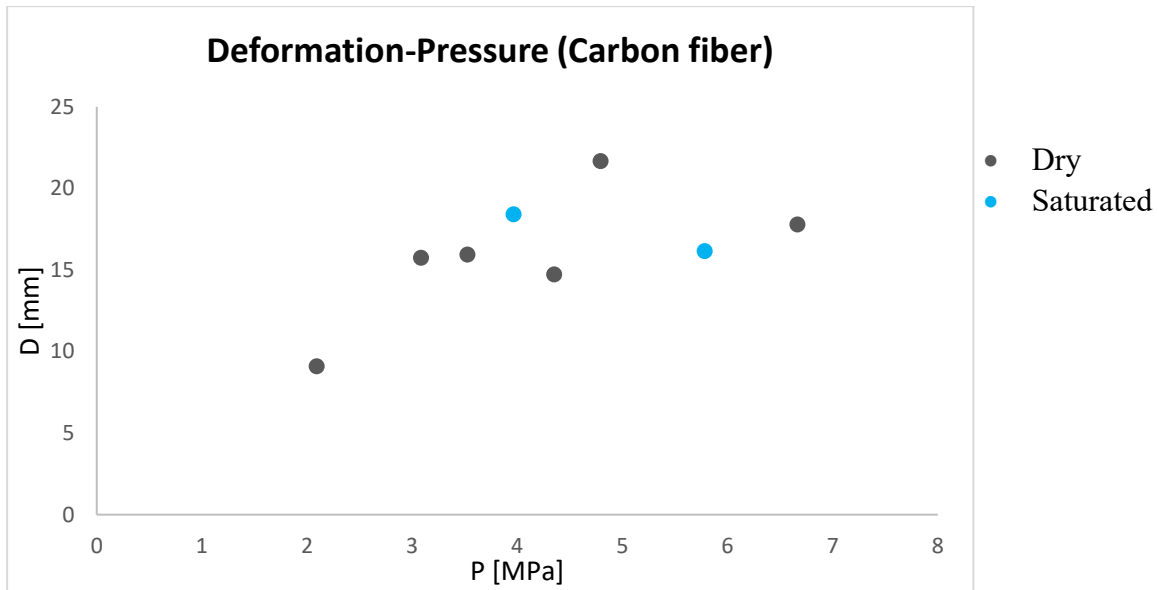


Figure 4.4: deformation-pressure graph of carbon fiber composites samples.

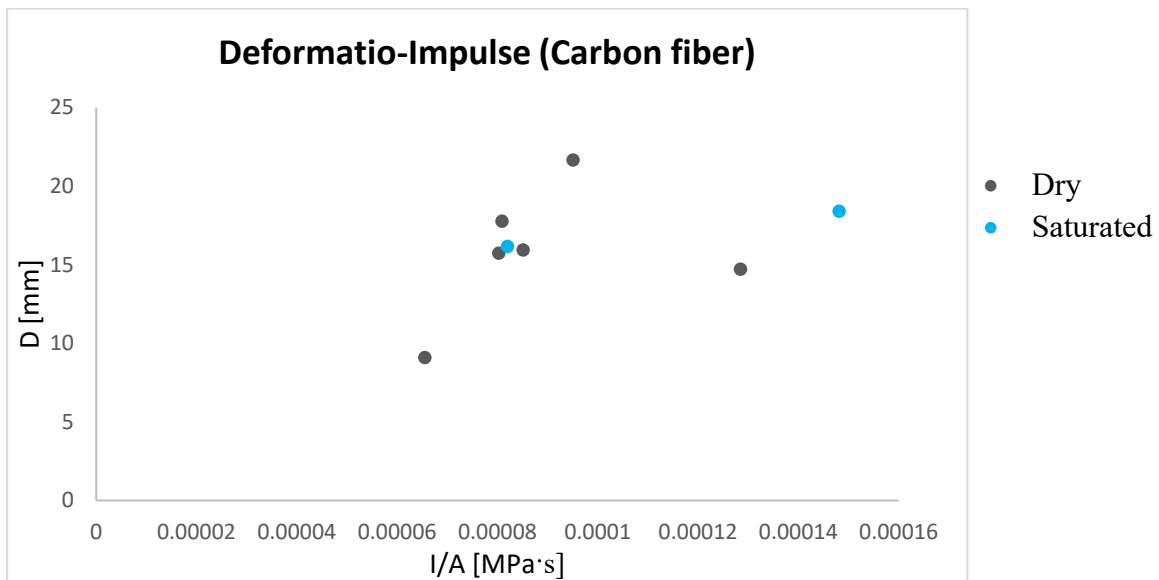


Figure 4.5: deformation-impulse graph of carbon fiber composites samples.

It is possible to note that the shot pressure is not the same and it is because carbon samples and glass samples were used to find the most appropriate pressure to study and compare the behaviour of all the samples. It is important to choose a pressure that is similar, in order to compare different specimens and materials. It is the reason why the CF14 sample was tested several times, firstly with a pressure of the shot of 2 bar, but on the sample there is not any sign of damage, then the pressure was raised to 3.6 and 4 bar, and the sample was damaged. A shot pressure of 6 bar was considered useless, because there were not any changes, there was

the same fracture in the same point, the only difference was obviously in the higher displacement reached by the sample.

In fact, as seen in the last graph, the samples CF16 and CF17 showed the higher values of displacement.

Regarding the saturated samples, it is difficult to state if they behave different than the dry ones, it is not notable any difference in the behaviour, but it can be due to the low number of saturated samples tested.

The fact that these specimens break during the test can also affect the signal, this can be the reason why CF16 shows a deformation peak so high compared with others.

Finally, as regards the damage, it is always located on the bottom of the sample. The failure is “upside-down T” shaped, in fact there is a more pronounced vertical line and another line perpendicular to it (Figure 4.6). some samples after test are shown in the next photos, where it is also possible to see the fracture patterns.

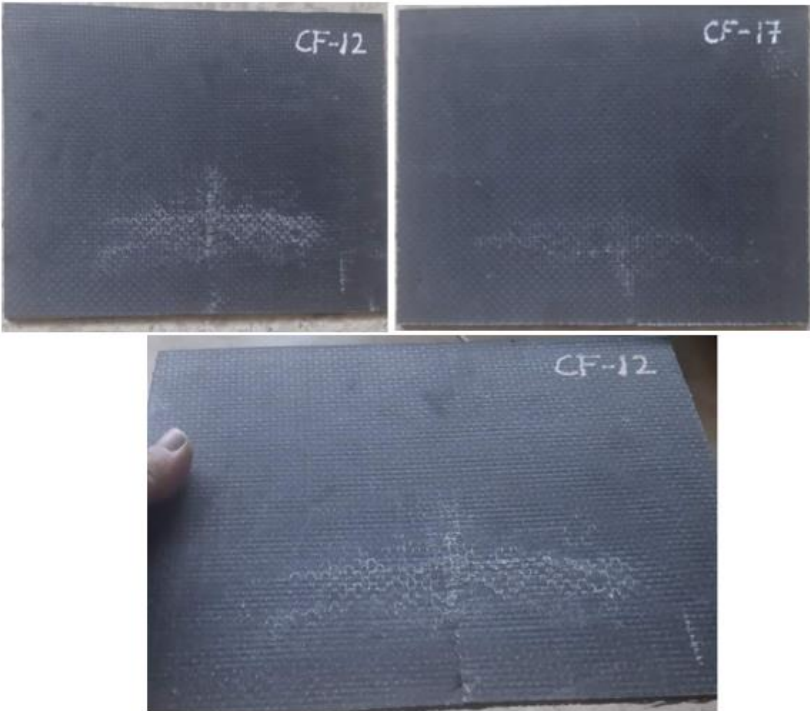


Figure 4.6: Carbon fiber samples photos after test and showing of the T shape fracture.

4.2.2 Glass fiber composites

As in the previous paragraph, *Table 4.3 and 4.4* show the results of the dry and saturated samples tested, respectively.

<i>Specimen</i>	<i>P_{shot} [bar]</i>	<i>v_{projectile} [m/s]</i>	<i>P_{max} [MPa]</i>	<i>D_{max} [mm]</i>	<i>I/A [MPa·s·10⁻⁵]</i>	<i>Damaged</i>
<i>GF15</i>	1.4	6.2	1.40	5.52	5.60	No
<i>GF15-2</i>	6	16.3	<u>2.11</u>	<u>14.10</u>	<u>14.02</u>	No
<i>GF16</i>	4.6	12.1	4.07	14.31	2.63	No
<i>GF17</i>	5	15.4	/	14.31	/	No
<i>GF18</i>	4.5	13.3	6.17	14.72	8.27	No

Table 4.3: results obtained of the glass fiber dry specimens.

The value of the GF15 tested for the second time are highlighted because the signal saturated, while there is not a maximum value for the GF17 sample, because the sensor pressure just dropped off during the shot, then there is not this measure.

Just like the case of carbon fiber, half of the specimen was saturated with salt-water, and two specimens were tested, while two samples were subjected to the heat cycle.

<i>Specimen</i>	<i>P_{shot} [bar]</i>	<i>v_{projectile} [m/s]</i>	<i>P_{max} [MPa]</i>	<i>D_{max} [mm]</i>	<i>I/A [MPa·s·10⁻⁵]</i>	<i>Damaged</i>
<i>GF13</i>	4.5	9.6	5.95	13.90	9.12	No
<i>GF14</i>	4.5	15.9	4.57	16.56	5.91	No

Table 4.4: results obtained of the glass fiber saturated specimens.

Considering the maximum values of pressure and deformation is possible to obtain a graph that shows the evolution of the deformation vs pressure reached in the chamber.

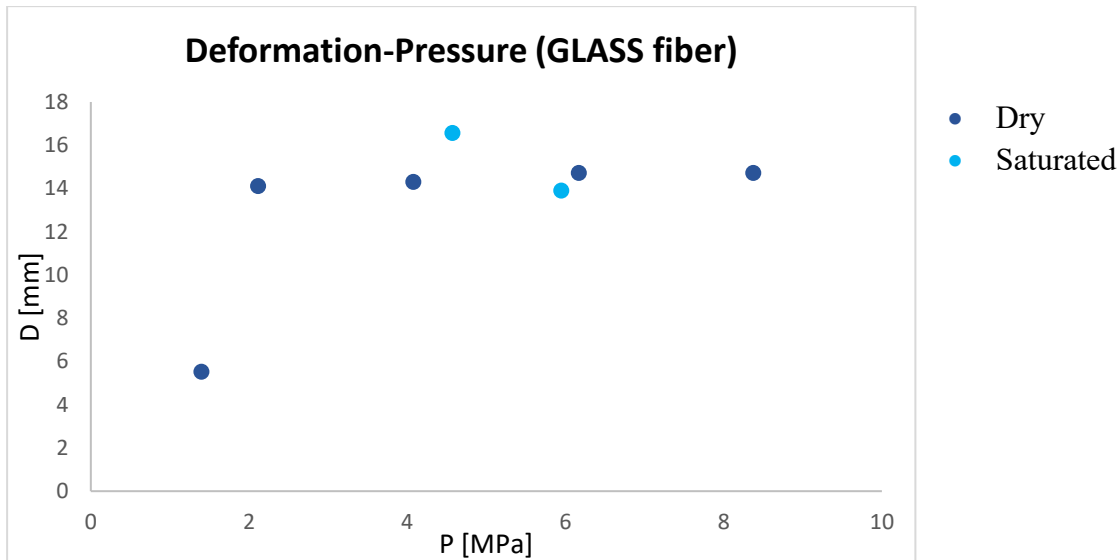


Figure 4.7: deformation-pressure graph of glass fiber composites samples.

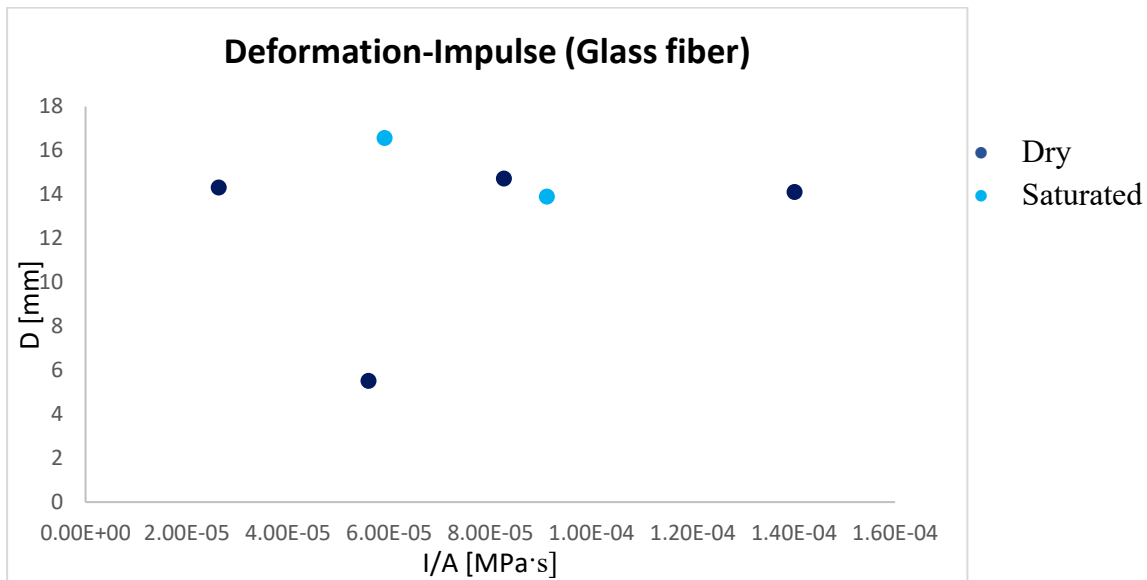


Figure 4.8: deformation-impulse graph of glass fiber composites samples.

As in the case of carbon fiber, some glass fiber samples were used to establish the appropriate pressure of the shot. In fact, the GF15 sample, was shot with a pressure of 1.4 bar, but since there were not any signs on the sample, then it was retested shooting at 6 bar, but also at this pressure the glass fiber sample did not show any sign of failure or of damage, considering also that carbon fibers did not show any differences between a pressure of 5 and 6 bar, it was decided to use always a pressure of about 5 bar for all the rest of tests and sample types. Anyway, bigger pressure or bigger impulse per area led to bigger deformation, as seen in the tables and in the graph. Glass fiber composites dry samples show a maximum

deformation of about 14 mm with pressures reached in the chamber in the range of 4-6 MPa, the value of 2MPa can not be considered because of the saturation of the measurement; saturated sample have a maximum value of the deformation peak of about 14 and 16, with a pressure of about 5 and 6 Mpa. It seems, again, that saturated samples do not show significant deformation. Anyway, samples were not broken and do not show damage. Some glass fiber samples after test are shown in *Figure 4.9*.



Figure 4.9: glass fiber composites samples after test.

4.2.3 Hybrid Basalt-Glass fiber composites

Basalt-glass composites are hybrid samples, this means that in the composite there are two fiber types, in this case basalt and glass fibers. The disposition of the fibers occurs in two phases, it means that during the manufacturing process were overlapped first all the layers of one tissue type and then the second type. The process led to a composite having one fiber type on a side and the other type on the other side, in fact, this is evident considering the different colour of the two sides of the composites, because glass is clear, while basalt is dark. Because of this disposition of the fibers in the composite, the panels were tested half in a side and half in the other side, in order to assess a possible different the behaviour when the panel receive the impact on the side of the basalt or on the side of the glass.

Results of these samples in the case of dry and saturated condition are shown in *Table 4.5 and 4.6*, where it is also shown the different side of the test with a letter in parentheses (B if the impact is received on the side where there is the basalt and G if the side addressed to the impact is glass).

<i>Specimen</i>	<i>P_{shot} [bar]</i>	<i>v_{projectile} [m/s]</i>	<i>P_{max} [MPa]</i>	<i>D_{max} [mm]</i>	<i>I/A [MPa·s²·10⁻⁵]</i>	<i>Damaged</i>
<i>HGB3 (B)</i>	4.5	14.52	4.85	13.08	8.91	No
<i>HGB4 (B)</i>	5	15.68	7.88	19.42	22.38	Yes
<i>HGB7 (G)</i>	5	16.36	5.40	16.97	9.96	Yes
<i>HGB8 (G)</i>	4.8	15.96	7.05	15.33	9.04	Yes

Table 4.5: results obtained for carbon-glass fiber dry specimens.

<i>Specimen</i>	<i>P_{shot} [bar]</i>	<i>v_{projectile} [m/s]</i>	<i>P_{max} [MPa]</i>	<i>D_{max} [mm]</i>	<i>I/A [MPa·s²·10⁻⁵]</i>	<i>Damaged</i>
<i>HGB1 (B)</i>	5	15.76	4.74	17.78	9.06	Yes
<i>HGB2 (G)</i>	5	16.07	6.34	15.53	8.91	Yes
<i>HGB5 (G)</i>	5	15.96	6.45	17.37	10.51	Yes
<i>HGB6-2(B)</i>	4.9	14.49	6.34	16.56	8.87	Yes

Table 4.6: results obtained for carbon-glass fiber saturated specimens.

In this last table, the HGB6 sample has the number two, because it was tested two times and the results shown are referred to the second test. During the first test the nylon cap took off from the projectile and was shot before of it crossing the trigger, meaning that it was not registered any measure, because in the 42 seconds immediately after the starting of the trigger, the projectile did not yet hit the chamber.

Deformation peaks versus pressure peak and versus impulse per area are shown in *Figure 4.10 and 4.11*.

In this case again it seems that saturated samples do not exhibit larger deformation than dry ones, as it is noticeable from the graph, while the number of specimens is too low to assess any effect of the impact side, actually.

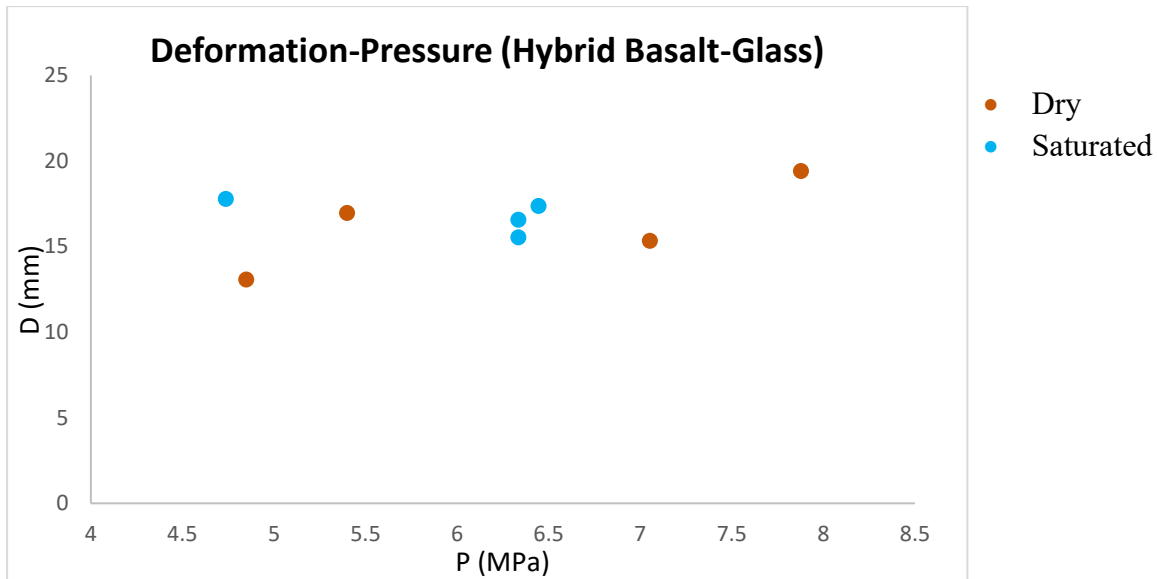


Figure 4.10: deformation-pressure graph of hybrid basalt-glass samples.

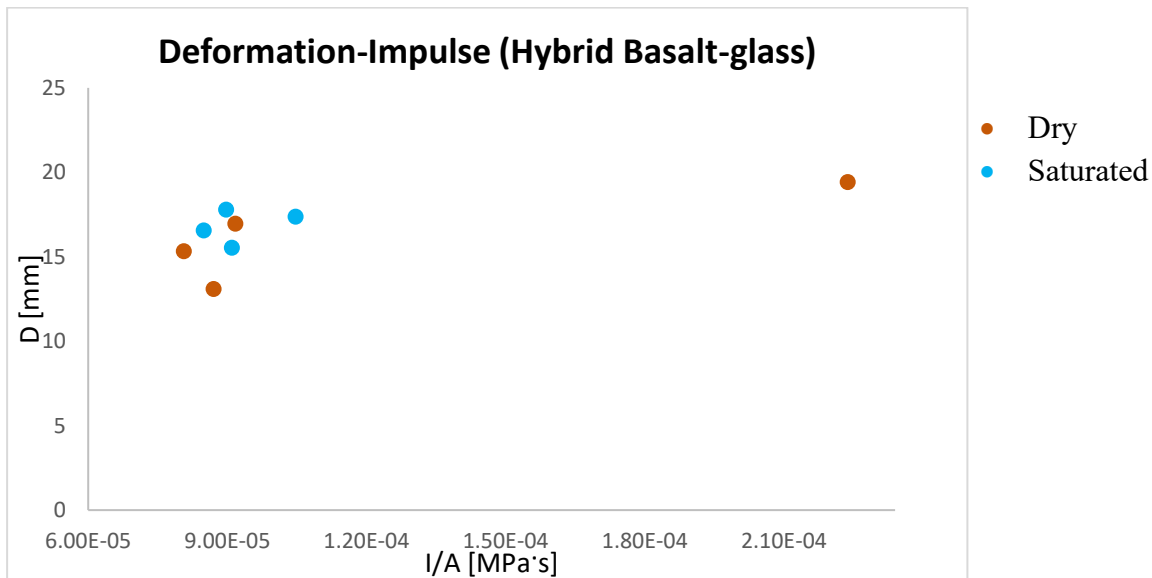


Figure 4.11: deformation-impulse graph of hybrid basalt-glass samples.

Anyway, hybrids basalt-glass samples show a maximum deformation in the range of about 15-17 mm in the maximum pressure range reached in the chamber. The only difference is the HGB4 sample, which reaching a maximum pressure of 8 MPa, shows a deformation of about 20 mm.

Regarding the damage suffered by the panels after tests, there are not any signs of fracture, but there is delamination that can be seen by naked eye as shown in the figures. The delamination is more appreciable when the test is conducted on the glass side, but it does not

mean anything, it is just because of the transparence of glass, in fact, even when the basalt side is hit it is possible to see delamination, even if it is not so evident as in the other case.

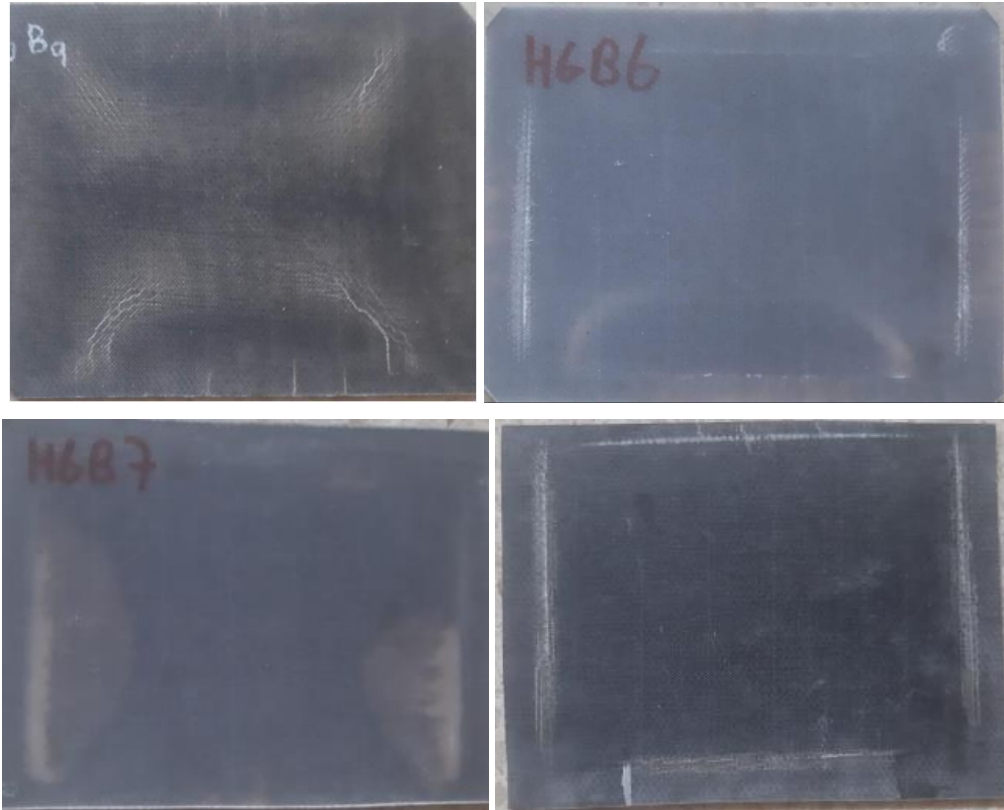


Figure 4.12: photos of hybrid basalt-glass panels after tests.

4.2.4 Hibrid Carbon-Glass fiber composites

Carbon-glass composite is the other hybrid composite type tested. As the basalt-glass, it has a random disposition of the fiber, then in one side of the panel there is the glass and on the other side the carbon. Also in this case, the different colour of the panel allow to see the difference, because glass is clear while carbon is black. In order to assess the effect of un-symmetry, half panels are impacted on the side of carbon and half on the side of glass. In this case the number of panels is double, then the difference can be more appreciable.

The results of hybrid carbon-glass tested in dry and saturated condition are shown in *Table 4.7 and 4.8*, respectively.

<i>Specimen</i>	<i>P_{shot}</i> [bar]	<i>v_{projectile}</i> [m/s]	<i>P_{max}</i> [MPa]	<i>D_{max}</i> [mm]	<i>I/A</i> [MPa·s·10 ⁻⁵]	<i>Damaged</i>
HGC5(G)	4.9	14.31	2.51	12.26	11.38	Yes
HGC6(C)	5	14.59	4.10	12.06	14.22	Yes
HGC7(G)	5.1	14.82	4.10	8.38	6.61	No
HGC8(C)	5.1	15.29	4.38	10.42	8.10	No
HGC9(G)	4.9	12.70	4.41	13.08	8.31	Yes
HGC12(G)	4.9	15.18	4.08	15.13	8.81	Yes
HGC13(C)	5	15.18	6.45	17.78	8.48	Yes
HGC16(C)	4.9	13.93	4.68	14.92	8.82	Yes

Table 4.7: results obtained for hybrid dry carbon-glass fiber specimens.

<i>Specimen</i>	<i>P_{shot}</i> [bar]	<i>v_{projectile}</i> [m/s]	<i>P_{max}</i> [MPa]	<i>D_{max}</i> [mm]	<i>I/A</i> [MPa·s10 ⁻⁵]	<i>Damaged</i>
HGC1 (G)	5	15.18	4.27	13.08	14.52	No
HGC2 (C)	5	16.06	8.37	17.78	9.35	No
HGC3 (G)	5	16.16	7.71	15.13	9.27	No
HGC4 (C)	5	11.31	3.88	12.06	9.34	No
HGC10-2(G)	5	15.46	4.99	14.51	9.81	Yes
HGC11 (G)	5	15.73	6.14	14.92	16.35	Yes
HGC14-2(G)	5	15.92	5.40	13.29	9.16	Yes
HGC15 (C)	4.9	<u>2.79</u>	6.04	15.74	14.07	No

Table 4.8: results obtained for hybrid saturated carbon-glass fiber specimens.

HGC10 and HGC14 samples are tested two times, because again the nylon caps jumped ahead of the projectile and started the trigger, then during these tests no measure was registered, then the results reported refer to the second tests performed on each sample. In the case of HGC15 it is notable that the speed of the projectile is lower than usual, it was for the same reason that is the nylon cap took off from the projectile and the trigger started, but in this case, the measures were registered.

The graphs of the results obtained are shown in the next figures.

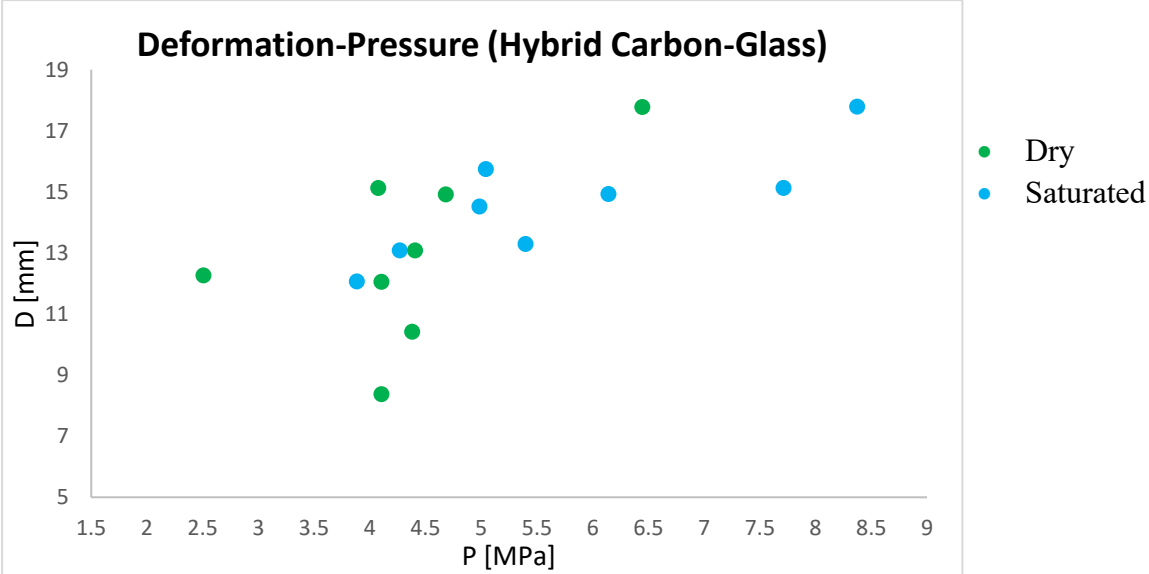


Figure 4.13: deformation-pressure graph of hybrid carbon-glass samples.

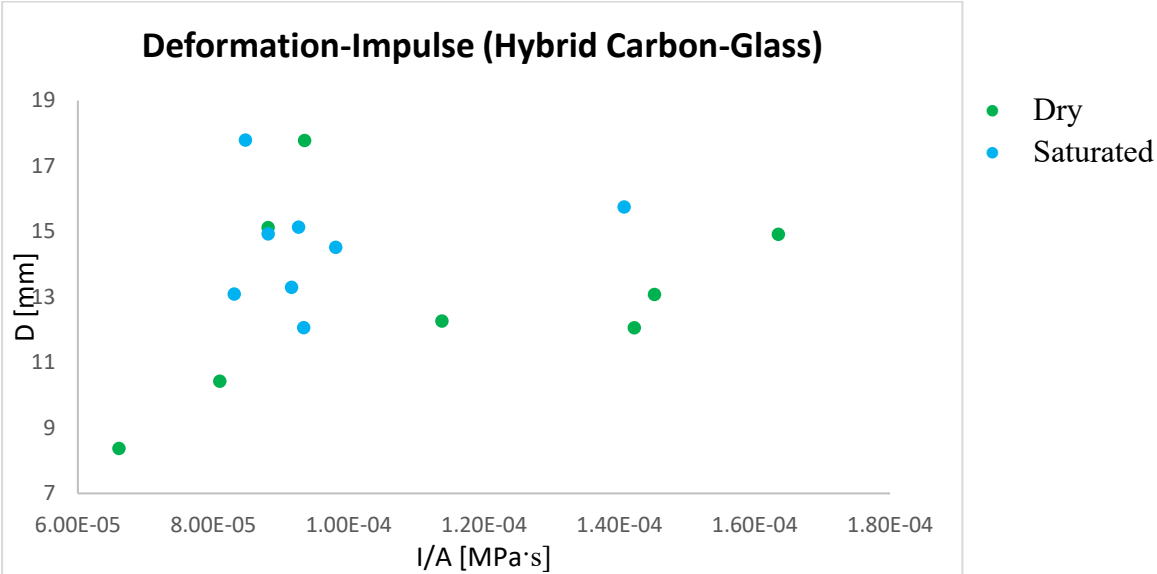


Figure 4.14: deformation-impulse graph of hybrid carbon-glass samples.

As previously mentioned, there is no significant effect of saturation. In order to understand a possible difference between the side tested it is highlighted with different colour as in the next graph.

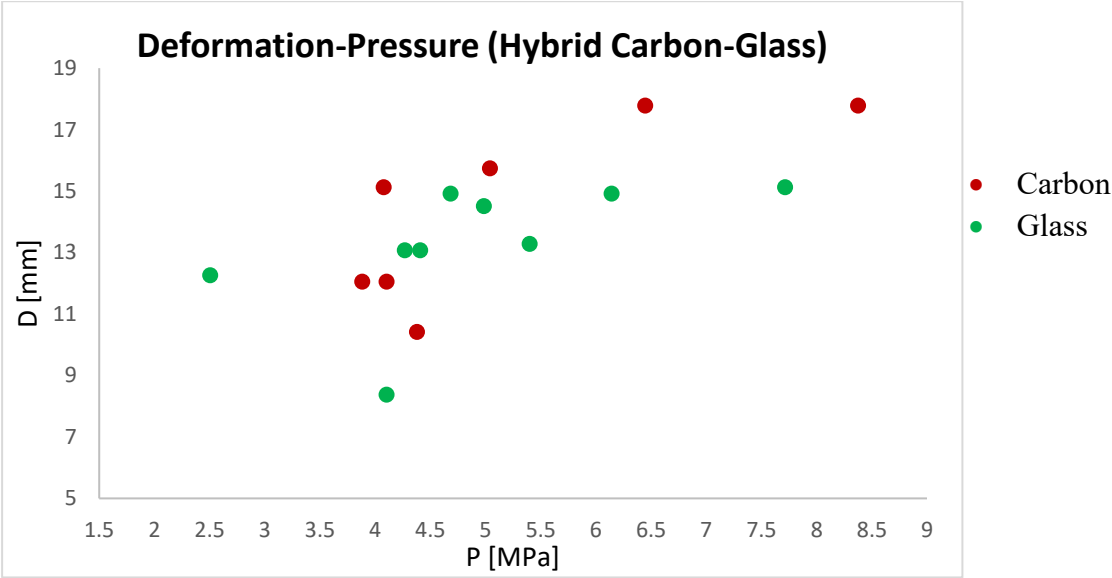


Figure 4.15: Deformation-pressure graph of hybrids carbon-glass showing the different side tested.

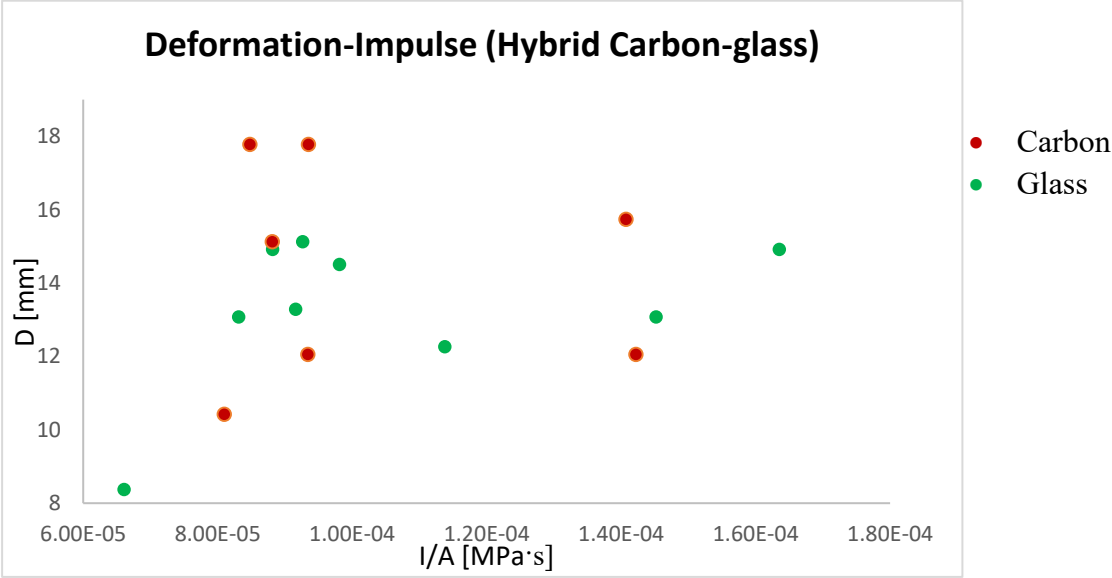


Figure 4.16: Deformation-impulse graph of hybrids carbon-glass showing the different side tested.

It is difficult to appreciate a real difference between the two different tested sides, because half samples are saturated, two are tested for the second time, and the range of pressure is

quite wide. Generally, it seems that there are no appreciable differences in the behaviour considering the tested sides, but to be sure, more tests would be necessary.

Concerning the panels after tests, they do not break but they show signs of delamination that has a pattern as shown in the following photos, the delamination is more appreciable when the test is conducted from the glass side, but it is just because glass is clear and carbon is dark, just like in the case of basalt-glass samples.

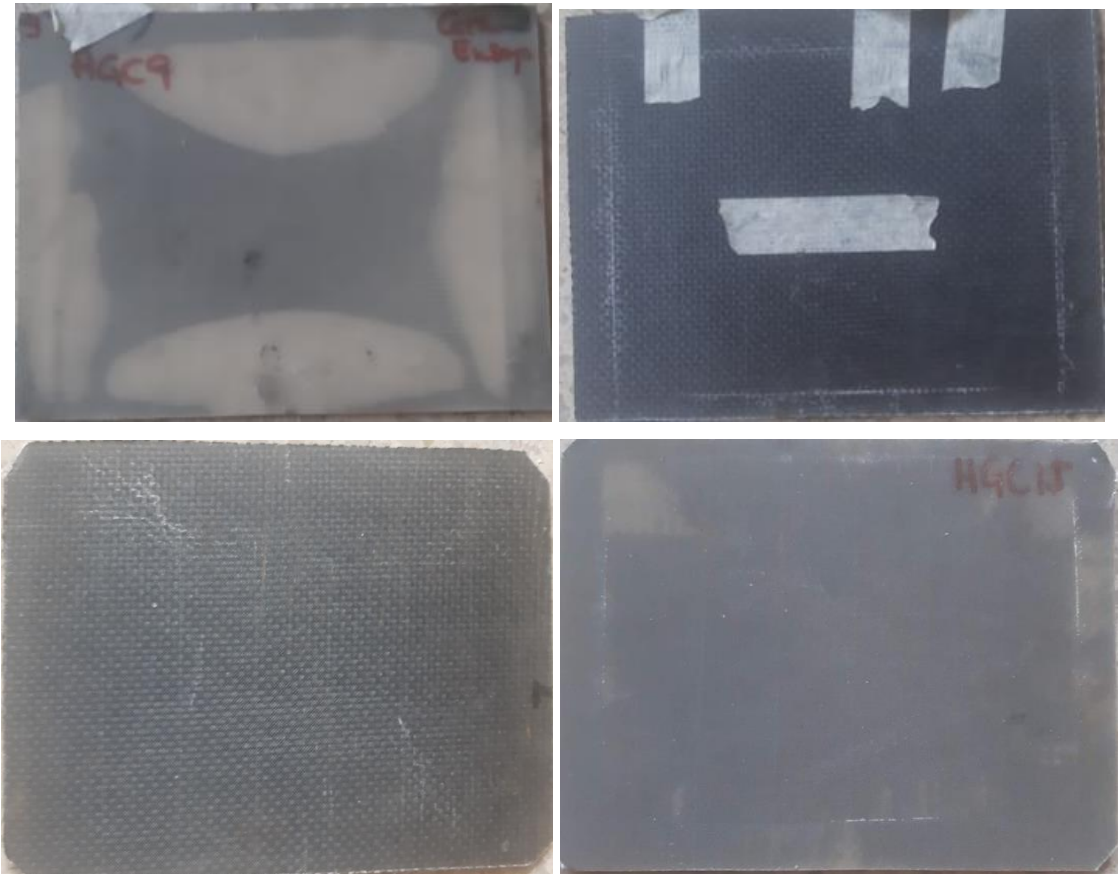


Figure 4.17: Hybrids carbon-glass composites after tests.

4.3 Results comparison

For the sake of comparing the results, the following plots gather the results of dry specimens made of different composites (*Figure 4.18 and 4.19*). *Figure 4.19 and 4.20* gather the results obtained with saturated specimens.

Although all results are quite similar, if focus is on the pressure with higher density of results, that is to say, between 4 and 6 MPa of peak pressure, it is found lower peak displacement values for carbon-glass hybrid specimens. Conversely, carbon fiber specimens exhibit the

largest values of peak displacements. Similar results can be extracted from deformation versus impulse plot. If it is considered that carbon fiber specimens registered significant levels of damage, it can be deduced that this configuration (carbon fiber composite with vinylester matrix) is the one that provides the poorest performance.

Generally, hybrid composites perform quite well in terms of displacement peak. However, it must be reminded that both configuration (glass-basalt and carbon-glass) exhibited delamination failure after the test which may compromise the residual strength of the panels after being subjected to blast load. Maybe a more homogeneous distribution of the hybrid fibers inside the matrix would avoid this delamination failure. In this sense, further experiments should be carried out to confirm this fact.

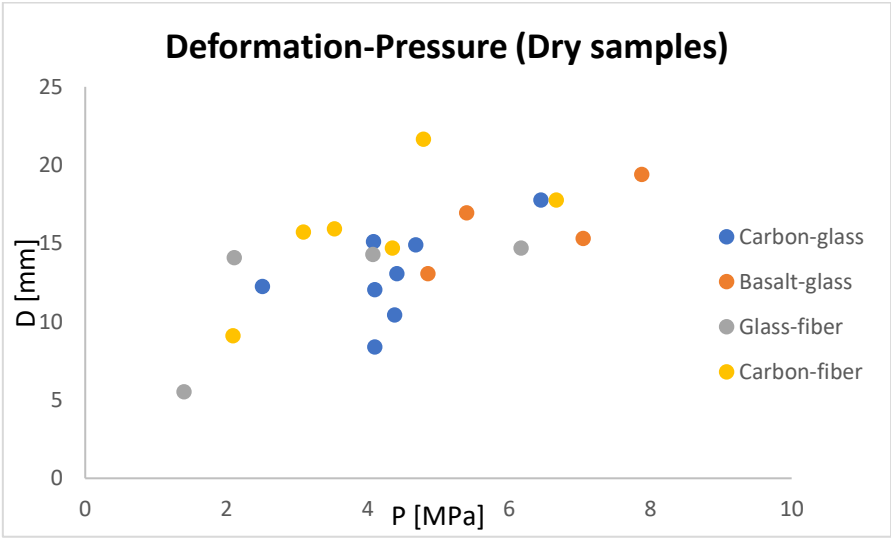


Figure 4.18: Deformation-Pressure comparison of dry samples.

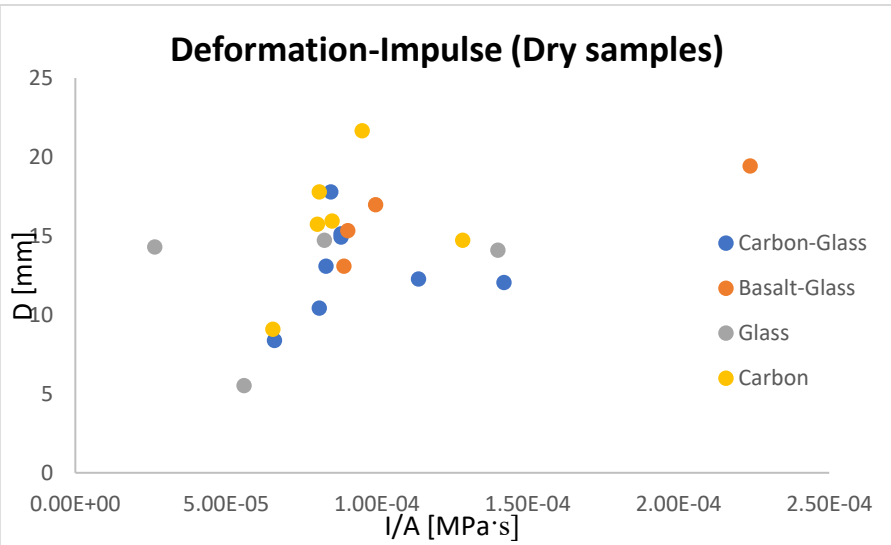


Figure 4.19: Deformation-Impulse comparison of dry samples.

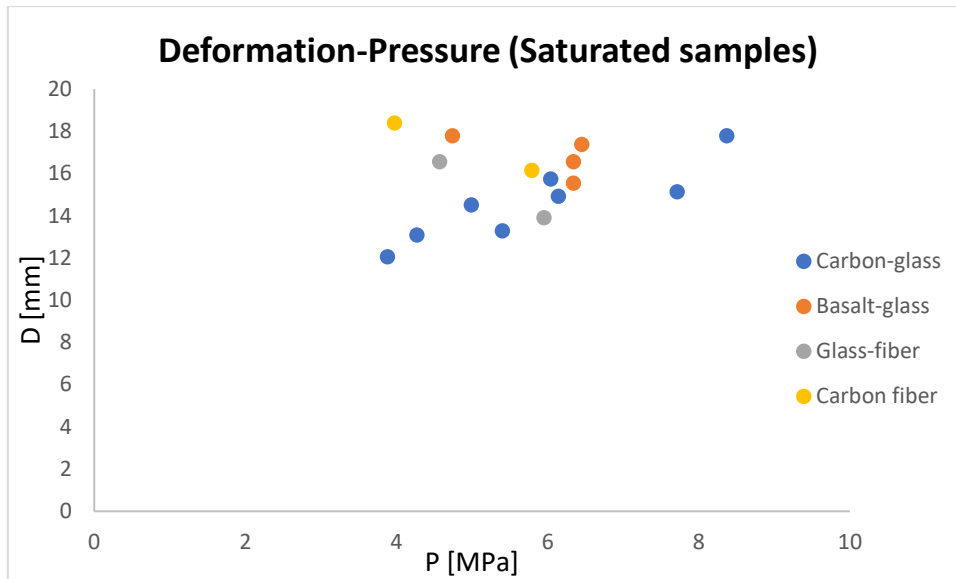


Figure 4.20: Deformation-Pressure comparison of saturated samples.

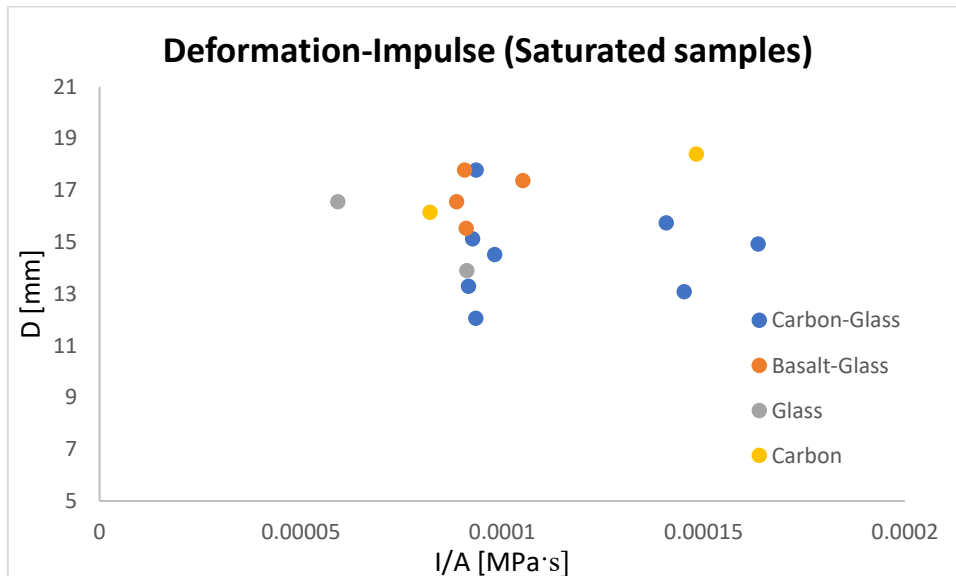


Figure 4.21: Deformation-Impulse comparison of saturated samples.

In summary the best behaviour corresponds to the glass fiber reinforced composites. It must be noted, however, that these results are difficult to be extrapolated to other fiber contents: different amounts of fibers and thickness could lead to different results. Obviously, further experimental data are required to extract more conclusive results.

Regarding the saturated samples, similar comments can be made by looking at *Figure 4.20 and 4.21*. This result supports the idea that sea water saturation do not affect the performance of these composites.

Chapter 5

Analytical model

In this chapter the analytical model based on the mathematical equations written by the professor Vicente Sánchez [38] is discussed. Starting from that, it was developed a calculation program that considers some boundary conditions, obtained by first developing a model for a circular panel and then extending it to a rectangular one. The model takes into account the material properties, the geometry and the type of impact. The solution that the model aims to obtain is the behaviour of composite materials facing with water blast explosion, just like in the experimental part, but in this case the study is theoretical. The objective of the analytical model is to obtain results comparable with the experimental results.

Finally, the objective of this part is to present the results with the model prediction.

5.1 Analytical model of blast effect on composite panels [38]

In order to obtain the analytical model that will be used to develop a program, two cases will be considered: circular or rectangular and large panel.

5.1.1 Circular panel

In the first case it is considered a panel assumed orthotropic and clamped on the edges, under a planar wave.

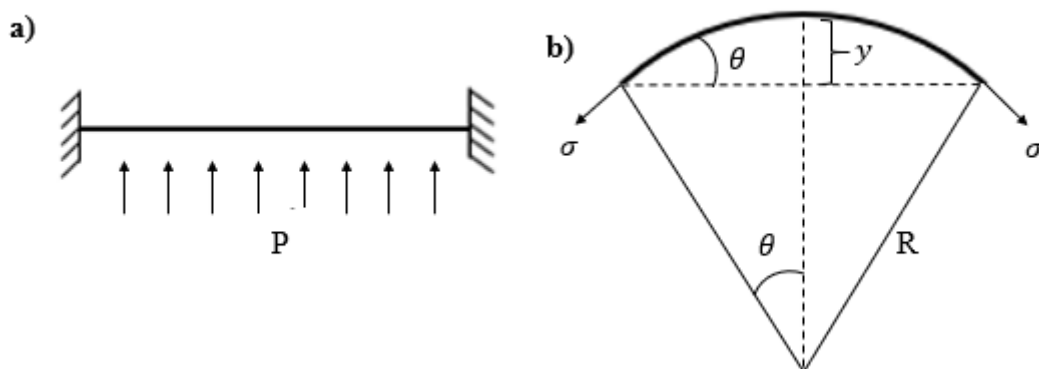


Figure 5.1: circular panel clamped subjected to a pressure P and panel deformed after a time t .

Applying the force for long enough time t , the shape of the deformed specimen can be considered spherical with a radius R and a deflection sustained is called y . It is then possible to write the following equation:

- Applied force:

$$F_p = P\pi \frac{\phi^2}{4} \quad (1)$$

(where ϕ is the diameter of the panel).

- Resistant force:

$$F_r = \sigma t R \sin \theta \quad (2)$$

(where t is the thickness of the panel and σ is given by the young modulus multiplied for the deformation: $\sigma = E \frac{R2\theta - \phi}{\phi}$).

- Deflection:

$$y = R(1 - \cos\theta) \quad (3)$$

Then the relation between R and θ is: $\frac{\phi}{2} = R \sin\theta$

Applying the Newton's law: $F = ma = m \frac{dv}{dt} = \frac{d}{dt}(mv)$, then:

$$(F_p - F_r)dt = (m + m_{H_2O})dv + dm_{H_2O}V \quad (4)$$

Where m is the mass of the specimen ($m = \pi \frac{\phi^2}{4} t\rho$; ρ is the density of the panel) and the mass of the water varies with time and deformation and then with volume ($m_{H_2O} = \frac{\pi y^2}{3} (3R - y)\rho_{H_2O}$).

In the equations there are some constants (ϕ , t , ρ , E , ρ_{H_2O} , m) and some quantities depending on time (θ , R , σ , y and velocity of the specimen v), while P can be constant or variable.

To solve the problem, firstly, it is considered:

$$\sigma = 0; \theta = 0; v = 0; y = 0$$

To account for $R=\infty$ when time is 0, it is written R as: $R = \frac{y}{1 - \cos\theta} = \frac{\phi}{2 \sin\theta}$ and then:

$$m_{H_2O} = \rho_{H_2O} \frac{\pi y^3}{3} \left(\frac{3}{1-\cos\theta} - 1 \right) = \frac{\pi y^3}{3} \cdot \frac{2+\cos\theta}{1-\cos\theta} \rho_{H_2O} \quad (5)$$

$$\sigma = \frac{E(2R\theta - \phi)}{\phi} = E \left(\frac{\theta}{\sin\theta} - 1 \right) \quad (6)$$

The mass of water is initially set equal to zero, the pressure varies with time and Δt indicates the time variation. The increment Δt and the pressure P are external variables, then deformation, angle and mass of water increases with time. The new quantities are introduced in the equation 4 to obtain Δv and $\Delta y = v \Delta t$. A new time step starts. The quantities given will be σ and y . The computation ends when σ reaches the critical value of the material or when v is zero (safe condition), in this last case the solution will be the last value y obtained.

5.1.2 Computation example

In this paragraph it is shown a simple example on a composite material with the following parameters:

$P=10$ MPa (constant)

$\phi=150$ mm

$t=6$ mm

$E=100$ GPa

$\rho=1700$ kg/m³

m will be then: $m = \pi \frac{\phi^2}{4} t \rho = 1700 * 6 * 10^{-3} \pi \frac{0.15^2}{4} = 0.18$ kg

If pressure is constant, the applied force will be also constant and equal to:

$$F_P = P \pi \frac{\phi^2}{4} = 10^7 \pi \frac{0.15^2}{4} = 1.77$$
 N

As said in the previous paragraph, the first step is to set $v=0$, $\theta=0$, $\sigma=0$, $m_{H_2O}=0$, $y=0$.

Considering $\Delta t=10^{-6}$ it is obtained:

$$1.77 * 10^5 \Delta t = 0.18 \Delta v$$

And then $\Delta v=1$ m/s and $\Delta y=10^{-6}(1+0)/2=5*10^{-7}$ m

Second step consists in the setting of these two values:

$v=1$ m/s; $y=5*10^{-7}$ m

the angle can be obtained: $\frac{\sin\theta}{1-\cos\theta} = \frac{\phi}{2y} = \frac{0.15}{2.5*10^{-7}} = 1.5 * 10^5$

Then $\theta=0.007^\circ=1.2*10^{-4}$ rad.

From the equation 5 the mass of water will be:

$$m_{H_2O} = 2.6 * 10^{-7} kg$$

Stress is calculated with equation 6:

$$\sigma = 3 * 10^{-4} MPa$$

Now there are all the quantities to apply the Newton's law (4):

$$(1.77 * 10^5 - 300 * 6 * 10^{-3} \pi * 0.15 \sin 0.007) \Delta t = (0.18 + 2.6 * 10^{-7}) \Delta v + 2.6 * 10^{-7}$$

Considering again $\Delta t=10^{-6}$:

$\Delta v=0.98$ m/s and then $v=1.98$ m/s and it is possible to obtain Δy :

$$\Delta y = \frac{1+0.98}{2} 10^{-6} = 1.49 * 10^{-6} m, \text{ and } y=1.99*10^{-6} m$$

Continuing always in the same way.

In the case of fiber reinforce composite panels, the resistance force (eq. 2) should be replaced with:

$$F_r = \frac{\sigma S n_l \pi \phi}{l} \quad (7)$$

In equation (7) σ is the stress supported by the fibers, S is the cross-section area of a fiber, n_l is the numbers of layers containing in the panel and l is the distance between two fibers in a layer. On the other hand, σ and E are the stress and Young's modulus of the fibers and all the equation still continue to be valid.

5.1.3 Rectangular panel

This case is more complex because it is also considered the shape of the deformed panel as it can be seen in the next figure:

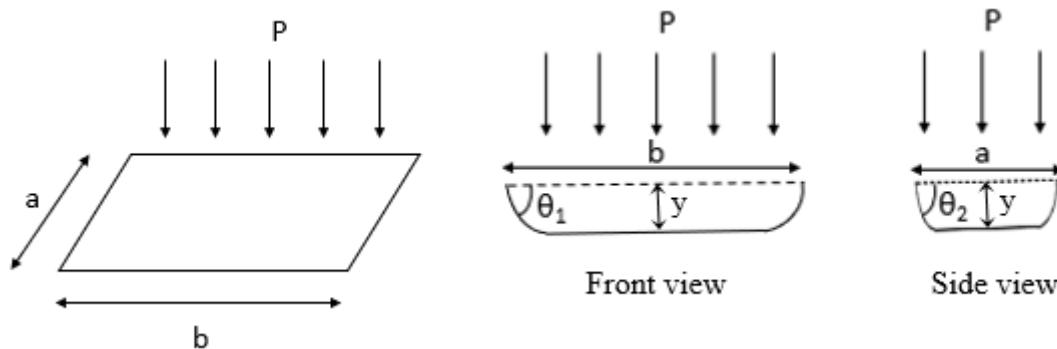


Figure 5.2: force applied on a rectangular panel and its deformed shape.

It is not easy to calculate the relation between the displacement y and the angles θ_1 and θ_2 . Also, the volume occupied by the water pushed by the pressure is not easy to obtain. It is necessary to make some simplifications, then the shape of the deformed panel is approximated to the shape of a folded plane, obtained using the slip-line theory. The approximated shape is represented in the next figure.



Figure 5.3: approximated shape of the deformed rectangular panel.

Distance x is assumed with the hypothesis that the stress (and the strain) in the fibers is the same in both directions of the panel:

$$\frac{2\frac{x}{\cos\theta_1} + (b-2x) - b}{b} = \frac{\frac{a}{\cos\theta_2} - a}{a} \quad (8)$$

Manipulating mathematically:

$$\frac{x(\frac{2}{\cos\theta_1} - 2)}{b} = \frac{1}{\cos\theta_2} - 1 \quad (9)$$

There is a relation between the angles θ_1 and θ_2 :

$$y = x \tan \theta_1 = \frac{a}{2} \tan \theta_2 \quad (10)$$

The approximation of the deformed shape of the panel allows to obtain a volume of a triangular prism minus two triangular pyramids:

$$V_{H_2O} = \frac{1}{2} ayb - \frac{2}{3} \frac{1}{2} ayx \quad (11)$$

It led to the following pushing force and resistance force:

$$F_p = pab \quad (12)$$

$$F_r = \sigma t 2(a + b) = \frac{2\sigma n_l S(a+b)}{l} \quad (13)$$

The stress will be then the same in both directions:

$$\sigma = E \left(\frac{1}{\cos\theta_2} - 1 \right) \quad (14)$$

The assumptions allow to calculate velocity and displacement just like shown in the case of the circular panel.

5.2 Model Implementation

As said, the model is written based on the professor Vicente Sánchez's equations. The software used is GNU Octave, a software for numerical analysis like MATLAB.

Input to the program are geometrical variable of the panel, materials properties (Young modulus, number of layers, fibers cross section, distance between fibers) and pressure. The pressure archive it is obtained as follows. In the QtiPlot files of each sample there is the pressure column, as said in the previous chapter the number of values is more than hundred thousand, then the computation will be too much long. For this reason, the first and the last part of the curve where the values are close to zero will not be used in the calculations. Then, the table is duplicated, in order to not to lose the original values, and to deal only with time and pressure data (in Pa), and more than seventy thousand values are eliminated.

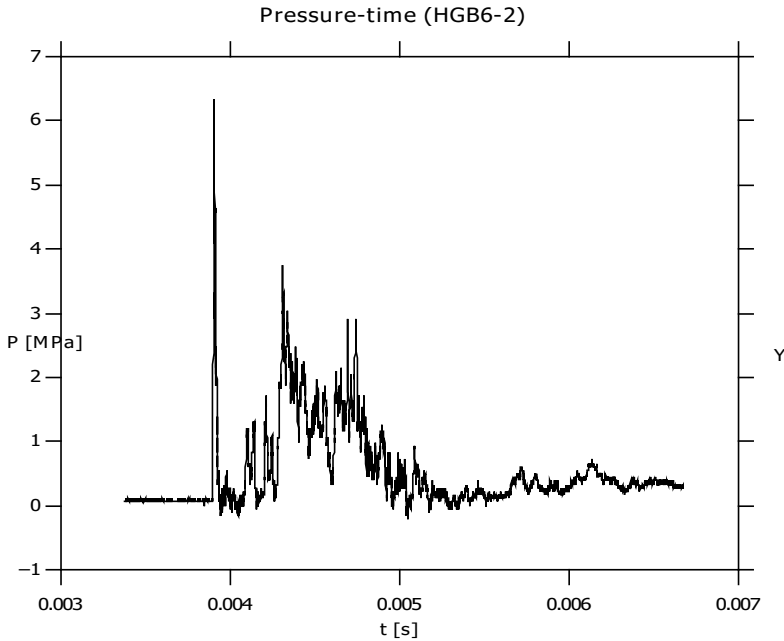


Figure 5.4: pressure-time graph after zero values deleting.

Next step is to obtain the csv file, so the values are copied on excel and saved in the desired format to be managed by the software. At the end of the computation, the software saves a csv file containing the calculated deflection values.

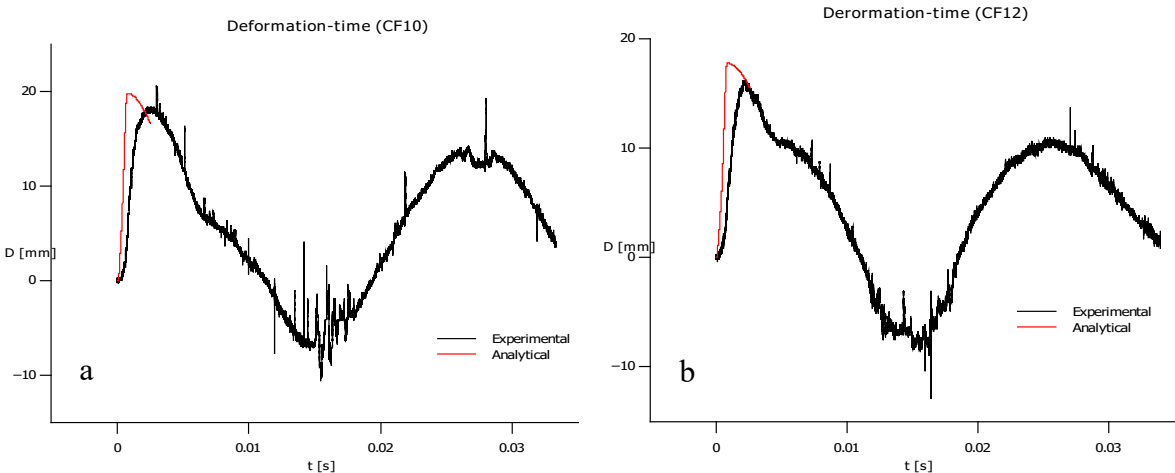
5.3 Results

In the next paragraphs it is proposed the comparison between the deflection curves obtained experimentally and those obtained with the model. In QtiPlot it is imported the output deflection file of the analytical model and then it is possible to compare the two curves.

. The input variables on the material characteristics are known for the single fiber types (carbon, glass and basalt). The properties for hybrid samples are calculated with lever rule, considering the number of layers for each fiber type in the same panel. The values obtained have been put in the software and the solutions compared with experimental curves.

5.3.1 Carbon fiber specimen

Figure 5.5 (a-h) show the comparison between the experimental curves and the results obtained with analytical model, for all pressure histories recorded for carbon fiber tests.



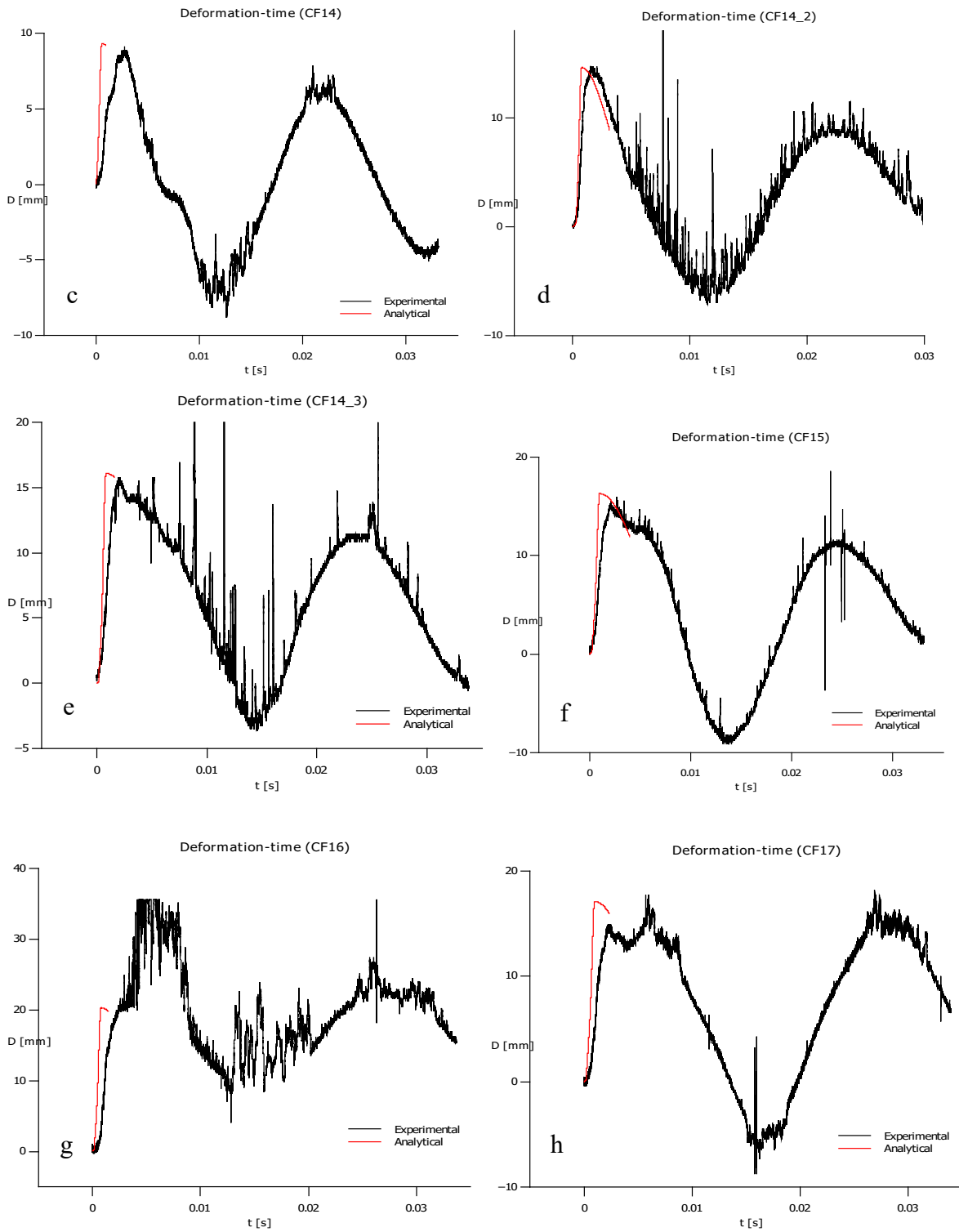


Figure 5.5: a-h: analytical and experimental deformation-time curves of CFRP.

5.3.2 Glass fiber specimen

Figure 5.6 (a-f) show the comparison between the experimental curves and the results obtained with analytical model, for all pressure histories recorded for glass fiber tests.

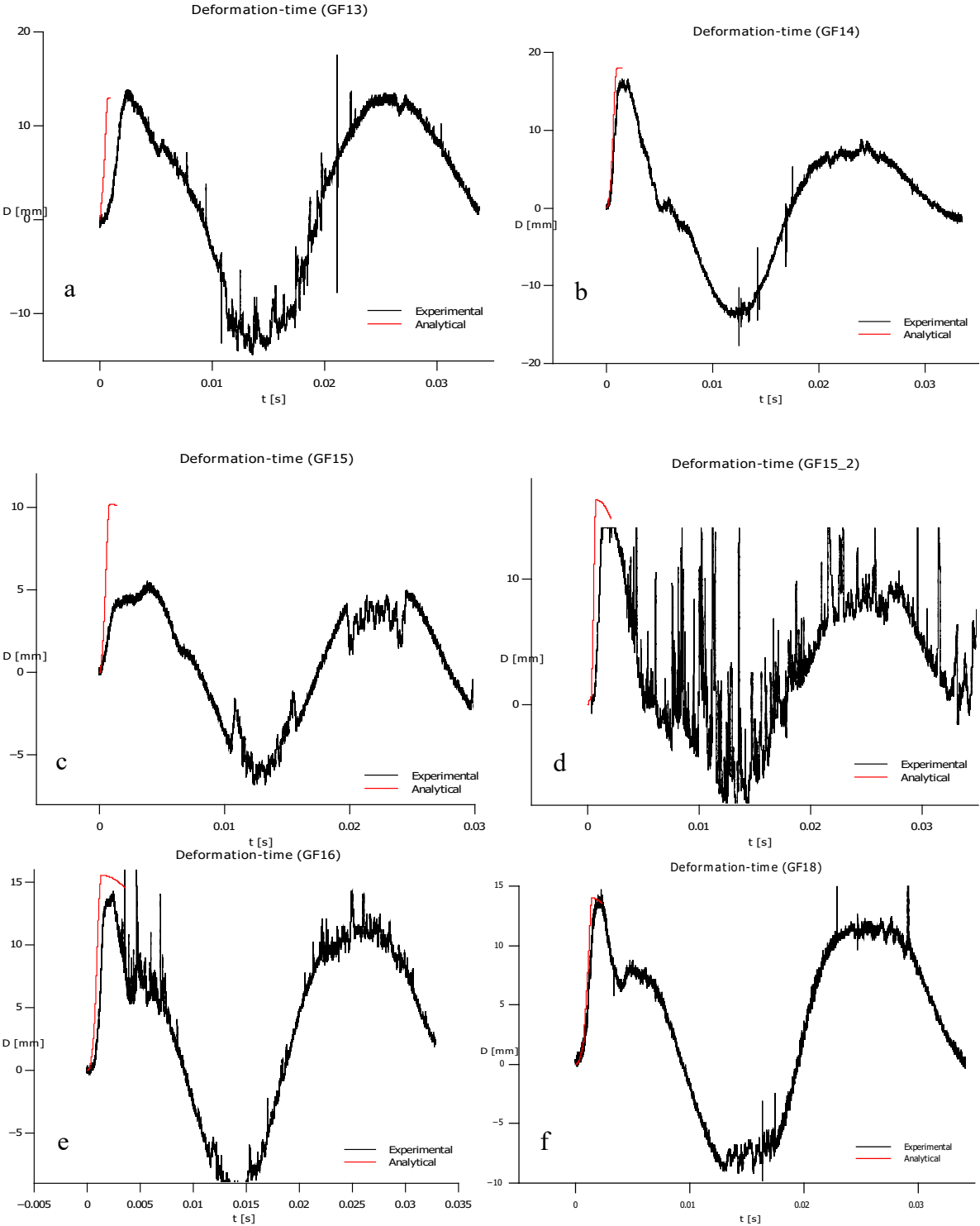
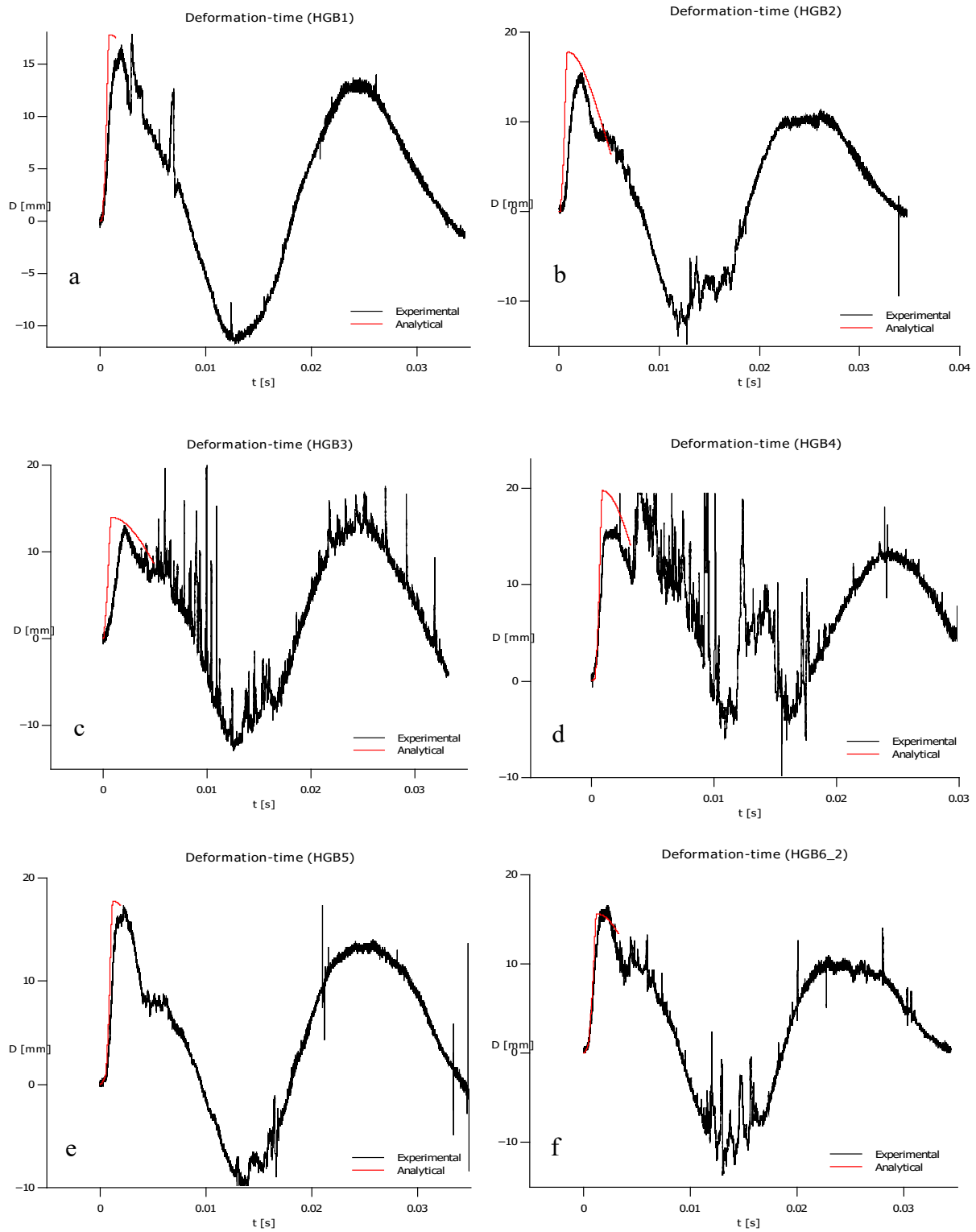


Figure 5.6: a-f: analytical and experimental deformation-time curves of GFRP.

5.3.3 Basalt-glass specimen

Figure 5.7 (a-h) show the comparison between the experimental curves and the results obtained with analytical model, for all pressure histories recorded for basalt-glass tests.



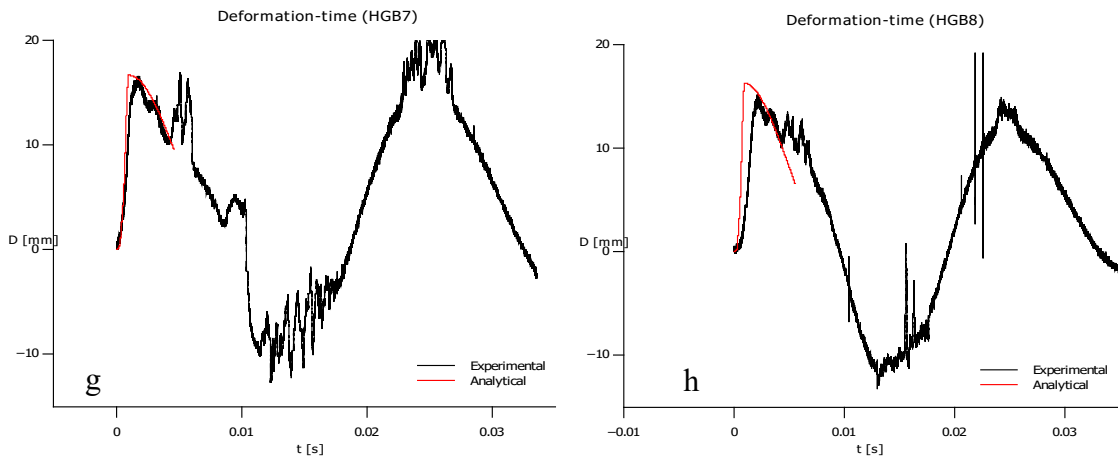
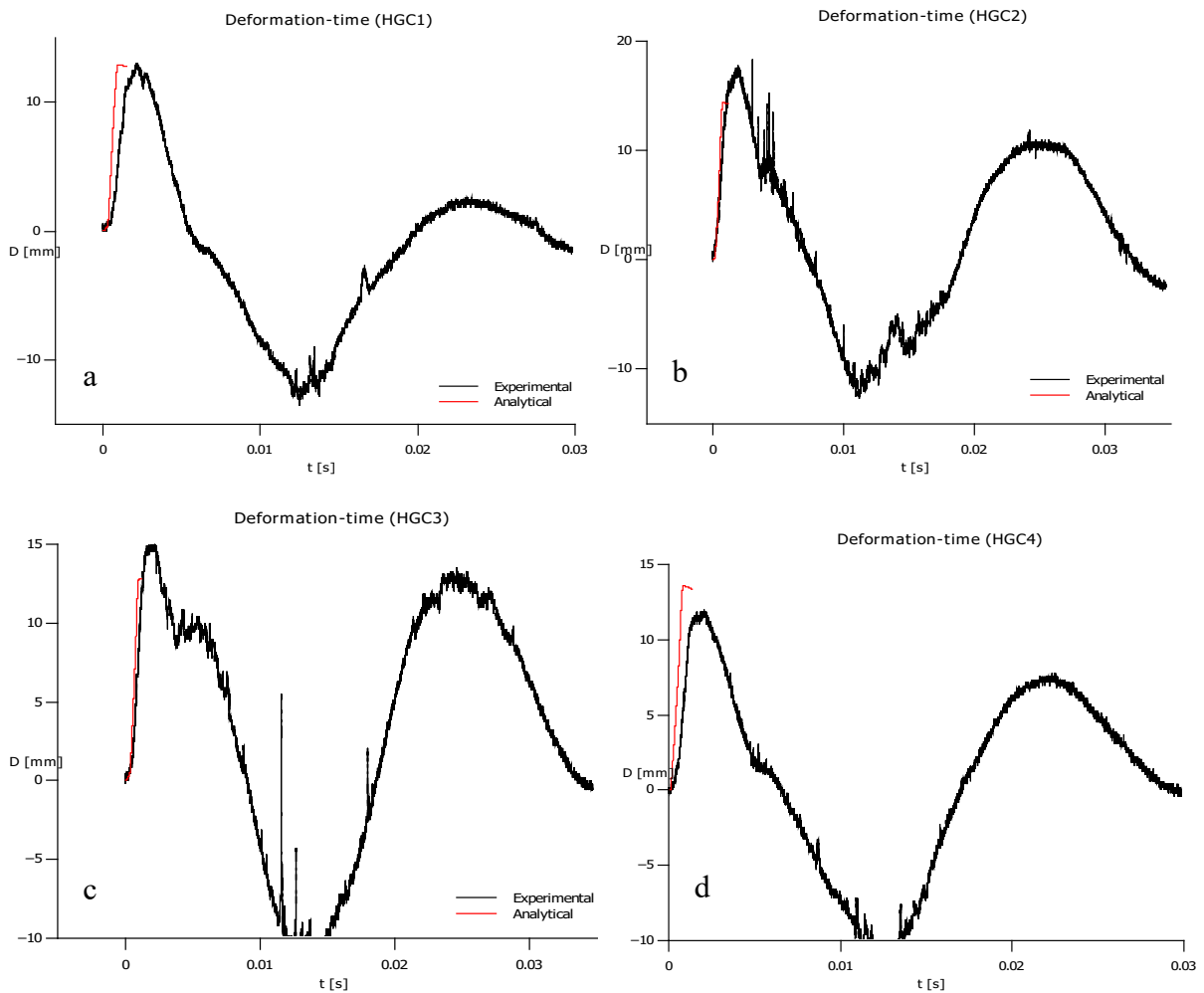
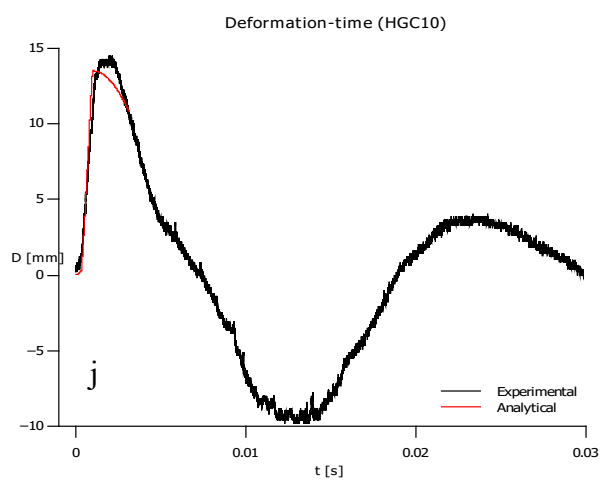
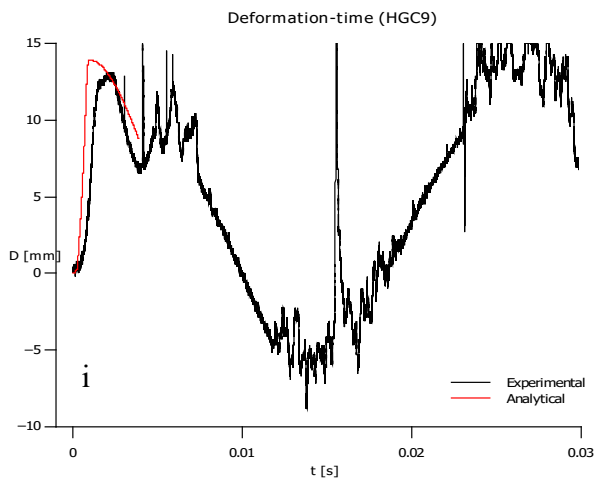
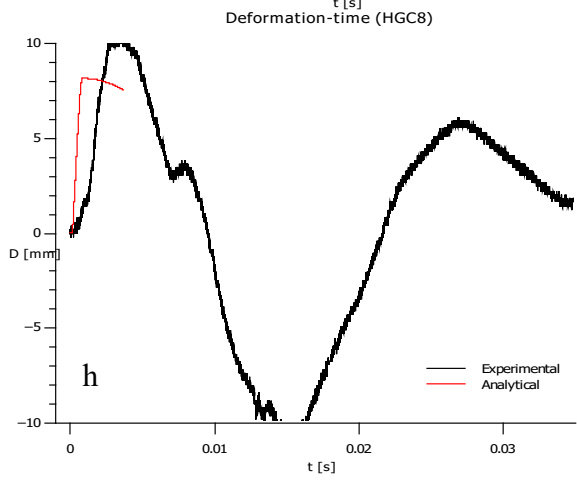
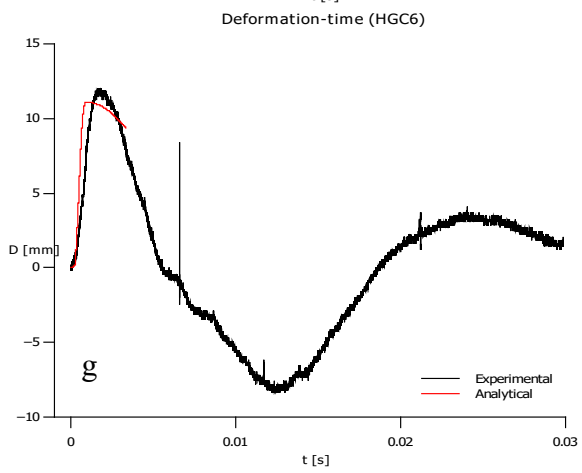
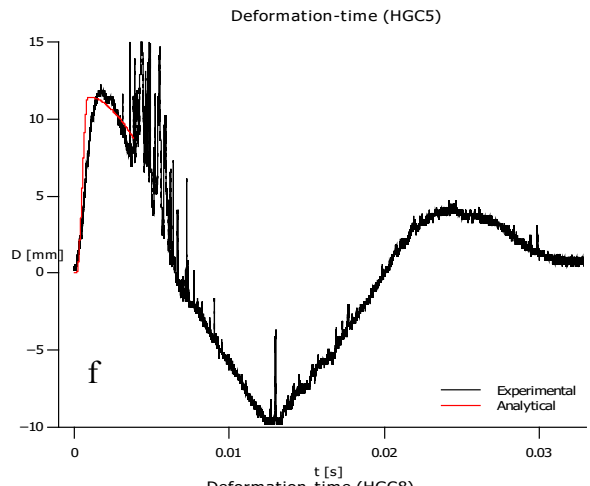
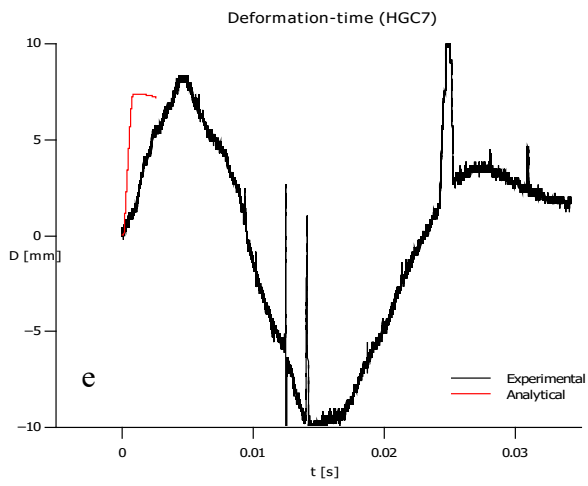


Figure 5.7: a-h: analytical and experimental deformation-time curves of HGB.

5.3.4 Carbon-glass specimen

Figure 5.8 (a-o) show the comparison between the experimental curves and the results obtained with analytical model, for all pressure histories recorded for carbon-glass tests.





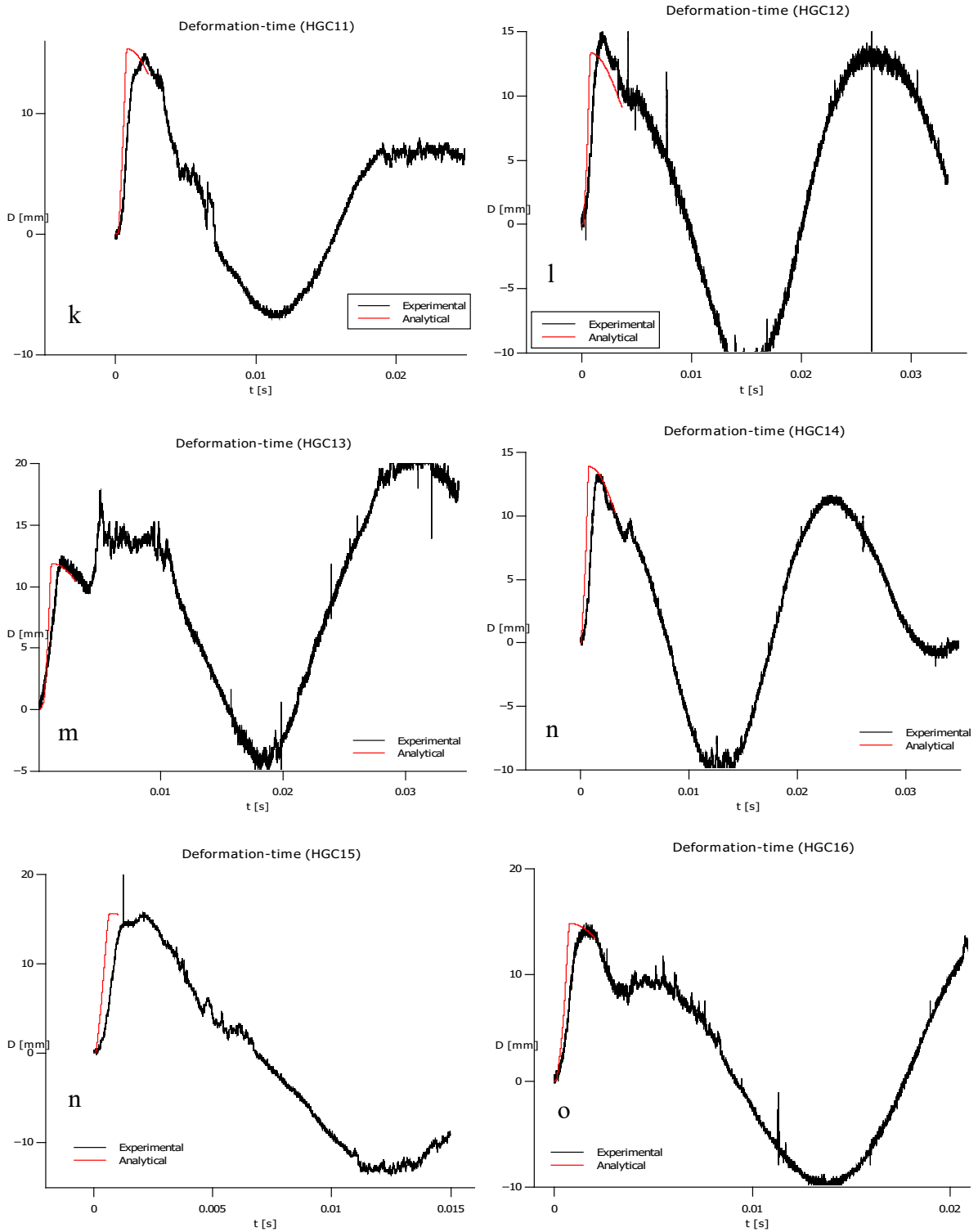


Figure 5.8: a-o: analytical and experimental deformation-time curves of HGC.

5.4 Results discussion

It is possible to notice that the analytical curves calculated provide a good prediction of the experimental behaviour, at least during the first stages of the test. In particular, peaks values of the deflection are about equals. Also, the initial slope is very similar, but, in some cases, it is quite different. It is because the specimens do not behave perfectly during the tests, in fact they are not perfectly fixed in the framework, so they can show a behaviour more compliant. As consequence of this not perfectly behaviour in the framework, the experimental curves do not show always the same slope, even if the material is the same. It is because the device used is not standardized and then it does not always behave in the same way.

If it is considered that the higher stress values reached in the specimens, it corresponds to the maximum deflection, it can be stated that this analytical model is a suitable tool for predicting the behaviour of composite panels subjected to blast. Compared to conventional Finite Element Models, this analytical tool is faster and much simpler, making it ideal for designing purposes. Analytical model is a potential instrument, because it can be used not only for the materials considered in this application, but also for other materials, in fact, it is just needed to change the input variables on the geometry and on the properties.

Chapter 6

Conclusion and future work

In this last chapter a brief summary of this master thesis work needs to be carried out, in order to highlight the main aspects of the project.

In the months spent at *Politecnica de Madrid*, the behaviour of composite materials used in naval field and subjected to water blast explosion was studied. First of all, a literature survey was carried out, in order to better understand the importance of the goal of the project. In fact, during the last years, several studies on these materials have been conducted. The behaviour of these composite materials subjected to static, quasi-static and dynamic impact was deeply studied, while there are not enough researches on the subjection to ballistic impacts. Materials used in naval field must support several critical conditions, like thermal cycling, dynamic loads and impulsive attacks among others. This led to the need pursued in this project.

In order to carry out this object, an experimental device, able to simulate a submarine mine, was designed based on the Hopkinson bar device. It was never used before and consists of the combination of an incident bar with an aluminium chamber. The incident bar was screwed to a piston (the frontal face of the box) and was hit by a projectile powered with compressed air. The impact was converted in a plane wave in the water inside the aluminium box and it was this plane wave itself to hit the sample, fixed behind the aluminium box. The experimental device was also provided with an instrumental system which allowed to obtain experimental measures, like the deformation suffered by the sample and the pressure in the chamber.

The focus was on four FRP (fiber reinforced polymers) types made in vinylester reinforced with: carbon, glass, basalt-glass and carbon-glass. It means that it was studied not-hybrid and hybrid configuration. In the case of the hybrid configuration (two fiber types in the same panel), it was also considered the possible different behaviour if the test is conducted from the side of glass, or from the side of carbon and basalt. Another focus of this project was on the

study of the possible influence after the immersion in seawater. In fact, half samples were put in a bath of saltwater until the saturation level.

Another objective of this master thesis work was to develop an analytical model that allowed to predict the behaviour of composite materials subjected to water blast explosion. The analytical model was based on Vicente Sánchez's equations and it was implemented on matlab. The input of the software was the pressure history obtained with experimental device and the output was a deformation archive calculated by the program. For each sample it was calculated the analytical deformation, in order to compare all the analytical and experimental results and to understand if the model would be reliable.

The experimental measures were analysed in order to compare all the conditions considered and to find the material that better behave in this application studied.

Regarding the hybrid materials, half of the specimens were tested in a side and half on the other side, but no appreciable differences were found, meaning that the hybrid composites behaved in the same way depending on the side involved in the impact. As regards the immersion in water, it was found that the deformations reached by saturated samples were very similar to the ones reached by dry specimens. It means that the immersion did not influence the behaviour of these composite materials.

It was also found that CFRP (carbon fiber reinforced polymer) is the composite type that behave worse of anyone. In fact, all the CFRP samples were broken after the tests and they showed the higher deformation values. Hybrid samples and especially carbon-glass showed the lowest deformation values, but it cannot be considered the best material in this application, because more than half specimens were delaminated after tests. Finally, GFRP (glass fiber reinforced polymer) were the only ones to not show any signs of damage after tests, therefore it can be concluded that they were the best materials for this application. It was also important to say that these conclusions can be applied just in the case of this project, meaning that a different, thickness, a different number of layers, a better homogeneous configuration of the fibers could led to different results. The reason behind the better behaviour of GFRP seems to be its higher compliance, which allows to reach higher deflection levels without compromising its integrity.

Regarding the analytical model, experimental and analytical deformation were compared, and it was found that analytical curves are very similar to experimental ones, especially for the peak values reached, which also is the most important parameter, because it represented the maximum deformation caused by the blast and, in principle, the highest stress levels for the

specimens. It can be concluded that analytical model is suitable for the prediction of the behaviour of composite materials subjected to submarine blast load.

Possible future works can be carried out. It can be conducted X-ray analysis to better evaluate the internal damage in the samples tested and to measure the residual stresses. It can be tested under different environmental conditions, such as different temperatures, considering that materials used in naval field can be subjected to thermal shock. Different thickness, number of layers, fibers disposition or, for example, a more homogeneous disposition of fibers in hybrid materials in order to confirm if the trends obtained in this work can be extrapolated to other configurations.

Moreover, it could be designed an improved experimental device based on that used in this project, considering that many difficulties slowed down the tests. However, the experimental device was been designed to study the behaviour of any type of material, therefore, in future can be used this device or another improved one to test different types of materials.

Finally, the analytical model predicted quite well the behaviour of the materials considered, then it can be used to study any type of materials, simply changing the input variables on the geometry and on the properties of the panel.

Appendix

Matlab software

```
clear
%geometry and properties%
a=0.17; %dimension of the panel in m
b=0.225; %dimension of the panel in m
n=; %number of layers
S=; %cross-section area of the fiber
l=; %distance between fibers
E=; %Young Modulus in Pa
rho=; %Density in kg/m3
sr=; %critical stress of the fiber in Pa
e=0.003; %thickness of the panel in m
mpiston=1.132+1.017; %piston mass
frozamiento=100; %friction

%select the pressure archive%
ruta='../Ensayos/SAMPLE/';
input_presion='presion.csv';
output_deflexion='deflexion';

file=fopen([ruta,input_presion],'r');%pressure in MPa, time in s
P=csvread([ruta,input_presion]);
fclose(file);
%file_res=fopen([ruta,'Registro_proceso_calculo'],'w')
%fprintf(file_res,'Fecha %s\n',date)

%ITERATIVE PROCESS%
[f,c]=size(P);

tp=P(:,1);%time vector
p=P(:,2);%pressure vector

t(1)=0;
rhoH2O=1000; %Kg/m^3%
m=rho*e*a*b;

s(1)=0;%stress in the sample
```

```

v(1)=0;%panel speed
dv(1)=0;
y(1)=0.00001;%deflection
theta(1,1)=0.00001;%angle with normal to sample
theta(2,1)=0.00001;
fp(1)=p(1)*1e6*a*b;%pushing force
fr(1)=0;%resistant force
mH2O(1)=0;%mass of the water in the box
dmH2O(1)=0;
i=2;
x(1)=0;
sigma=s(1);

while(sigma<sr && i<=number of values in the pressure archive used)

dt(i-1)=tp(i)-tp(i-1);
t(i)=t(i-1)+dt(i-1);
[sol,niter]=newton_raphson_rectangular(@fun_rectangular,@dfun_rectangular,theta,a,b,y(i-1),1E-3);
theta(1,i)=sol(1);
theta(2,i)=sol(2);
epsx(i)=2*y(i-1)*(1-cos(sol(1)))/(sin(sol(1))*b
epsy(i)=(1/cos(sol(2)))-1
x(i)=y(i-1)/theta(1,i);
s(i)=(theta(2,i)/abs(theta(2,i)))*E*((1/cos(theta(2,i)))-1);

fp(i)=p(i)*1E6*a*b;
fr(i)=s(i)*n*S*2*(a*sin(sol(1))+b*sin(sol(2)))/l

if (s(i)>s(i-1))
mH2O(i)=rhoH2O*(0.5*a*b*y(i-1)-(1/3)*a*y(i-1)*x(i));
dmH2O(i)=mH2O(i)-mH2O(i-1);
dv(i)=((fp(i)-fr(i))*dt(i-1)-dmH2O(i)*v(i-1))/(m+mH2O(i));
else
mH2O=rhoH2O*0.2*0.25*0.15;
dv(i)=((fp(i)-fr(i))*dt(i-1))/(m+mH2O+mpiston+frozamiento);
end

v(i)=v(i-1)+dv(i);
dy(i)=v(i)*dt(i-1);
y(i)=y(i-1)+dy(i);
sigma=s(i);
i=i+1;
end

D=[t',1000*y'];%save the deflection in mm
csvwrite([ruta,output_deflexion],D);

```


References

- [1] Badini C. (2013), *Materiali compositi per l'ingegneria*, Celid, 248 pp.
- [2] Pagliara G., (n.d.), *Compositi a matrice o a rinforzo ceramico*, lezioni di tecnologia ceramica.
- [3] Licciulli A (2009), *Materiali compositi e loro rinforzi*, Corso di scienza e ingegneria dei materiali, Università del Salento.
- [4] Anon (2012), *Materiali compositi*, dispense corsi di laurea a distanza, Scienza dei materiali, Politecnico di Torino.
- [5] Altevista (2011), *Materiali Compositi*. [online] disponibile a: <http://adpaloha.altevista.org/wp-content/uploads/2012/11/Materiali-Compositi_____.pdf> [Ultimo accesso 15/05/19].
- [6] Vannucci (2008), *Cosa sono i materiali compositi*, Capitolo 1, Dispense Scuola di dottorato di ingegneria, Università di Pisa.
- [7] Rossetti G., (n.d.), *Progettazione con materiali*, presentazione disponibile a: <slideplayer.it/slide/13404486/> [ultimo accesso 21/11/19].
- [8] Octima, (2016), *poliestere, vinilestere o epossidica*, PDF disponibile a: <https://www.octima.it/wp-content/uploads/2016/01/09_Nau_Gurit.pdf>.
- [9] Marinò A. (2016), *Costruzioni navali in composito*, dispense, Università degli studi di Trieste.
- [10] Albicini L. (2016), *I materiali compositi avanzati (FRP-FRG). Classificazione e applicazioni nel restauro e ricostruzione post-sisma*, tesi di laurea, Scuola di ingegneria e architettura, Università di Bologna.
- [11] Fidia s.r.l. (n.d.), *Tessuti in fibra naturale di basalto BFRP*, disponibile a: <http://www.fidiaglobalservice.com/ita/tessuti_basalto.html> [ultimo accesso: 29/10/19].
- [12] Naik S., (2013), *Stress wave propagation in split Hopkinson pressure bar*, master thesis, department of civil engineering, National institute of technology Rourkela.
- [13] Mazón P., (2018), *Estudio del comportamiento a impacto de alta velocidad en materiales compuestos del sector naval*, tesi di laurea, Department of material's engineering, Politecnica de Madrid.
- [14] Mouritz A.P., Gargano A., Pingkarawat K., Das R., Pickerd V., Delaney T., (2017), *Effect of seawater on the explosive blast response of a carbon fiber laminate*, **109** (A), 382-391.
- [15] Arora H., Del Linz P., Dear J. (2017), *Damage and deformation in composite sandwich panels exposed to multiple and single explosive blasts*, **104**, 95-106.
- [16] Dear J.P., Rolfe E., Kelly M., Hooper P.A., Arora H., (2016), *X-Ray CT Analysis after Blast of Composite Sandwich Panels*, **167**, 176-181.
- [17] D'Angelo G., (2017/2018), *High speed impact properties of composite materials*, Department of management engineering, Università degli studi di Napoli Federico II.
- [18] Dhand V., Mittal G., Rhee K.Y., Park S., Hui D., (2015), *A short review on basalt fiber reinforced polymer composites*, **73**, 166-180.
- [19] Linkedin, (2011), *Composite materials*, disponibile a: <<https://player.slideplayer.com/12/3505368/data/images/img18.jpg>>.

- [20] Alijibori H., Ridha N., Alosfur F., Salim M., (2016), *A study on Thermal Diffusivity and Dielectric Properties of Epoxy Matrix Reinforced by Fibers Material*, **14**, 42-53.
- [21] Cannon plastec, immagine disponibile a:
<<https://www.cannonplastec.com/technologies/composites/>>.
- [22] Gokce A., Advani S.G., (2005), *Modeling, optimization and control of resin flow during manufacturing of textile composites with liquid molding*, 242-291.
- [23] SubsTech (2012), *Poltrusion*, disponibile a:
<<https://www.substech.com/dokuwiki/doku.php?id=pultrusion>>.
- [24] Absullah F., Mahmoud F., Al-ameed E., (2017), *Effect of adding nano-powder on composite pipes behaviour subjected to multi stresses*, **21**, 184-200.
- [25] Gotro J., (2016), *Polymer composites part 4: Overview of matrix resins*, disponibile presso: Polymer Innovation Blog.
- [26] Caretto F., Cannataro G., Casciaro G., (2017), *Analisi dell'adesione tra fibra di basalto e matrici termoplastiche*, ENEA-RT-2017-16.
- [27] Cabral T., (2016), *A first approach to structural health monitoring of adhesive bonded joints in pipelines using integrated fiber optic sensors*, Department of Mechanical Engineering, Universidad Federal de Santa Catarina.
- [28] Wang R., Zheng S., Zheng Y., (2011), *Reinforced materials*, 29-99, 547-548.
- [29] Park S., Heo G., (2015), *Precursors and manufacturing of carbon fibers*, 31-66.
- [30] Monni F., (2011), *Utilizzo della fibra di basalto per il recupero e la conservazione di murature storiche*, 205-208.
- [31] Quionne Tech S.L., (2016), *Basalt fiber from a volcanic lava to an advanced composite*, disponibile a : < <http://www.quionnengineering.com/939/>> [ultimo accesso: 26/11/19].
- [32] Wikipedia (2019), *La Fayette-class frigate*, disponibile a:
<https://en.wikipedia.org/wiki/La_Fayette-class_frigate> [ultimo accesso: 29/10/19].
- [33] Pixdaus, *FNS Tornio, Finnish Navy Hamina class attack*, disponibile a: <<http://pixdaus.com/fns-tornio-finnish-navy-hamina-class-fast-attack-boat-naval-/items/view/304738/>> [ultimo accesso: 29/10/19].
- [34] Minoia R., (2012), *Mappa degli attacchi dei pirati sulle rotte del giro del mondo*, disponibile a:
<<http://blog.veleggiando.it/post/mappa-degli-attacchi-dei-pirati-sulle-rotte-del-giro-del-mondo.aspx>> [ultimo accesso: 29/10/19].
- [35] Anon (2017), *Composite ships for the next generation of ship owners*, disponibile presso: Damen Magazine.
- [36] Gargano A., Pingkarawat K., Blacklock M., Pickerd V., Mouritz A.P., (2017), *Comparative assessment of the explosive blast performance of carbon and glass fibre-polymer composites used in naval ship structures*, **171**, 306-316.
- [37] Neşer G., (2017), *Polymer based composites in marine use: History and future trends*, **194**, 19-24.
- [38] Sánchez V., Gálvez F., Sancho R., Cendón D., (2017), *A new analytical model to simulate high-speed impact onto composite materials targets*, **108**, 322-333.